

**Dissertation zur Erlangung des Doktorgrades
der Fakultät für Chemie und Pharmazie
der Ludwig-Maximilians-Universität München**



**An electrophysiological Approach to Analyze
Lysosomal Cation Channels of the TRP Channel Superfamily**

Cheng-Chang Chen

aus Tainan, Taiwan

2014

Erklärung

Diese Dissertation wurde im Sinne von § 7 der Promotionsordnung vom 28. November 2011 von Prof. Dr. Christian Wahl-Schott betreut.

Eidesstattliche Versicherung

Diese Dissertation wurde eigenständig und ohne unerlaubte Hilfe erarbeitet.

München,23.10.2014.....

.....

(Cheng-Chang Chen)

Dissertation eingereicht am 23.10.2014

1. Gutachter Prof. Dr. Christian Wahl-Schott

2. Gutachter Prof. Dr. Martin Biel

Mündliche Prüfung am 05.11.2014

Table of contents

Erklärung	2
Ehrenwörtliche Versicherung.....	Fehler! Textmarke nicht definiert.
1 Introduction.....	3
1.1 The aims of this thesis.....	16
2. Material and Methods.....	18
2.1 Material.....	18
2.1.1 Chemicals and consumables.....	18
2.1.2 Compounds and chemical syntheses.....	20
2.2 Methods.....	21
2.2.1 cDNA constructs and transfection.....	21
2.2.2 Cell culture.....	21
2.2.3 Generation of stable HEK293 cell lines.....	22
2.2.4 Generation and Isolation of MEFs from TPC2 ^{-/-} knockout mice.....	23
2.2.5 Patient cell lines.....	23
2.2.6 Calcium imaging.....	24
2.3 Modified whole-lysosome patch-clamp electrophysiology.....	24
2.3.1 Cut and isolated lysosome.....	24
2.3.2 Lysosome attach and giga seal formation	25
2.4 Whole-lysosome planar patch-clamp recording.....	25
2.4.1 Preparation of lysosomes	26
2.4.2 Planar patch-clamp electrophysiology	28
2.5 Data Analysis.....	31
3. Results	33
3.1 Characterization of the lysosomal two-pore channel 2.....	33
3.1.1. Direct whole-lysosome patch-clamp method to characterize TPC2 mediated currents from intact lysosomes	33
3.1.2. Whole-lysosome Planar Patch-clamp method to characterize TPC2 mediated currents from intact lysosomes	36
3.1.3. PI(3,5)P2 and NAADP evoke TPC2 channels in the lysosome.....	37
3.1.4. Regulation of TPC2 by NED-19 and ATP	40
3.1.5. Ion permeability of TPC2	43
3.1.6. Different direct electrophysiological approaches	43

3.2.	Electrophysiological characterization of MLIV causing point mutants of TRPML1	44
3.2.1.	Subcellular localization of ML IV causing point mutants of TRPML1	44
3.2.2.	Small molecule agonists increase channel activity of TRPML1 mutant isoforms	46
3.2.3.	Further development of the lead structure SF-22.....	49
3.2.4.	Effect of MK6-83 on channel activity in ML IV patient derived cell lines.....	56
4.	Discussion.....	58
4.2	Characterization of TPC2 channels	61
4.3	Towards a treatment for MLIV disease.....	64
5.	Summary.....	67
6.	Literature.....	67
7.	Appendix.....	82
7.1.	Abbreviations.....	82
6.2	Chemical structures of the lead compound SF-22 and novel SF-22 analogues.....	84
7.2.	Curriculum vitae	85
7.3.	Acknowledgements	87

1 Introduction

The cell membrane is a biological membrane that consists of the phospholipid bilayer with embedded proteins. It is also known as the plasma membrane that separates the interior of cells from the outside environment and it is involved in several cellular processes, such as cell signalling and ion conductivity. However, the plasma membrane structure only forms 5 % of the whole cell lipid bilayer membrane. The membranes of intracellular organelles form more than 95 % of the total cell membrane system. Several types of intracellular ion channels play a role in the maintenance of ion homeostasis in subcellular organelles including the endoplasmic reticulum, nucleus, lysosome, endosome, and mitochondria. These intracellular ion channels in the various cellular organelles are fundamental for the control of numerous physiological functions, including muscle contraction, secretion, cell motility, immune response and degradation (Berridge et al., 2000; Leanza et al., 2013; Sftig et al. 2009) (**Fig.1**). The smallest intracellular organelle, the lysosome, is the main focus of this thesis.

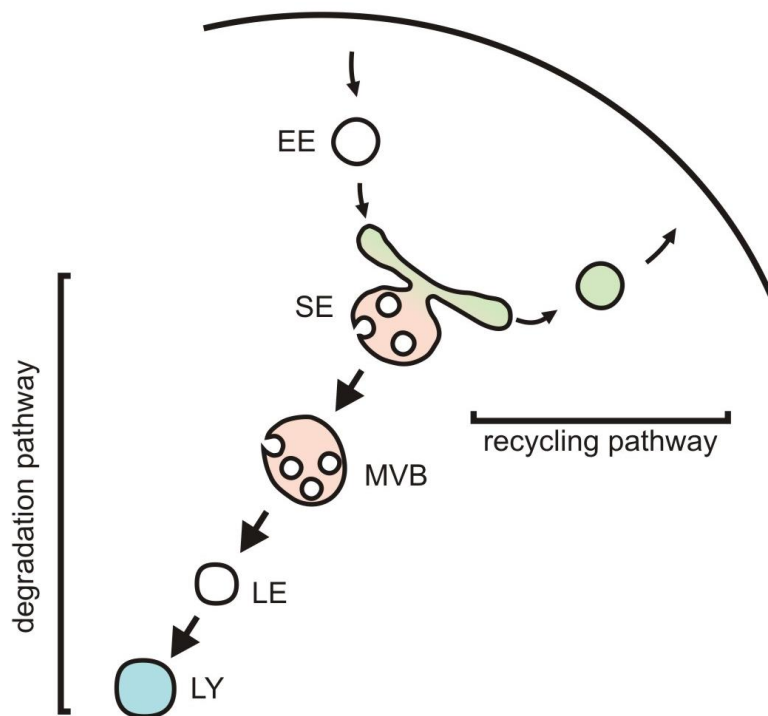


Figure 1: Cartoon illustrating endo-lysosomal degradation and recycling pathways. After internalization receptors of the plasma membrane are either hydrolyzed in the degradation pathway (e.g. Epidermal growth factor receptor) or trafficked back to the plasma membrane in the recycling pathway (e.g. Low-Density Lipoprotein receptor, transferrin receptor). SNARE proteins such as syntaxins regulate critical fusion events within these pathways. EE: early endosome; SE: sorting endosome; MVB: multivesicular body, LE: late endosome; LY: lysosome.

More than 50 years ago Christian de Duve used centrifugal fractionation and discovered a saclike structure surrounded by a membrane which contains hydrolytic enzymes. Duve named them "lysosomes", which is Greek for digestive body (de Duve et al., 1955; de Duve et al., 1962; de Duve 2005). Lysosomes as dynamic organelles constitute up to 5 % of the intracellular volume and are of heterogeneous size (100 – 1000 nm) and morphology (Holtzamn et al., 1972; Mellman 1989). More than 60 different degradative enzymes have been identified in lysosomes to hydrolyze proteins, DNA, RNA, polysaccharides, and lipids (Saftig and Klumperman 2009; Eskelinen et al., 2003; Lee et al., 2010; Zhang et al., 2010; Korolchuk et al., 2010). Lysosomes have been recognized as the terminal degradative compartment of the endocytic pathway and they have been found to be required for the digestion of the intracellular material during the process of autophagy (Schiaffino et al., 1963; Luzio et al., 2007). The luminal environment of lysosomes is maintained at an acidic pH because of proton-pumping vacuolar ATPases (Mellman et al., 1986). The pH of intraluminal lysosomes and endosomes is around 4.6 and 6.0, respectively (Morgan et al., 2011; Grabe et al., 2001). Lysosomes contain acid hydrolases and many lysosomal membrane proteins including ion channels which receive and degrade macromolecules from the secretory, endocytic, autophagic and phagocytic membrane-trafficking pathway (Luzio et al., 2007). The gene mutations or dysfunctions of lysosomal membrane proteins cause the majority of lysosomal storage diseases (LSDs), which represent the leading cause of childhood-onset neurodegeneration (Parkinson-Lawrence et al., 2009; Schöpfer et al., 2010; Valenzano et al., 2011). Because lysosomes play a variety of roles in the functioning of cells, an understanding of the electrophysiological properties of lysosomal ion channels is important in many areas of biology.

Intracellular acidic lumina of endolysosomes contain several types of cations. The concentrations of these ions vary from early and late endosomes to lysosomes. However, the quantification of most ions in the lumen of different acidic organelles across diverse cellular sources has not been undertaken systematically. Generally, the intraluminal concentrations of sodium and potassium are reported to range from 20 to 150 mM and from 20 to 107 mM, respectively (Wang et al., 2012; Morgan et al., 2011; Steinberg et al., 2010). The estimated intraluminal concentration of calcium

within acidic stores ranges from 200 to 600 μM in lysosomes (Morgan et al., 2011; Lloyd-Evans et al., 2008; Christensen et al., 2002) and from 3 to 37 μM in late endosomes (Gerasimenko et al., 1998; Morgan et al., 2011), meaning that there is a substantial ~ 5000 fold Ca^{2+} gradient in late endosome and lysosome system. Intracellular free calcium ions play a vital role in the majority of physiological processes (Carapoli et al., 2001). Ca^{2+} ions unlike most other intracellular signaling messengers, cannot be created or destroyed, so their regulation only relies on transport or buffering mechanisms. Cytoplasmic concentration of Ca^{2+} is tightly controlled by efflux mechanisms on the plasma membrane and intracellular storing/releasing mechanisms of the organelles such as the endoplasmic/sarcoplasmic reticulum (ER/SR) and acidic organelles (Haller et al., 1996). The Ca^{2+} concentration gradient influences the reactions ranging from muscle contraction and neuron excitation to regulation of gene expression and neurotransmitter release (Berridge et al., 2003; Clapham 2007). In addition, numerous studies have demonstrated that Ca^{2+} influx through voltage-gated Ca^{2+} channels triggers a late step of exocytotic vacuole fusion during neurotransmission and fundamentally regulates endolysosomal dynamics via concentration of juxta-organelle Ca^{2+} (Südhof 2008; Hay 2007; Peters et al., 1998). In yeast, the study of the trans-SNARE complex formation showed trans-SNARE interactions directly elicit Ca^{2+} efflux from the lumen of vacuoles (Merz et al., 2004). Lacking control of luminal Ca^{2+} concentration is known to inhibit the maturation of phagosomes in macrophages (Shaughnessy et al., 2007), and trafficking in neurons and subsequent neurodegenerative disorders (Lloyd-Evans et al., 2008; Lloyd-Evans et al., 2010). For these events, it has been postulated that Ca^{2+} is elicited through unknown Ca^{2+} channels from the lumen of vesicles and intracellular acidic organelles like lysosomes.

The lysosomal lumen has also been presumed to contain high concentrations of K^+ , Na^+ , H^+ and Fe^{2+} (Morgan et al., 2011; Morgan et al., 2013; Hentze et al., 2004, Kidane et al 2006). Recent approaches have determined the relative abundance of the total but not free ions in the lumen, although the absolute concentrations of ions could not be precisely measured due to the lack of knowledge about the lysosomal dynamic volume. Like the cytosol and the endoplasmic reticulum, lysosomes have been presumed to contain high K^+ and low Na^+ , using indirect measurements (Morgan et al 2011; Steinberg et al., 2010). In contrast, in the latest study it was postulated that Na^+ is the predominant monovalent cation in the lumen of the lysosome. Wang and colleagues used the lysosome fraction of HEK293 cells and applied a density-gradient centrifugation approach (Wang et al., 2012), which has been used successfully before to determine ionic compositions in a number of intracellular organelles, including mitochondria and synaptic vesicles (Cohn et al., 1968; Schmidt et al., 1980). Whereas positively charged lipid bilayers tend to fuse frequently (Anzai et al., 1993), Na^+ ions from vesicle influx into the cytoplasm affect membrane fusion during exocytosis (Parnas et al., 2000). In mammalian cells, lysosomes are considered to be the main source of cellular iron. They release iron

from the endosome-lysosome system after iron uptake by endocytosis of Fe²⁺-bound transferrin receptors, or after lysosomal degradation of ferritin-iron complexes and ingestion of iron-containing macromolecules via the autophagy pathway (Hentze et al., 2004, Kidane et al 2006).

Numerous ion channels have been identified in the lysosomal-endosomal compartment such as chloride channels (CIC) and transient receptor potential channels (TRP) (Clapham et al., 2001; Clapham 2003; Ramsey et al., 2006; Jentsch et al., 2005; Huang et al., 2014) (**Table 1**), which allow cations to leave or enter the lysosome; However, their physiological roles in situ have remained largely uncharacterized. The resting membrane potential of these acidic stores which is around +10 to +40 mV depending on the charge of luminal organelle is more positive than the cytosol (Morgan et al., 2011; Koivusalo et al., 2011), that is generally considered to be highly favourable to cation release.

Ion Channel	Expression	Function	Human Disease
TRPM1	Skin and eyes	Tumor suppressor, potential role in mediating synaptic transmission in bipolar cells	Mutations in TRPM1 are associated with congenital stationary night blindness, Metastasis and poor prognosis in melanoma
TRPM2	Brain	Oxidant stress sensor, mediates H ₂ O ₂ dependent cell death	Guamanian amyotrophic lateral sclerosis/parkinsonism dementia complex
TRPM7	Broad	Synaptic vesicle function, Anoxia-induced cell death	Guamanian amyotrophic lateral sclerosis/parkinsonism dementia complex
TRPML1	Broad	Role in sorting/transport in late endocytic pathway; regulates lysosomal lipid and cholesterol trafficking; endolysosomal pH regulation and cation/heavy metal (iron) homeostasis	Mucopolipidosis type IV (MLIV) is associated with mutations in TRPML1; symptoms include severe psychomotor retardation and retinal degeneration
TRPML2	Thymus, spleen, kidney, trachea, liver, lung, colon, testis, thyroid, inner ear, lymphocyte B cells	Endolysosomal pH regulation and cation homeostasis; vesicle fusion and transport	N.D.
TRPML3	Hair cells of the inner ear, organ of corti, utricle, stria vascularis, (skin) melanocytes,	Overexpression increases endosomal pH; endosomal pH regulation and cation	Deafness, circling behavior, head bobbing, and coat color dilution is associated with

	kidney, lung, liver, olfactory bulb, nasal cavity, thymus, colon, trachea, brain	homeostasis; vesicle fusion and transport	mutations in MmTRPML3 (Varitint-waddler mutations Va and Va ^l)
TRPV1	Central and peripheral nervous system and less in other tissues	Thermosensation and nociception	N.D.
TRPV2	Central nervous system, spleen and lung	Thermosensation and nociception	N.D.
TRPV5	intestine, kidney, placenta	Ca ²⁺ reabsorption	Osteoporosis, hypercalciuria
TRPV6	kidney, intestine	Ca ²⁺ reabsorption	Alopecia, dermatitis, decreased intestinal Ca ²⁺ reabsorption
TRPC3	Heart tissue	BDNF-induced chemoattractive turning	Cerebellar ataxia (moonwalker mouse)
TRPC5	cerebral vascular tissue	Regulation of growth cone extension	Susceptibility to pyloric stenosis
TPC1	Broad	NAADP receptor complex?; vesicle fusion and transport?; endolysosomal pH and Ca ²⁺ regulation?	N.D.
TPC2	Broad	NAADP receptor complex?; vesicle fusion and transport?; endolysosomal pH and Ca ²⁺ regulation?	Polymorphisms in human TPC2 are associated with blond versus brown hair
CIC3	Broad	Acidification of synaptic vesicles, endosomes	
CIC4	Broad	N.D.	
CIC5	Kidney, intestine	Acidification of endosomes	Dent's disease (proteinuria, kidney stones)
CIC6	Nervous system	Acidification of late endosomes	
CIC7	Broad	Acidification of osteoclast resorption lacuna	Osteopetrosis, retinal degeneration, lysosomal storage
P2X4	Broad	Membrane trafficking?	

Table 1: Ion channels on the endolysosomal system. Tissue expression, function and associate human diseases are summarized from recent studies (Clapham et al., 2010; Jentsch et al., 2005; Schieder et al., 2010b; Grimm et al., 2012; Grimm et al., 2014; Novarino et al., 2010; Huang et al., 2014). Many of these ion channels are also present widely or mainly in other organelles and/or in the plasma membrane. TRP, transient receptor potential channel; CIC, chloride channel; N.D., not determined.

The transient receptor potential ion channels are cation permeable and belong to the voltage-gated-like ion channel superfamily (Li et al., 2011). The TRP family comprises 29 cation channel genes (**Fig. 2**), which are expressed in many tissues and different cell types (Nilius et al., 2007; Nilius 2007). The general topology of TRP channels comprises cytoplasmic amino acid and carboxyl termini of variable length and six transmembrane domains (TM1-TM6) with the pore-forming loop between TM5 and TM6. Tetrameric assembly of either homomeric or heteromeric TRP polypeptides forms TRP channels (Schaefer 2005) (**Fig. 3**). The TRP family contains seven subfamilies that are classified according to sequence and topological homology (**Fig. 2**) (Ramsey et al., 2006; Venkatachalam and Montell 2007; Owsianik et al., 2006; Grimm et al., 2012). TRPV (vanilloid), TRPM (melastatin) and TRPC (canonical) share substantial sequence identity in TMs and several other common sequence elements and domains, contain a TRP box, and a highly conserved structure of the C-terminus near TM6 (Owsianik et al., 2006; Venkatachalam and Montell 2007). TRPV and TRPC possess multiple N-terminal ankyrin repeats in common, which have been hypothesized to mediate specific protein-protein interactions (Eder et al., 2007), to link to the cytoskeleton, or to allow multimerization of channel complexes (Erler et al., 2004). The transient receptor potential channel mucolipin 1 (TRPML1) and two-pore channel 2 (TPC2) are more distantly related members of the TRP family (**Fig. 2**). These two lysosomal cation channels are the main focus of this thesis and will be discussed in more detail in the next section.

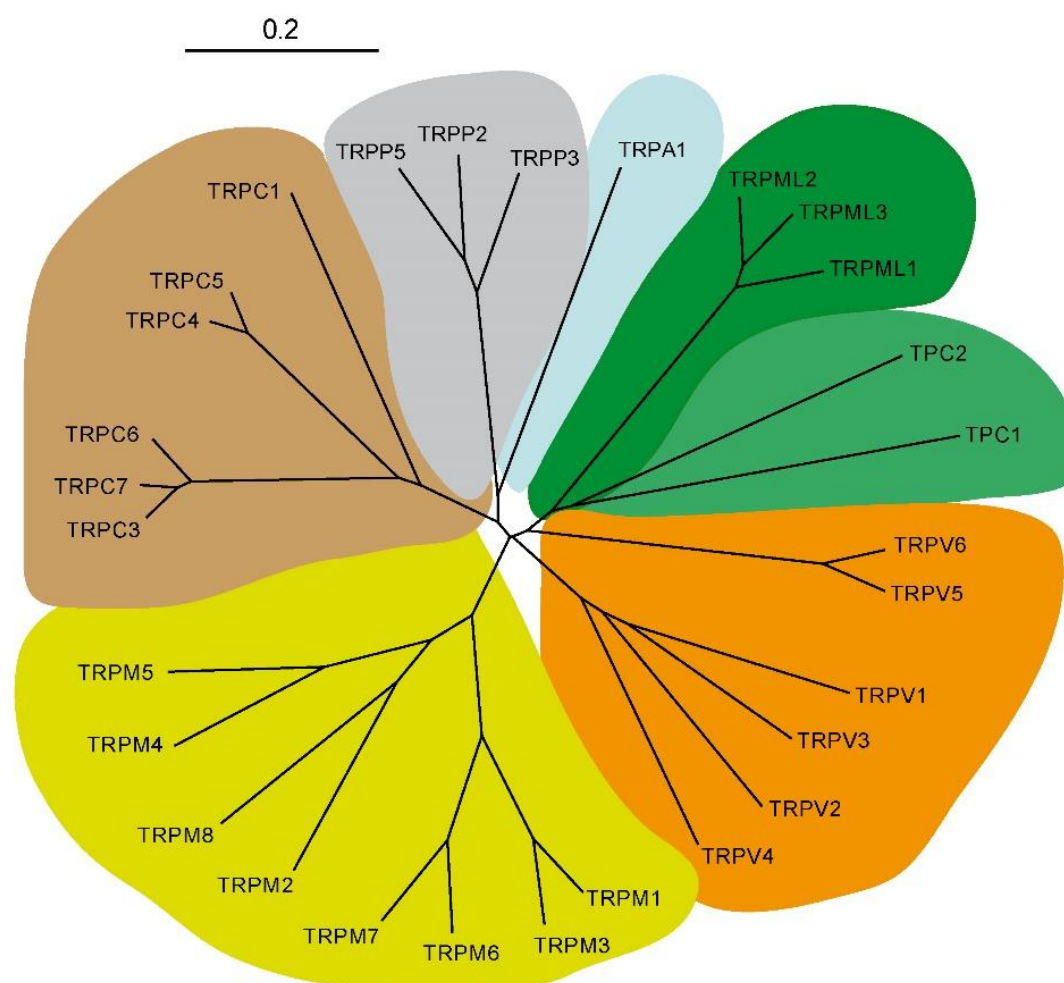


Figure 2: Representation of the amino acid relationships of the minimal pore regions of TRP ion channel superfamily in human. The alignment of pore domains was generated using DNMAN software (Lynnon Corporation, Pointe-Claire, Quebec, Canada). The unrooted tree was generated using NJplot software (<http://pbil.univ-lyon1.fr/software/njplot.html>). The scale bar indicates the degree of genetic divergence in arbitrary units. TRPC2 is a pseudogene in human. TPC3 is absent in human.

Two-pore channels (TPCs) were first cloned from rat kidney and predicted to be involved in Ca^{2+} signaling (Ishibashi et al., 2000). TPCs are expressed in endosomes and lysosomes (Calcraft et al., 2009; Brailoiu et al., 2009; Zong et al., 2009) as well as plant vacuoles (Peiter et al., 2005). TPCs contain two repeats of a 6 transmembrane pore-forming domain (**Fig.3**) (Morgan et al., 2014; Zhu et al., 2010) and are closely related to the voltage-gated cation channels (VGCCs) and TRP channels (Galione et al., 2009). TPCs assemble as dimers through interactions between transmembrane domains (Churamani et al., 2012; Rietdorf et al., 2011). Pore loop I and II contain glycosylated residues to provide protection from the harsh luminal acidic environment (Ruas et al., 2010; Hooper et al., 2011; Lin-Moshier et al., 2012). There are three isoforms of TPCs. While TPC1 and TPC2 are universal isoforms, TPC3 is absent from the genomes of several species including human, mice, rat, and flies (Zhu et al., 2010; Cai et al., 2010). TPC2 is predominately found in late-endosomes and

lysosomes. TPC1 tends to distribute to less acidic early-endosomal sections (Morgan et al., 2011; Zhu et al., 2010; Morgan et al., 2014). Human TPC2 polymorphisms have been postulated to play a role in hair pigmentation, which implies a potential role of TPC channels in melanosomes which are lysosome-related organelles in melanocytes (LROs) (Sulem et al., 2008).

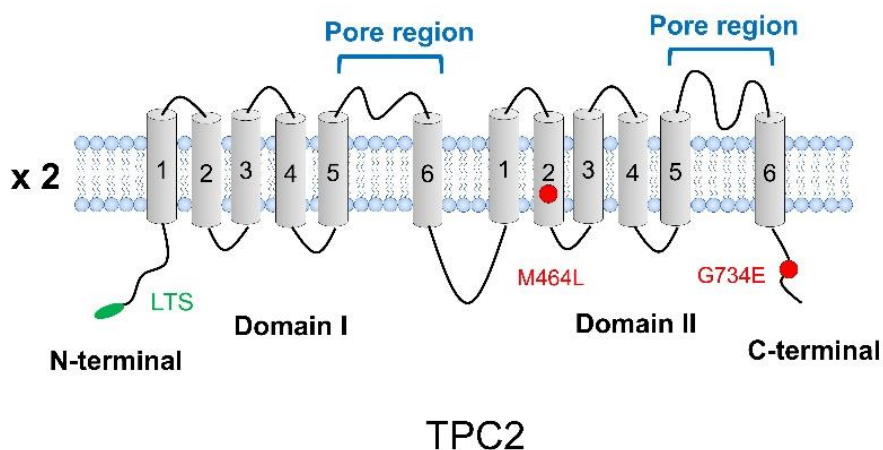


Figure 3: Topology of TPC2 channels. The predicted lysosomal targeting sequence (LTS) motifs are marked by green color. N, C – terminal regions are located in cytoplasm. TPC2 contains the estimated positions of two polymorphisms in human TPC2 associated with blond versus brown phenotype.

The cytosolic second messengers that cause Ca^{2+} release from intracellular Ca^{2+} storage organelles, include inositol 1,4,5-trisphosphate (IP_3), cyclic ADP-ribose (cADPR), and nicotinic acid adenine dinucleotide phosphate (NAADP) (Berridge et al., 2002; Lee 2012, Morgan et al., 2011; Patel et al., 2011; Zhu et al., 2010). Due to the localization of TPCs and their homology with VGCC, TPCs were prime candidates for the NAADP-regulated channels (Berridge et al., 2002; Genazzani et al., 1997; Mandi et al., 2006; Zhang et al., 2009; Zhang et al., 2007; Morgan et al., 2014).

Recently, numerous studies suggested that manipulation of TPC2 expression affects NAADP-induced Ca^{2+} release from lysosomal stores (Brailoiu et al., 2009; Brailoiu et al., 2010a; Calcraft et al., 2009; Davis et al., 2012; Dionisio et al 2011; Ogunbayo et al., 2011; Pereira et al., 2011; Ruas et al., 2010; Tugba Durlu-Kandilci et al., 2010; Yamaguchi et al, 2011; Zong et al., 2009). Several additional pieces of associated evidence strongly support TPC2 as NAADP receptor: high affinity NAADP binding proteins complex with TPC2 (Calcraft et al., 2009; Ruas et al., 2010; Walseth et al., 2012), sensitivity to the NAADP antagonist Ned-19 (Brailoiu et al., 2010b; Pitt et al., 2010), and a bell-shaped NAADP concentration-response curve (Calcraft et al., 2009; Pitt et al., 2010; Zong et al., 2009). TPC2 was described as NAADP-mediated Ca^{2+} -permeable channel by different groups and several indirect

electrophysiological approaches: embedded TPC2 protein into artificial bilayer (Pitt et al., 2010; Rybalchenko et al., 2012) and TPC2 re-targeted to the plasma membrane (Brailoiu et al., 2010b).

Importantly, recent studies reported that TPC2 can also be activated by an endolysosome-specific phosphoinositide PI(3,5)P₂ (Wang et al., 2012 and Cang et al., 2013). Cytoplasmic membrane lipids are reported to be central regulators of membrane trafficking and important cellular responses (Di Paolo et al., 2006). The function of lysosomes may be controlled by the lipid composition of the lysosome (Ktistakis et al., 2013; Sridhar et al., 2013). Many of the functions of lysosomes are thought to be dependent on PI(3,5)P₂ (phosphatidylinositol (PI)-3,5-bis phosphate), and the conversion of PI-3 phosphate (PI3P) to PI(3,5)P₂ (Michell et al., 2006; Ho et al., 2012). PI(3,5)P₂ is a low abundance PIP variant present in non-stimulated cells under basal conditions (Dove et al., 2009; Ikonomov et al., 2011) reaching levels of less than 10% of those of PI(3)P in cells (Zhang et al., 2007). PI(3,5)P₂ is generated from PI(3)P via PIKfyve/Fab1 which is a PI 5-kinase that mainly localizes to late endosomes and lysosomes (Poccia et al., 2009; Dove et al., 2009; Ikonomov et al., 2011; Duex et al., 2006a; Duex et al., 2006b; Botelho et al., 2008). Hence, PI(3,5)P₂ is hypothesized to predominantly localize to the endolysosomal system (Dove et al., 2009; Zhang et al., 2007; Chow et al., 2007; Bonangelino et al., 2002). Recent studies showed human mutations in PI(3,5)P₂-metabolizing enzymes and regulators cause muscle and neurodegenerative diseases such as Charcot-Marie-Tooth and amyotrophic lateral sclerosis (Chow et al., 2007), PI(3,5)P₂-deficient cells cause intracellular endolysosome/vacuole enlargement and defective membrane trafficking (Chow et al., 2007; Dove et al., 2009; Kerr et al., 2010; Shen et al., 2011). However, the controversies of ligand-gating and ion permeability of TPC2 that need to be further investigated.

TRPML channels are the other cation channels that can be activated by PI(3,5)P₂ in the endolysosomal system (Dong et al. 2010). Cloning of mucolipins (MCOLN1-3, TRPML1-3) has started with the identification of MCOLN1 on human chromosome 1 (Bargal et al., 2000). Mucolipins were later named TRPML channels because of structural and sequence similarities with TRP cation channels. TRPML1 contains two di-leucine sorting motifs which are responsible for the transport of the protein to membranes of late endosomes and lysosomes (Vergarajauregui et al., 2006; Miedel et al., 2006; Pryor et al., 2006; Cheng et al., 2010; Puertollano et al., 2009). TRPML2 was discovered through database searches and TRPML3 was identified in mice with the varient-waddler (Va) phenotype (Di Palma et al., 2002). The gain-of-function mutant isoforms Va (A419P) and VaJ (A419P + I362T) cause severe auditory, vestibular, and melanocytes phenotypes. The A419P mutation renders the channel constitutively active leading to large inward fluxes of calcium and sodium (Grimm et al., 2007; Grimm et al., 2010; Kim et al., 2007; Kim et al., 2010; Xu et al., 2007; Nagata et al., 2008; Dong et al., 2009; Samie et al., 2009; Lev et al., 2010). TRPML3 is expressed in multiple

intracellular compartments including the plasma membrane (Kim et al., 2009). TRPML2 is found in endosomes and lysosomes (Venkatachalam et al., 2006; Grimm et al., 2010) and TRPML1 is expressed predominantly in lysosomes (Treusch et al., 2004; Pryor et al., 2006; Venkatachalam et al., 2006; Nilius et al., 2007; Zeevi et al., 2009). Initially, channel function of TRPML1 was assessed by indirect electrophysiological approaches using the varitint-waddler equivalent mutant isoform of TRPML1 (V432P) or isoforms with deleted lysosomal targeting sequence (LTS) motifs, resulting in TRPML1 translocation to the plasma membrane. TRPML1 was characterized by these indirect electrophysiological approaches as an inwardly rectifying non-selective cation channel that can be potentiated by low pH (LaPlante et al., 2002; Raychowdhury et al., 2004; Cantiello et al., 2005; Kiselyov et al., 2005; Xu et al., 2007; Dong et al., 2008; Grimm et al., 2010)

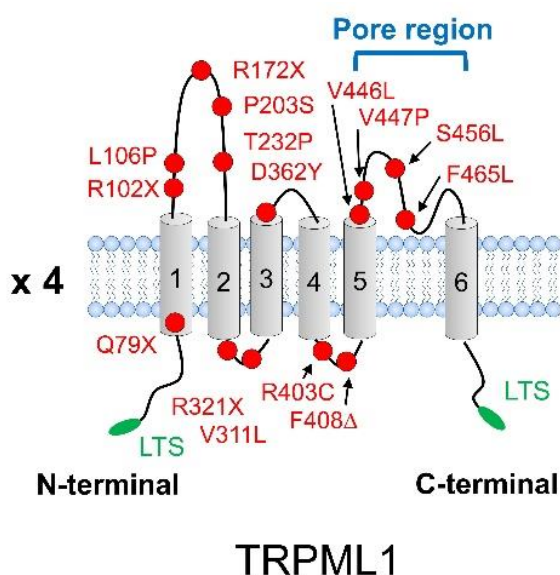


Figure 4: Topology of TRPML1 channels. Cartoon of the human TRPML1 point mutations in exon regions. X stands for termination codon.

Naturally occurring mutations in the human TRPML1 gene cause mucopolipidosis type IV (MLIV) which is an autosomal recessive lysosomal storage disorder (LSD) characterized by severe psychomotor retardation and ophthalmologic abnormalities including corneal opacity, retinal degeneration and strabismus. Most patients are unable to walk or speak independently. Patients also frequently have constitutive achlorhydria associated with a secondary elevation of serum gastrin levels (Bassi et al., 2000; Sun et al., 2000). Storage bodies of lipids and water-soluble substances are observed by electron microscopy in almost every cell type of the patients (Bargal et al., 2000; Soyombo et al., 2005; Vergarajauregui et al., 2008). More than 15 different MLIV-causing mutations have been identified throughout the TRPML1 gene. Unfortunately, many patients carry mutations that result in

a stop codon or frame shift of the ORF (open reading frame). As a result, the TRPML1 protein is completely absent, or abnormally short and lacks the ion conducting pore between TMD5 and TMD6. However, some patients carry single point mutations which do not destroy the open reading frame, i.e. L106P, T232P, D362Y, R403C, F408Δ, Y436C, V446L, V447P, S456L, or F465L (**Fig. 4**) (AlBakheet et al., 2013; Altarescu et al., 2002; Goldin et al., 2004; Manzoni et al., 2004; Sun et al., 2000; Tüysüz et al., 2009).

To analyze the function of lysosomal ion channels such as TPC2 and TRPML1, novel electrophysiological methods have to be established. The patch-clamp technique is a useful and versatile method for studying electrophysiological properties of ion channels. The method was developed by Erwin Neher and Bert Sakmann in 1976. With the ability to form gigaseals and the establishment of the various recording configurations, recordings of currents passing through single channels from cell surface or cell-free membranes as well as limited intracellular patching became possible. Since the early 1980s, the patch-clamp techniques has become the gold standard for the functional characterization of ion channels and it is well established in the fields of biophysics and pharmacological drug development (Neher et al., 1976; Neher 1992; Sakmann 1992).

In conventional patch-clamping, a glass micropipette with a few micrometres in diameter at the tip is used as an electrode which is placed on the surface of the plasma membrane of an intact cell. Then, by application of air suction an omega shaped piece of plasma membrane is generated and subsequently drawn into the glass pipette (Milton et al., 1990). Eventually, a “gigaseal” (from seal resistance $> 10^9 \Omega$) is established between the cell membrane and the glass pipette, which is required to avoid leakage current and allow for high-resolution measurements. This cell-attached configuration is the original formation preceding all other variants of the patch-clamp technique.

However, the conventional patch-clamp technology is limited by two major disadvantages for the investigation of intracellular ligand gated ion channels. First, it is difficult to isolate intact organelles from a cell. Second, because of the small size of the vacuoles it is not readily applicable to measure ion channels localized in the membrane of intracellular organelles such as lysosomes, endosomes, mitochondria, golgi apparatus, and cisternae of the endoplasmic reticulum (ER). Therefore, two indirect approaches were applied to resolve the biophysical properties of ion channels of intracellular membrane systems: 1. Redirect lysosomal channels to the plasma membrane. 2. Reconstitute lysosomal channels into artificial membranes.

Sorting of transmembrane proteins and ion channels to endosomes and lysosomes is mediated by signals present within the cytosolic domains of the proteins. Two major classes of lysosomal sorting signals exist which are referred to as “tyrosine-based” (NPXY or YXXØ) and “dileucine-based”

([DE]XXXL[LI] or DXXLL) consensus motifs (Trowbridge et al., 1993; Sandoval et al., 1994; Bonifacino et al., 1999; Bonifacino et al. 2003). X stands for any amino acid and Ø stands for an amino acid residue with a bulky hydrophobic side chain.

The N terminus of mammalian TPC2 includes a conserved dileucine-based motif conforming to the consensus sequence [DE]XXXL[L/I] which targets transmembrane proteins to lysosomes (Bonifacino et al., 2003; Brailoiu et al., 2010). Its deletion translocates TPC2 to the plasma membrane, where it is accessible to conventional patch-clamp analysis (Brailoiu et al., 2010; Yamaguchi et al., 2011). TRPML1 can also be translocated to the plasma membrane by removal of both TRPML1-specific dileucine motifs (Miedel et al., 2006; Venkatachalam et al., 2006; Vergarajauregui and Puertollano 2006; Grimm et al., 2010).

Another experimental strategy is the measurement of the electrophysiological function of lysosomal channels reconstituted into artificial membranes. The formation of lipid bilayers by the spreading of phospholipid dispersions was introduced in the 1960-1970s by Mueller and Montal (Montal et al., 1972). Further applications of this lipid bilayer recordings were established by many research groups in the following years (Sitsapesan et al., 1991; Favre et al., 1999). Alternatively, purified channel proteins or membrane vesicles can be reconstituted into liposomes and can be analyzed by means of conventional patch-clamp (Tank et al., 1982). For example, Pitt et al. purified the human recombinant TPC2 complex for subsequent reconstitution into artificial lipid bilayers under voltage-clamp conditions, and suggested high nanomolar concentrations of NAADP to open TPC2 resulting in Ca^{2+} release depending on luminal pH (Pitt et al., 2010). The single channel recordings of reconstituted purified TRPML1 in lipid bilayers suggested TRPML1 to be a non-selective cation channel (LaPlante et al., 2002; Raychowdhury et al., 2004; LaPlante et al., 2004).

The main drawback of these indirect electrophysiological methods is that ion channel proteins are extracted from their physiological environment. Many important factors, such as essential components of the lysosomal membrane as well as specific modulators and accessory subunits, which are associated in vivo with the ion channel protein are lost in these indirect electrophysiological measurements. By contrast, factors in the plasma membrane can potentially interfere with the activity of the translocated lysosomal ion channel. Furthermore, the procedure of purification of proteins can possibly affect the ion channel or form additional conductances which lead to incorrect interpretations of current recordings from bilayers. In order to prevent these problems, two direct whole-lysosome patch-clamp methods were developed recently: modified whole-lysosome patch-clamp (Dong et al., 2008; Dong et al., 2010; Wang et al., 2012; Cang et al., 2013) and whole-lysosome planar patch-clamp (Schieder et al., 2010a,b). These two novel

electrophysiological approaches can maintain the integrity of intact lysosomes and allow to characterize ion channels directly in lysosomal membranes in unprecedented detail.

1.1 The aims of this thesis

Previous work indicated that TPC2 and TRPML1 channels are expressed in the membrane of lysosomes and play important physiological roles in the endolysosomal pathway. So far, indirect electrophysiological approaches are not the ideal tool for a reliable characterization of intracellular ion channels. By building on the properties of lysosomal cation channels as discussed in the introductory chapter and the application of novel whole-lysosome patch-clamp techniques, this thesis aims to address the following subjects:

Comparison between the whole-lysosome patch-clamp and the whole-lysosome planar patch-clamp.

As direct whole-lysosome patch-clamp methods were initially postulated as the most efficient electrophysiological techniques to study lysosomal ion channels, this thesis begins by discussing the protocols and advantages of the modified whole-lysosome patch-clamp and whole-lysosome planar patch-clamp techniques.

Analysis of the channel properties of TPC2 and TRPML1 in lysosomes

This question will be answered by the isolation of intact lysosomes for planar patch-clamp studies. By direct recording of ion channels on lysosomes from stable HEK cells, native mouse embryonic fibroblasts and human fibroblasts, the characteristics of TPC2 and TRPML1 channels are discussed. Agonists and antagonists of TPC2 and TRPML1 are investigated and discussed.

Characterization and functional analysis of small molecule activators of native and mutant TRPML1.

Loss of function or dysfunction of TRPML1 is resulting in MLIV, which implies that MLIV mutant isoforms are pathophysiologically relevant proteins that have the potential to be targeted by novel therapeutics. To investigate the potential of small molecule ligands to rescue TRPML1 mutant channel activity, the direct whole-lysosome planar patch-clamp technique is employed.

Overall, this thesis attempts to achieve a deeper understanding of the electrophysiological properties of TPC2 and TRPML1 channels by applying whole-lysosome patch-clamp techniques, and to make full use of this method to test small molecule TRPML1 activators for their potential to restore mutant

channel function.

2. Material and Methods

2.1 Material

2.1.1 Chemicals and consumables

All chemicals used were obtained by Sigma-Aldrich if not mentioned extraordinarily. The quality was “ACS grade” or “for molecular biological use”. For all solutions high pure and deionized water was used (Millipore, Milli-Q Academic Ultra Pure Water Purification System). In experiments in which a high purity was required all solutions were autoclaved.

5-ml microfuge test tube

175-cm² dishes for cell culture (Sarstedt, #831803)

2-, 10-, 200- and 1000- μ l pipettes

25-cm cell scrapers (BDFalcon, #353086)

Agar (Applicam, #A0949)

Adenosine 5'-triphosphate (ATP) magnesium salt

Bleach solution (Nanion) Sodium hypochlorite solution (NaClO), 12% Cl

Borate - Sodium tetraborate anhydrous

Boric acid

Borosilicate glass with Filament, fire polished (BF150-75-10, Sutter)

CaCl₂·2H₂O

CaMSA

Cell culture flasks (75 cm²; Greiner Bio one, #658175)

Complete protease inhibitor cocktail, EDTA-free (Roche, #04693132)

DMSO

Dulbecco's modified Eagle medium containing 25 mM glucose (DMEM supplemented with 4.5 g/l glucose and pyruvate and Glutamax;

Invitrogen, #31966-021).

EGTA

Fetal bovine serum (FBS; Biochrom, #S0615)

HCl

Human embryonic kidney (HEK) 293 cells stably overexpressing ion channels under investigation

HEPES

Hygromycin B, 50 mg/ml solution (Carl Roth, #CP12.2)

K-gluconate

KCl

KF

KH₂PO₄

KMSA

KOH

Mannitol

Methanesulfonic acid

MgCl₂

Micropipettors

Microscope cover glasses 12mm (Glaswarenfabrik Karl Hecht GmbH)

Na₂HPO₄-2H₂O

NaCl

NaMSA

NPC-1 chips (single use, disposable) microstructured glass chip containing an aperture of $\sim 1 \mu\text{m}$ diameter (Nanion)

Pen-strep (penicillin 10,000 units/ml; streptomycin 10,000 $\mu\text{g/ml}$; Biochrom)

Poly-L-Lysine hydrobromide

Series 20 Chamber platform Model Ph1 (Warner)

Sterile syringe filters $0.2 \mu\text{m}$ (VWR, #5140061)

Sterile syringes (VWR, #612-0120)

Sucrose (Sigma, #84100)

Tris(hydroxymethyl)aminomethane (Tris, Prolabo, #103156x)

Vacuolin-1

2.1.2 Compounds and chemical syntheses

MK6-83 5-methyl-N-[2-(piperidin-1-yl)phenyl]thiophene-2-sulfonamide

NAADP Nicotinic acid adenine dinucleotide phosphate tetrasodium salt (TOCRIS)

NED-19 (1*R*,3*S*)-1-[3-[[4-(2-Fluorophenyl)piperazin-1-yl]-4-methoxyphenyl]-2,3,4,9-tetrahydro-1*H*-pyrido[3,4-*b*]indole-3-carboxylic acid (TOCRIS)

PI(3,5)P2-diC8 L- α -D-myo-Phosphatidylinositol 3,5-bisphosphate (A.G.Scientific)

PI(4,5)P2-diC8 L- α -D-myo-Phosphatidylinositol 4,5-bisphosphate (A.G.Scientific)

SF-21 4-chloro-N-(2-morpholin-4-ylcyclohexyl)benzenesulfonamide (MolPort)

SF-22 5-chloro-N-(2-piperidin-1-ylphenyl)thiophene-2-sulfonamide (MolPort)

SF-23 5-chloro-N-(2-morpholin-4-ylphenyl)thiophene-2-sulfonamide (MolPort)

SF-24 4-methyl-N-(2-phenylphenyl)benzenesulfonamide (MolPort)

All substances were dissolved according to manufacturers' instructions. Stock solutions of 10 mM in DMSO were prepared for NED-19, SF-21, SF-22, SF-23, SF-24 and MK6-83. Stock solutions of 100 μM in water were prepared for NAADP, PI(3,5)P2 and PI(4,5)P2. All stock solutions are stored aliquot in tightly sealed vials at $-20 \text{ }^\circ\text{C}$.

2.2 Methods

2.2.1 cDNA constructs and transfection.

Unless otherwise stated, all of the channel clones were GFP or YFP tagged for the identification of channel-protein-expressing endolysosomes used for lysosome preparation and whole-lysosome recordings. Human isoform of TPC2 was cloned into the HindIII/EcoRI sites of peGFP-C3 vector in modified whole-lysosome patch-clamp experiments as described before (Cang et al., 2013). Human wild-type TRPML1 was subcloned into pcDNA3 expression vector (Invitrogen Life Technologies, Breda, The Netherlands) as described before (Grimm et al., 2010). Murine wild-type TPC2 was subcloned into pcDNA5FRT expression vector (Invitrogen) as described before (Schieder et al., 2010a). Mutations in the putative selectivity filter of murine TPC2 N256A were introduced using the QuikChange site-directed mutagenesis kit (Stratagene, LA Jolla, CA).

2.2.2 Cell culture

HEK293 cells (Human Embryonic Kidney) were maintained in DMEM supplemented with 10% FBS, 100 U penicillin/mL, and 100 µg streptomycin/mL and kept at 37°C in a humidified atmosphere of 10% CO₂ in air. MEFs (Mouse embryonic fibroblasts) and human skin fibroblasts were maintained in 5% CO₂. Cells were transiently transfected with Fugene (Roche) or GeneExpresso Max Transfection Reagent (Excellgen) according to the manufacturer's protocols and used for LSM experiments 24-48 hours after transfection. For planar patch-clamp electrophysiology, two or three days before performing the experiments, plate HEK293 cells or fibroblasts per dish in two 175-cm² tissue-culture dishes with 25 ml of DMEM culture medium for each dish. Grow the cells homogeneously to 90 – 95 % confluence on the day of the experiment. For modified patch-clamp electrophysiology, one or two days before performing the experiments, plate HEK293 cells per well with 0.1 % poly-L-lysine coating microscope cover glasses (12 mm) in 24 wells plates with 1 ml of DMEM culture medium for each well. Every microscope cover glasses were autoclaved and soaked into 0.1 % Poly-L-lysine Boric buffer for 24 hours. Before plating cells, the glasses were rinsed with distilled water and stored in distilled water at room temperature. After reaching confluence, cells were partly digested with 0.05% trypsin (Invitrogen) to give a cell suspension, diluted in desired medium and propagated in new flasks or culture dishes for electrophysiology experiments.

Cell Culture Medium

Fetal bovine serum	10 %
Pen-Strep	100 U/ml
DMEM	500 ml

Mix components and filter-sterilize. Store at 4°C; pre-warm to 37°C before use.

Poly-L-Lysine Coating Solution

Poly-L-lysine	0.1 %
Boric acid	80 mM
Borate	10 mM

Sterilize by passing through a 0.2 µm filter and store at 4°C

For long-term cell storage, stocks of each cell line were maintained in a liquid nitrogen cell bank at -195°C. Cells were prepared for storage as a single-cell suspension in a freezing medium of FBS with 10% DMSO which was cooled slowly to -80°C in a Styrofoam cooling box, 24 hours before transfer to the cell bank.

Freezing medium

Fetal bovine serum	10ml
DMSO	10ml
DMEM	80ml

Pre-cooled before use. Store at 4°C for two weeks.

2.2.3 Generation of stable HEK293 cell lines

Stable HEK293 cell lines for enhanced GFP-tagged murine wild type TPC2 and mutant TPC2 were generated using the Flp-In™ system (Invitrogen) according to manufacturer's protocol. Hygromycin B (Sigma-Aldrich) was used for selection of stable cell lines. Stable HEK293 cell lines for enhanced YFP-tagged human wild type TRPML1, TRPML2, TRPML3 and mutant TRPML1 were generated using pcDNA3 vectors (Invitrogen) which contain the neomycin resistance gene for selection of stable cell lines using 600 µg/ml G418 (Sigma-Aldrich).

Selective Culture Medium

Fetal bovine serum	10 %
Pen-Strep	100 U/ml
Hygromycin B	100 µg/ml (pcDNA5FRT/TPC2)
G418	600 µg/ml (pcDNA3/TRPML)
DMEM	500 ml

Mix components and filter-sterilize. Store at 4°C; pre-warm to 37°C before use.

Transfected host cell line with pcDNA5/FRT (TPC2) or pcDNA3 (TRPML) construct using the desired protocol. 48 hours after transfection, split the cells in 10 cm dish using fresh medium containing selective antibiotic at pre-determined concentration required for cell line. Feed the cells with selective culture medium every 3-4 days until selective antibiotic-resistant foci can be identified. Pick and expand colonies in 6-well plates.

2.2.4 Generation and Isolation of MEFs from TPC2^{-/-} knockout mice

All generations and isolations of MEFs were performed by Sami Hassan as described previously (Grimm et al., 2014, Jat et al., 1986). TPC2^{-/-} mice were generated by deleting exon 7 and introducing an early stop codon. We generated a targeting vector that, after homologous recombination, resulted in a modified TPC2 allele carrying two *loxP* sites flanking exon 7. A neo^R cassette, which was used for G418/geneticin selection, was removed with Flp recombinase before the ES cells were injected into host blastocysts to generate chimeric mice. After germline transmission and continued breeding, PCR with genomic DNA from progeny of WT, heterozygous and homozygous animals showed proper recombination and inheritance of the TPC2^{lox} allele. Subsequently, exon 7 was deleted by pairing TPC2^{lox} mice with mice expressing Cre-recombinase under a CMV promoter. Exon7 encodes TMD5 and part of the pore-loop in domain I of TPC2 from TPC2^{-/-} and WT mice.

2.2.5 Patient cell lines

Human skin fibroblast cells from a ML IV patient (TRPML1^{-/-}, clone GM02048) and a WT control (TRPML1^{+/+}, clone GM03440) were obtained from the Coriell Institute for Medical Research (NJ, USA). Other human fibroblast cell lines were contributed by Dr. Schiffmann (Institute of Metabolic Disease, Baylor Research Institute, Dallas, TX, USA).

2.2.6 Calcium imaging

All experiments obtained from Calcium imaging in this study were performed by Dr. Dr. Christian Grimm as described previously (Grimm et al., 2008; Grimm et al., 2010). Calcium imaging experiments were performed using fura-2 as described previously. Briefly, HEK293 cells were plated onto glass coverslips, grown over night and transiently transfected with the respected cDNAs using TurboFect transfection reagent (Thermo Scientific). After 24-48 h cells were loaded for 1 h with the fluorescent indicator fura2-AM (4 μ M; Invitrogen) in a standard bath solution (SBS) containing (in mM) 138 NaCl, 6 KCl, 2 MgCl₂, 2 CaCl₂, 10 HEPES, and 5.5 D-glucose (adjusted to pH 7.4 with NaOH). Cells were washed in SBS for 30 min before measurement. Calcium imaging was performed using a monochromator-based imaging system (Polychrome IV monochromator, TILL Photonics).

2.3 Modified whole-lysosome patch-clamp electrophysiology

Modified whole-lysosome patch-clamp electrophysiology was performed in isolated lysosomes using an established patch-clamp method (Dong et al., 2010a; Wang et al., 2012; Cang et al., 2013). HEK293 cells stably expressing the tetracycline-inducible wild type human TPC2 GFP-tagged gene were treated with tetracycline overnight prior to the experiments. Cells were treated with 1 μ M Vacuolin-1, a lipid-soluble polycyclic triazine that can selectively increase the size of lysosomes up to 5 μ m (Huynh and Andrews, 2005), for overnight. Large vacuoles were observed in most vacuolin-treated cells. No significant difference in TPC channel properties were seen for enlarged vacuoles obtained with or without vacuolin-1 treatment (Dong et al., 2010a; Wang et al., 2012).

Enlarged lysosomes of sizes from 3-10 μ m were visually identified and dissected manually with a glass electrode. Under the phase contrast microscope, enlarged lysosomes were viewed as phase-bright (see Fig5A, red circled). To prevent the cells from detaching from the cover glass, must plate the cells on poly-L-lysine coating cover glass as described above.

2.3.1 Cut and isolated lysosome

Selected the target lysosome which was enlarged and nearby the edge of cell plasma membrane. The size of target lysosome should be smaller than half of cell to prevent detaching from cover glass during cutting and isolating. To facilitate slicing of the plasma membrane with a glass pipette, cells with enlarged lysosomes, closer to the edge of cells, were used because cell thickness increased toward the center. The first glass pipette with slight negative pressure was approached against the cell membrane at a position close to the lysosome to be patched and then rapidly cut or rip the edge of plasma membrane. Lysosomes were pushed out through the cut position with the same pipette

tip. Multiple attempts were required to free the enlarged lysosomes from the cell. Isolation was successful for 10%-20% of attempts in HEK293 cells. Compare with cell plasma membrane, the surface of isolated enlarged lysosomes looked thinner and bright. The bulk of isolated enlarged lysosomes are similar with soap-suds, weak and almost transparent. Occasionally, surrounding structures such as sections of plasma membrane and actin filaments were still connected with isolated enlarged lysosomes and lead to fail sealing. However, connection with a small number of actin filaments were necessary to fix isolated enlarged lysosomes for stabilized patching to avoid floating away from the field of vision.

2.3.2 Lysosome attach and giga seal formation

The fresh fine polished borosilicate glass pipette were used for patch-clamp. The patch pipette resistance was 3 – 6 megOhms. Give positive pressure 0.02 - 0.03ml (1ml syringe for pressure control) and hold this pressure (lock valve) before approach the surface of bath solution. Use 0.05ml positive pressure which is easy for sealing but bad for break-in lysosome. To avoid dust surround pipette, positive pressure is essential. Rapid move pipette against the top of target lysosome (<10 sec) and then release the positive pressure. Giga seal (> 1 Gohm) formed in few seconds.

2.4 Whole-lysosome voltage-clamp recording

In cells transfected with GFP-tagged TPC2, only the GFP-positive lysosomes were selected for recording. Only one lysosome was recorded from each coverslip. Patch recordings were performed with a Multiclamp 700B amplifier (Molecular Device) and a Digidata 1440A data acquisition system (Molecular Device). Whole-lysosome currents were digitized at 10 kHz and filtered at 2 kHz. All experiments were conducted at room temperature (21-23°C). PClamp, Clampfit (Molecular Device) and Origin 6.0 (OriginLab) software were used to record and analyze data. Fast and slow capacitive transients were cancelled by the compensation circuit of the EPC-10. Membrane potentials were corrected for liquid junction potential which was calculated by pClamp.

Stock Solution Vacuolin-1 1mM

Dissolve 1 mg of vacuolin-1 in 1.732 ml of DMSO; mix complete and store at 4°C.

Cytoplasmic (bath) solution

K-gluconate	140 mM
NaCl	4 mM
MgCl ₂	2 mM
CaCl ₂	0.39 mM
EGTA	1mM
HEPES	10mM

pH adjusted to 7.2 with KOH, sterilized by passing through a 0.2 µm filter.

Luminal (pipette) solution

NaCl	145 mM
KCl	5 mM
MgCl ₂	1 mM
CaCl ₂	2mM
HEPES	10mM
MES	10 mM
Glucose	10 mM

pH adjusted to 4.6 with NaOH, sterilized by passing through a 0.2 µm filter.

2.4.1 Preparation of lysosomes

All steps in this part of the protocol must be performed on ice to minimize the activation of damaging from intracellular phospholipases and proteases. Lysosomes should be used for electrophysiological recordings within 1 to 3 hours of isolation to keep lysosomes fresh. The quality of the lysosomal preparation can be monitored by epifluorescence microscope if HEK293 cells stably expressing a GFP- or YFP-tagged lysosomal ion channels.

Remove the medium from the cells and wash the cells twice with pre-cooled 15 ml PBS.

Remove PBS and add 250 µl pre-cooled Homogenization Buffer.

Detach the cells with a cell scraper.

Transfer cell suspension to the glass-grinding vessel of the potter homogenizer.

Wash the plate once with 250 µl Homogenization Buffer to detach the remaining cells.

Transfer the cells to the same glass-grinding vessel containing the rest of the cells.

Assemble the potter homogenizer and homogenize the cells using a Teflon pestle operated at 900 rotations per minute (rpm). Stroke the cell suspension placed in the glass grinding vessel 12 times. The Teflon–glass coupling represents the best compromise between homogenization of the cells and the preservation of lysosomal integrity. Harsher techniques, including glass pestle in a glass potter, can easily damage lysosomes.

Transfer the homogenate to a 1.5 ml microfuge test tube and centrifuge at 14,000g for 15 min at 4°C. Pre-cooled the centrifuge before use.

Collect the middle part of supernatant and transfer it to a 10-ml polycarbonate centrifuge tube. In order to increase the quality of lysosome preparation, must avoid to collect the plate and surface of supernatant.

Add an equal volume (typically 1.6 ml) of 16 mM CaCl₂ (final concentration 8 mM) to precipitate lysosomes.

Transfer the tube to a rotary shaker and shake at 100 rpm for 5 min at 4°C.

Centrifuge at 25,000g for 15 min at 4°C in an ultracentrifuge.

Discard the supernatant and resuspend the pellet in one volume of ice cold Washing Buffer.

Centrifuge at 25,000g for 15 min at 4°C in an ultracentrifuge.

Discard the supernatant, resuspend pellet containing lysosomes in 20 µl of Washing Buffer, and transfer the suspension to a 1.5-ml microfuge tube.

Add 20 µl of Washing Buffer to the tube that contained the pellet to resuspend, with a 200-µl pipette tip, any remaining pellet. Transfer the suspension to the same microfuge tube from the previous step.

16 mM CaCl₂

Dissolve 0.2352 g of CaCl₂ in 100ml of distilled water; mix complete and store at 4°C.

Complete Protease Inhibitor Cocktail

Dissolve 1 tablet in 2 ml distilled water and vortex to prepare a 25× conc. EDTA-free solution and store at 4°C or prepare aliquots and store at -20°C for 12 weeks storage.

Phosphate-Buffered Saline (PBS)

NaCl	137 mM
Na ₂ HPO ₄ ×2H ₂ O	8 mM
KH ₂ PO ₄	1.76 mM
KCl	2.7 mM

Adjust pH to 7.4 with HCl, prepare 500-ml aliquots, heat sterilize, and store at room temperature up to several months.

Homogenization Buffer

Sucrose	0.25 M
Tris	10 mM

Adjust pH to 7.4 with HCl, sterilize by passing through a 0.2 µm filter, prepare 960 µl aliquots, and store at - 20°C for several months. Before use, add 40 µl of Complete Protease Inhibitor Cocktail (final concentration 1×) per aliquot of homogenization buffer.

Washing Buffer

KCl	150 mM
Tris	10 mM

Adjust pH to 7.4 with HCl, sterilize by passing through a 0.2 µm filter, prepare 3.84 ml aliquots, and store at - 20°C for several months. Before use, add 160 µl of Complete Protease Inhibitor Cocktail (final concentration 1×) per aliquot of Washing Buffer.

2.4.2 Planar patch-clamp electrophysiology

For whole-lysosome planar patch recordings, the Port-a-Patch (Nanion Technologies) was used. lysosomes were enlarged with the treatment of 1µM vacuolin-1 overnight (Schieder et al., 2010a;

Schieder et al., 2010b; Dong et al., 2008; Cang et al., 2013). The planar patch-clamp technology combined with a pressure control system and microstructured glass chips containing an aperture of around 1 μm diameter (resistances of 10-15 M Ω) (Nanion Technologies). Currents were recorded using an EPC-10 patch-clamp amplifier and PatchMaster acquisition software (HEKA). Data were digitized at 40 kHz and filtered at 2.8 kHz. Mean endolysosomal capacitance was 1.01 ± 0.04 pF ($n=47$). For all planar patch-clamp experiments, salt-agar bridges were used to connect the reference Ag/AgCl wire to the bath solution to minimize voltage offsets. Ag/AgCl-coated electrodes need to be regularly chloridated in bleach solution approximately 15 min until a black AgCl-layer is obvious on the silver wire. Generally, electrodes should be replaced every 2 months.

It is essential to form a high-resistance seal (gigaseal) with the membrane of the lysosome or organelle of interest. Gigaseals are formed usually with the aid of seal enhancer external solution (cytoplasmic side) which contains a high concentration of fluoride, whereas the intralysosomal solution contains a high concentration of Ca^{2+} . For tight-seal lysosomal patch-clamp recordings, it is crucial to have solutions containing high Ca^{2+} (> 60 mM) on one side of the glass chip and solution containing high fluoride at the other side during seal formation. Omitting either of the ions from the respective solutions after seal formation can cause loss of seal quality and patch-clamp stability. Inclusion of fluoride improves patch-clamp sealing and stabilizes the cell membrane, resulting in longer, more stable patch-clamp recordings (Kostyuk et al., 1975); the mechanism of this effect is unknown.

The membrane potential was held at -60mV, and 500ms voltage ramps from -200 to +100 mV were applied every 5s. All recordings were obtained at room temperature (21-23°C), and all recordings were analyzed using PatchMaster (HEKA) and Origin 6.1 (OriginLab). To dissect lysosomal currents from whole-lysosome planar patch-clamp recording, all currents in the absence of compounds were subtracted from the currents obtained in the presence of compounds as previously described (Schieder et al., 2010a). Liquid junction potential was corrected. The EC50 of graded dose response curves were fitted with the Hill equation.

External (cytoplasmic) solution (TPC2)

KF	60 mM
K-MSA	70mM
Ca-MSA	0.2 mM
Na-MSA	4 mM
HEPES	10mM

Adjusted pH to 7.2 with KOH, sterilize by passing through a 0.2 μ m filter, prepare 1ml aliquots, and store at -20°C for several months.

Internal (intralysosomal) solution (TPC2)

Na-MSA	85 mM
Ca-MSA	60 mM
MgCl ₂	1mM
HEPES	10 mM

Adjusted pH to 4.6 with MSA, sterilize by passing through a 0.2 μ m filter, prepare 1ml aliquots, and store at -20°C for several months.

External (cytoplasmic) solution (TRPML)

KF	60 mM
K-MSA	70mM
Ca-MSA	0.2 mM
HEPES	10mM

Adjusted pH to 7.2 with KOH, sterilize by passing through a 0.2 μ m filter, prepare 1ml aliquots, and store at -20°C for several months.

Internal (intralysosomal) solution (TRPML)

K-MSA	70 mM
Ca-MSA	60 mM
MgCl ₂	1mM
HEPES	10 mM

Adjusted pH to 4.6 with MSA, sterilize by passing through a 0.2µm filter, prepare 1ml aliquots, and store at -20°C for several months.

2.5 Data Analysis

The reversal (zero-current) potential, E_{rev} , for NAADP-mediated currents in enlarged lysosomes was determined from current amplitude evoked in response to NAADP during voltage clamp ramp protocol (+100 to -200mV, 500 ms). The relative permeability of P_{Ca}/P_x , where x is monovalent ion (Na^+ and K^+), was estimated by the following bi-ionic Equation 1 (Fatt and Ginsborg 1958; Xu et al., 2004) derived from the Goldman-Hodgkin-Katz (GHK) voltage equation.

$$P_{Ca}/P_x = \gamma_x [X]_{Cyttoplasmic} / (\gamma_{Ca} 4[Ca^{2+}]_{Luminal}) \{ \exp(E_{rev}F/RT) \} \{ 1 + \exp(E_{rev}F/RT) \} \quad (Eq.1)$$

Where R , T , F , E_{rev} , and γ are, respectively, the gas constant, absolute temperature (room temperature), Faraday constant, reversal potential, and activity coefficient. Activity coefficients of KF (γ_K) and NaF (γ_{Na}) were 0.75 (Robinson and Stokes 1965). Activity coefficients of KMSA (γ_K) and NaMSA (γ_{Na}) were likewise 0.75 (Bonner 1981). Activity coefficient of CaMSA was 0.52 similar to CaCl₂ (Dani et al., 1983). All results are presented as mean \pm S.E.M. An unpaired t test was performed for the comparison between two groups. Values of $p < 0.05$ were considered significant.

External (cytoplasmic) solution (bi-ionic P_{Ca}/P_K)

KF	60 mM
K-MSA	100 mM
HEPES	10 mM

Adjusted pH to 7.2 with KOH, sterilize by passing through a 0.2µm filter, and store at -20°C for several months.

3. Results

3.1 Characterization of the lysosomal two-pore channel 2

TPC2 is primarily localized on membranes of late endosomes and lysosomes. A direct regulation of the ion channel activities of TPC2 on lysosomes is still unclear. A major obstacle to address this key point is that the size of lysosomes is smaller than 0.5 μm which is inaccessible to conventional electrophysiological approaches. To selectively increase the diameter of late endosomes and lysosomes up to 5 μm , cells were pretreated with vacuolin-1, a lipid-soluble polycyclic triazine (Huynh and Andrews, 2005). Here, two electrophysiological methods are presented to record TPC2 currents from isolated lysosomes.

3.1.1. Direct whole-lysosome patch-clamp method to characterize TPC2 mediated currents from intact lysosomes

A modified whole-lysosome patch-clamp approach is adopted to characterize the properties of TPC2 in isolated intact lysosomes which were enlarged from cells pretreated with vacuolin-1 for overnight. The cell membrane was damaged manually with a glass capillary at a position close to the edge of the lysosome. The intact lysosome was pushed out through the cut position with a capillary top. The isolation was successful for 5 – 10 % of the attempts. **Figure 5A** shows an isolated enlarged lysosome forming a giga seal (>2 Gohm; 10 – 20 % of attempts) on the top of a glass pipette. Lysosomes could be observed as phase-bright spheres under the phase-contrast microscope. The surface of isolated enlarged lysosomes looked smooth and highly fragile. The surrounding cellular structures – such as actin filaments – were usually still connected to the isolated lysosome formation. Too many surrounding structures are an obstacle for giga seal. **Figure 5B** shows the enlarged lysosomes were patch-clamped in the modified direct whole-lysosome configuration. Inward currents indicate cation flowing out of the lysosome and outward currents indicate cations flowing from the cytoplasm into the lysosome (Bertl et al., 1992).

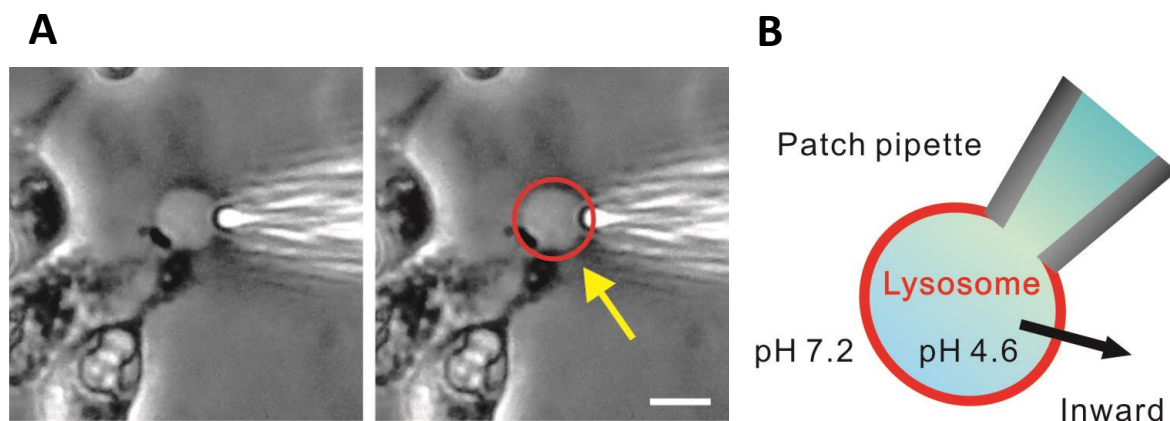


Figure 5: Illustration of the whole-lysosome recording using glass patch pipette. (A) The process of manual dissection of an enlarged lysosomes is shown, (right) the yellow arrow indicates the isolated enlarged lysosome (circled in red). Scale bar is 10 μm . (B) Cartoon of modified whole-lysosome patch-clamp configuration of whole-lysosome recording. The patch pipette was filled with low pH luminal solution to mimic the acidic environment of the lysosomal lumen. Inward current (negative) denotes positive charge flowing out of the lysosomal lumen into the cytosol.

HEK293 cells were transfected with enhanced green fluorescent protein (EGFP)-human TPC2 (Cang et al., 2013 Cell). Bath application of 10 μM PI(3,5)P2 in a water-soluble diC8 form large activated a TPC2-mediated non-rectifying current (16.1 ± 4.5 fold increase in basal activity) (**Fig. 6 a-b**). In 7 out of 7 enlarged lysosomes isolated from transfected HEK293 cells, TPC2-mediated currents in the presence of 10 μM diC8 PI(3,5)P2 were 1952 ± 245 pA at -100 mV with positive reversal potentials. Cytoplasmic/bath solution contained (in mM) $140\text{K}^+/4\text{Na}^+/2\text{Mg}^{2+}$ (pH 7.2); luminal/pipette solution contained (in mM) $145\text{Na}^+/5\text{K}^+/1\text{Mg}^{2+}/2\text{Ca}^{2+}$ (pH4.6 to mimic the acidic environment of the lysosomal lumen); the equilibrium potential of Na^+ was estimated to be $\sim +90$ mV; the equilibrium potential of K^+ was estimated to be < -80 mV. These results indicated that PI(3,5)P2 activates TPC2 in lysosomes and the channels are selective for Na^+ , but not K^+ . Similar results were obtained from HEK293 stable cell line of GFP-tagged murine wild type TPC2 (**Fig. 6 c-d**).

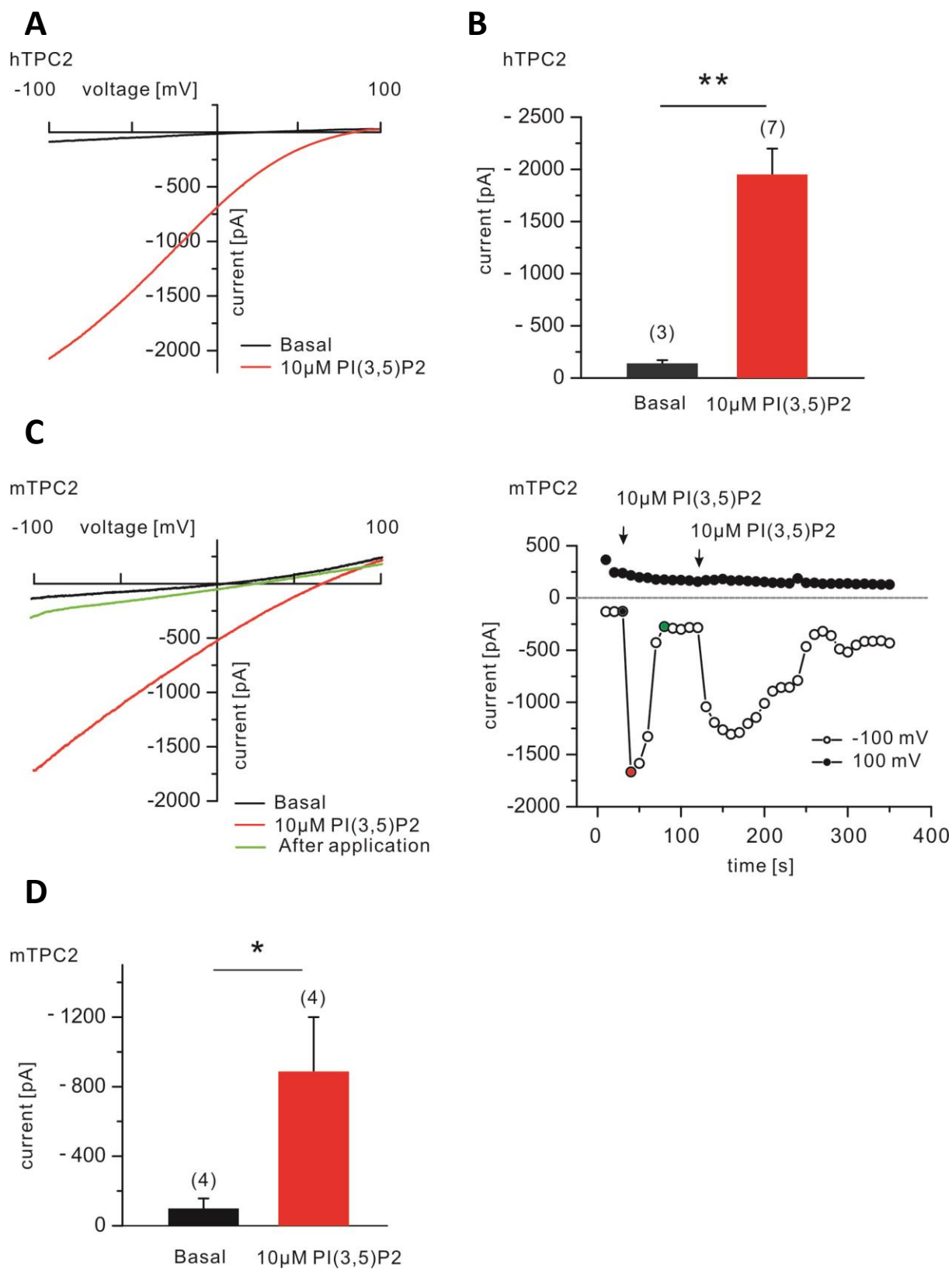


Figure 6: PI(3,5)P2-activated TPC2 inward currents. (A) Current-voltage relations of modified whole-lysosome patch-clamp experiments demonstrate that before (black) and after (red) the application of PI(3,5)P2 in a water-soluble diC8 form to the cytoplasmic side of enlarged lysosome isolated from vacuolin-treated human TPC2 overexpressing HEK293 cells activated

whole-lysosome currents with positive reversal potential (76.5 ± 3.7 mV, $n = 7$). Whole-lysosome recordings with ramp protocols (-100 to +100 mV; 500ms, holding potential 0 mV). (B) Statistics of current amplitudes at -100mV from experiments shown in A (2.0 ± 0.25 nA, $n = 7$). (C) PI(3,5)P2 activated whole-lysosome current with positive reversal potential in a mTPC2-positive lysosome isolated from stable HEK293 cell line. Right: Current amplitudes measured at -100 mV (open circle) and +100 mV (close circle) were used to plot the time course of activation. Left: representative current-voltage relations of mTPC2-mediated whole-lysosome currents before (black) and after (red and green) PI(3,5)P2 bath application at different time points, as indicated. (D) Statistics of current amplitudes at -100mV from experiments shown in C. Numbers of lysosomes are in parentheses. Data are presented as mean \pm SEM.

3.1.2. Whole-lysosome Planar Patch-clamp method to characterize TPC2 mediated currents from intact lysosomes

The successful ratio of this modified whole-lysosome patch-clamp approach for the characterization of lysosomal ion channels is limited. Intracellular membranes are much more fragile and usually not stable enough to withstand mechanical manipulation by glass capillaries during seal formation and rupturing of the membrane. To solve these problems, a novel whole-lysosome planar patch method was developed involving the immobilization of isolated organelles on a solid matrix planar glass chip (Schieder et al., 2010b). This approach contains a suction control system and a glass chip with a small hole ($<1\mu\text{m}$) that support the formation of gigaseals and allows electrophysiological recordings in spite of the unstable membranes of lysosomes.

Lysosomes were isolated from stable HEK293 overexpressing GFP-tagged-murine TPC2 (Schieder et al., 2010a). To increase the size of lysosomes, the cells were also treated with vacuolin-1. Purified isolated lysosomes were obtained using a lysosome preparation protocol. On average, per preparation 5 – 20 enlarged ($>5\mu\text{m}$) intact lysosomes from 8×10^6 HEK293 cells were collected (two 175 cm^2 tissue culture dishes with 90 to 95 % confluence). The integrity of the lysosomal preparation was verified using epifluorescence imaging (**Fig. 7A**). If the product of the lysosomal preparation contains large aggregates or no lysosomes, then it will be impossible to form giga seal and to record currents from lysosomes. In good quality lysosomal preparations only enlarged lysosomes were seen as perfect spheres containing GFP-TPC2 co-figuration on the surface. **Figure 7B** shows the whole-lysosome planar patch-clamp. The current conventions for electrophysiological experiments using the whole-lysosome planar patch-clamp technique are the same as for modified whole-lysosome patch-clamp. An inward current is defined as a current that flows out of the lysosome (luminal side of chip) into the cytosol (external side of chip).

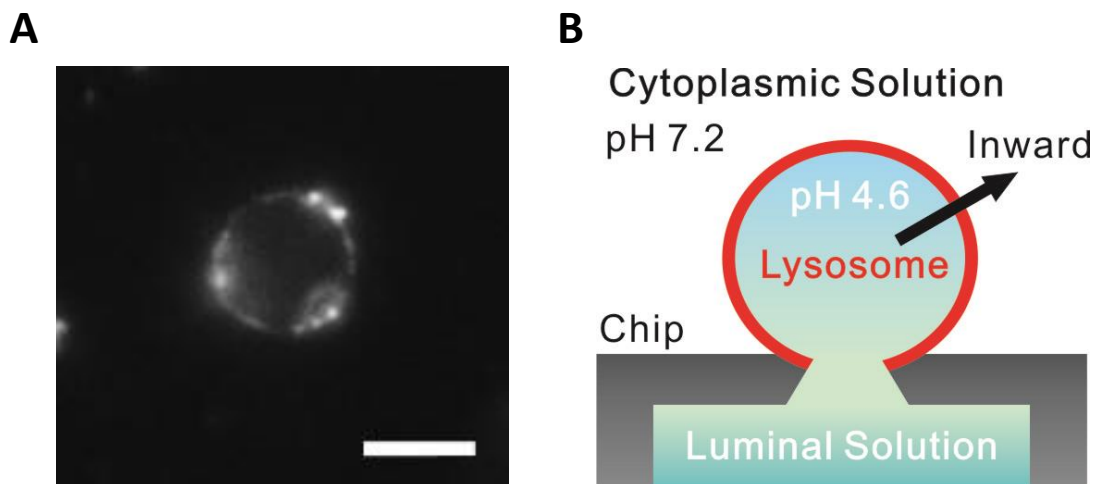


Figure 7: Schematic of whole-lysosome planar patch-clamp recording. (A) Epifluorescence image of vacuolin-treated lysosomes expressing GFP-TPC2. Scale bar is 5 μm . (B) Extralysosomal side of the planar glass chip containing the cytoplasmic solution, intralysosomal side of the chip containing the luminal lysosomal solution with low pH. Inward current denotes cation flowing out of the lumen into the cytosol (extralysosomal side). Suction is applied to the chip in order to attach a single lysosome (circled in red) to the chip and obtain the whole lysosomal configuration.

3.1.3. PI(3,5)P2 and NAADP evoke TPC2 channels in the lysosome

In enlarged lysosomes isolated from non-transfected HEK293 cells, little or no currents were detected in whole-lysosome recordings. External application of PI(3,5)P2 rapidly activated TPC2-mediated non-rectifying currents. Lysosomes that expressed a mutant TPC2 isoform carrying a N257A mutation in pore loop I showed no difference compared to non-transfected lysosomes (**Fig. 8**) (Schieder et al., 2010a). Other PIP2 isoforms such as PI(4,5)P2 are localized in the plasma membrane failed to activate TPC2 (**Fig. 8**).

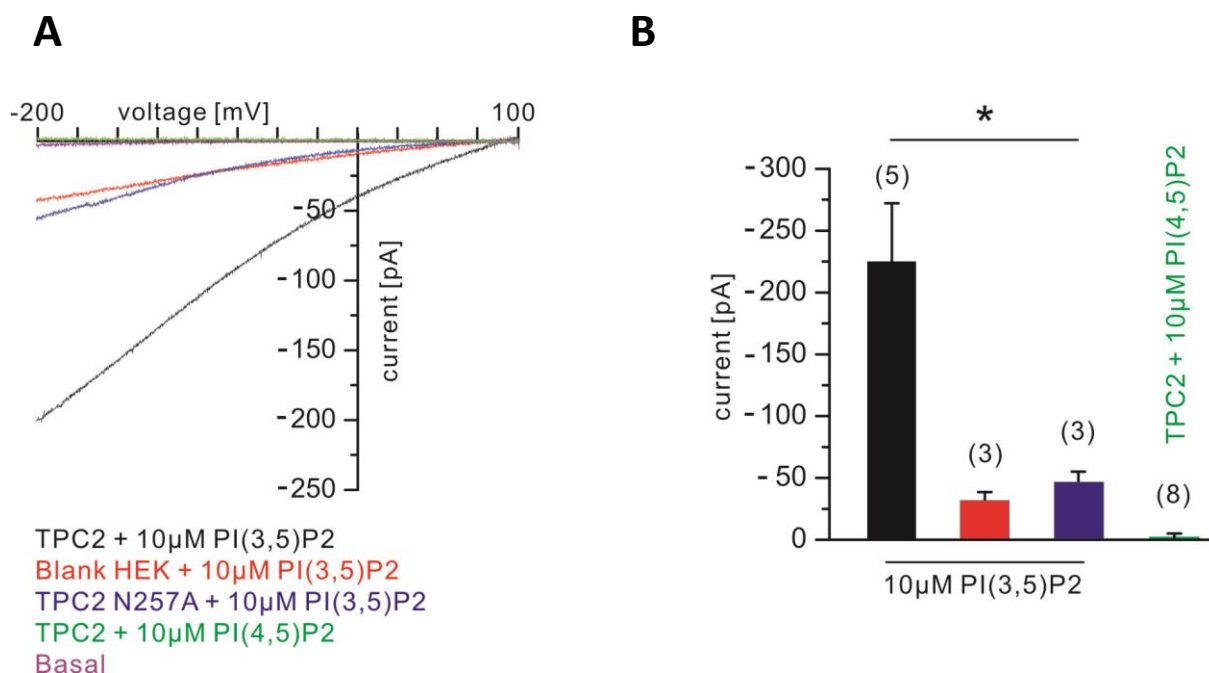


Figure 8: Specific activation of TPC2 by PI(3,5)P2. (A) Current-voltage relations of whole-lysosome planar patch-clamp experiments demonstrating that murine GFP-TPC2 is activated by PI(3,5)P2 (diC8, 10 μ M) when overexpressed in HEK293 cells. In contrast to TPC2 WT (black), the TPC2 pore mutant TPC2(N257A) (blue), was found to be non-responsive to an activation by PI(3,5)P2. Effects were not significantly different from effects observed in lysosomes isolated from untransfected HEK293 cells (red). Whole-lysosome recordings with ramp protocols (-200 to +100mV; 500ms, holding potential -60mV). (B) Bar diagram summarizing data at -200 mV from experiments shown in A. Numbers of lysosomes are in parentheses. Data are presented as mean \pm SEM. * = p < 0.05.

In lysosomes prepared from TPC2^{-/-} MEFs, currents elicited by postulated activators of TPC2, PI(3,5)P2 and NAADP were strongly reduced (**Fig. 9 and 10**). The equilibrium potential of Na⁺ was estimated to be \sim + 80 mV, the equilibrium potential of Ca²⁺ was estimated to be \sim + 70 mV, the equilibrium potential of K⁺ was estimated to be < - 100 mV. Application of PI(3,5)P2, an endogenous agonist of lysosomal TPC2 and TRPML1 channels (Wang et al., 2012; Jha et al., 2014; Dong et al., 2010) that evoked currents from lysosomes of WT MEF with a reversal potential of $+ 50 \pm 4$ mV (n=3). This implies PI(3,5)P2 activated both TPC2 and TRPML1 on lysosomes from WT MEF. Furthermore, PI(3,5)P2 activated TRPML1-like small rectifying inward currents in TPC2^{-/-} lysosomes and exhibited a more negative reversal potential of $+ 10 \pm 23$ mV (n=3) (**Fig. 9**), which suggests that endogenously expressed TRPML1 cation channels were present in TPC2^{-/-} MEF. NAADP (50nM) evoked TPC2-like currents from lysosomes of WT MEF were non-rectifying and exhibited a reversal potential of $+ 75 \pm 3$ mV (n=4) close to the equilibrium potential of Ca²⁺ and Na⁺ (**Fig. 10a**). NAADP dependent currents in WT lysosomes displayed a bell shaped dose response relationship (**Fig. 10b**) as described for the

native mammalian release channel (Cancela et al., 1999; Masgrau et al., 2003). TPC2 gets activated in the low nanomolar range of NAADP, reaches a peak at 50 nM and inactivates at higher concentrations of NAADP (200 nM). These NAADP evoked currents in WT and TPC2 $-/-$ MEFs suggest that NAADP-induced inward cation currents are mediated by endogenously expressed TPC2 channels and not by other postulated NAADP-activated lysosomal channels such as TRPML1 (Zhang and Li, 2007; Zhang et al., 2009) or TRPM2 which are activated by NAADP at hundred micromolar concentrations (Beck et al., 2006; Lange et al., 2008).

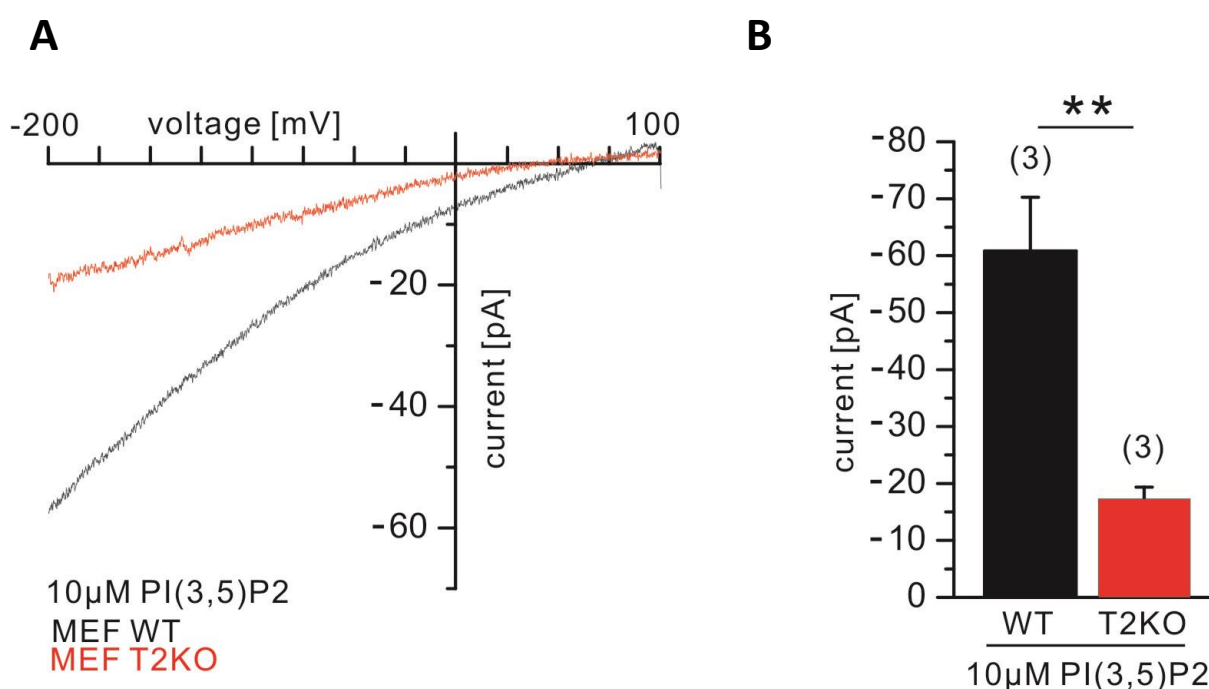


Figure 9: Genetic inactivation of TPC2 abolishes TPC2 currents in the lysosome. (A) Current-voltage relations of whole-lysosome planar patch-clamp experiments demonstrating that application of PI(3,5)P2 (diC8, 10 μ M) to the cytoplasmic side of lysosome evokes inward currents in lysosomes isolated from WT MEF while currents are strongly reduced in lysosomes isolated from TPC2 $-/-$ MEF. (B) Bar diagram summarizing data at -200 mV from experiments shown in A. Numbers of lysosomes are in parentheses. Data are presented as mean \pm SEM. ** = p < 0.01.

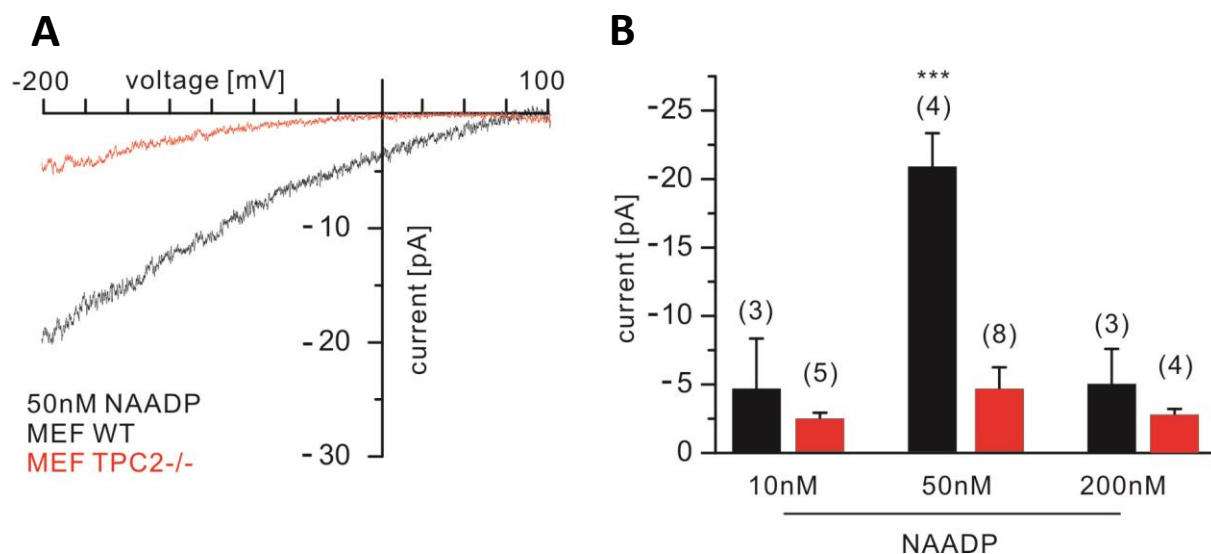


Figure 10: Bell-shaped dose-response-curve of NAADP evoked TPC2 currents with a maximum effect in the nanomolar. (A) Current-voltage relations of whole-lysosome planar patch-clamp experiments demonstrating that application of low nanomolar NAADP to the cytoplasmic side of lysosome evokes inward currents in lysosomes isolated from WT MEF while currents are strongly reduced in lysosomes isolated from TPC2^{-/-} MEF. (B) Bar diagram summarizing data at -200 mV from experiments shown in A and additional experiments using 10 or 200 nM NAADP instead of 50 nM. Numbers of lysosomes are in parentheses. Data are presented as mean ± SEM. *** = $p < 0.001$ (two-way ANOVA followed by Bonferroni's post test)

3.1.4. Regulation of TPC2 by NED-19 and ATP

The NAADP antagonist NED-19 (Naylor et al., 2009) inhibited NAADP-mediated Ca^{2+} release (Rosen et al., 2009). In lysosomes prepared from stable TPC2 overexpressing HEK293 cells, application of 10 μM NED-19 blocked PI(3,5)P₂ evoked TPC2 currents. These data provide additional evidence for NAADP mediated activation of TPC2 channels (**Fig. 11**).

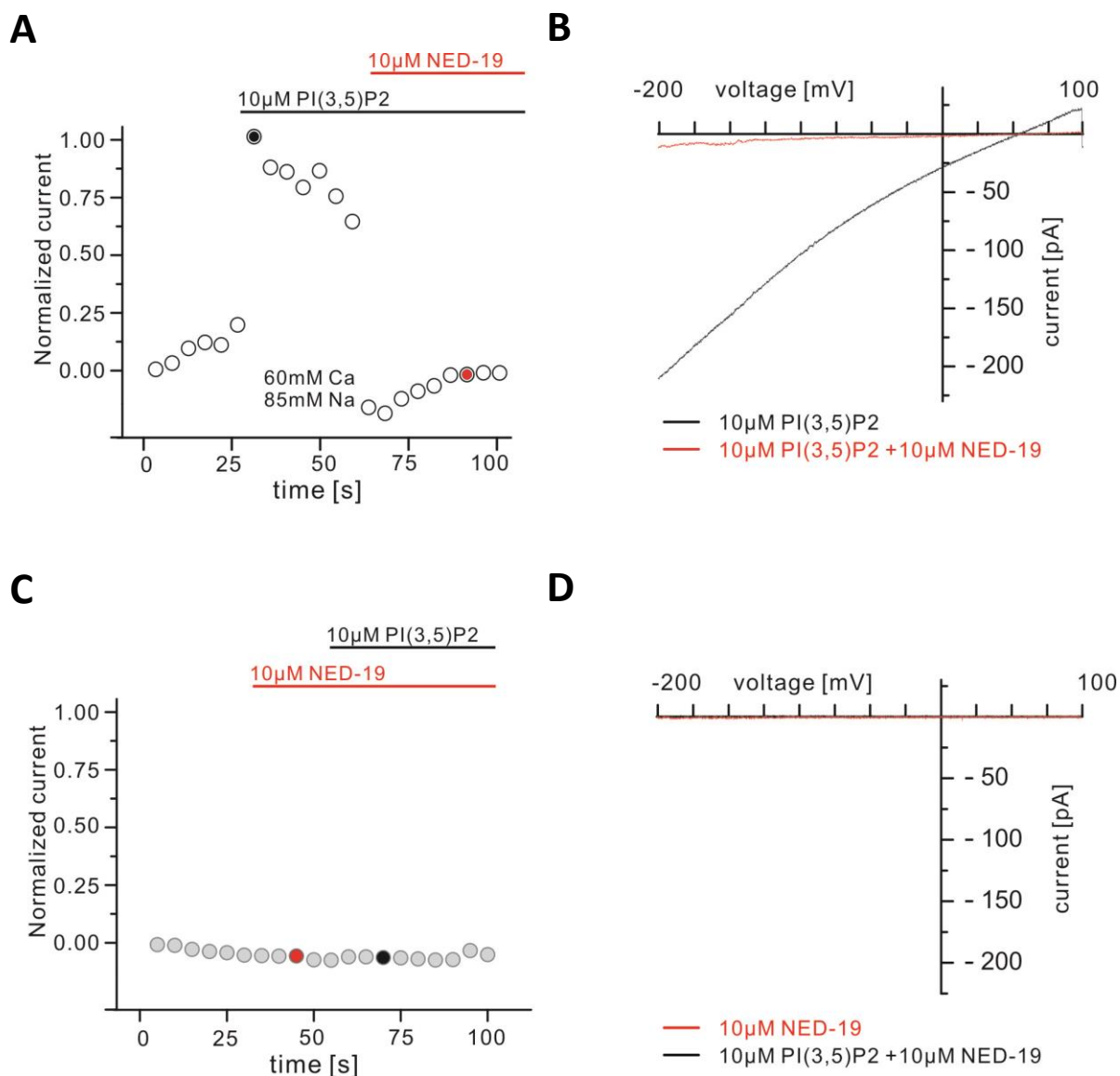


Figure 11: NED-19 Inhibitors PI(3,5)P2-mediated TPC2 cation currents. (A,C) Representative continuous recordings of isolated lysosomes from TPC2 overexpressing HEK293 cells. Whole-lysosome currents were elicited by repeated voltage ramps (-200 to +100 mV; 500 ms) with a 5 second interval between ramps; current amplitudes measured at -200 mV were used to plot the time course of activation. Application of 10 μ M PI(3,5)P2 (black) and 10 μ M NED-19 (red) are indicated by closed bars, respectively. (B, D) show representative current-voltage relations of TPC2-mediated whole-lysosome currents before and after NED-19 extralysosomal application at different time points in the presence of PI(3,5)P2.

Recently, it was reported that PI(3,5)P2-activated TPC2 currents are inhibited by cytosolic ATP (Cang et al., 2013). With a luminal solution containing high Ca^{2+} (60mM) and high Na^+ (85mM) and a cytosolic solution containing K^+ and PI(3,5)P2, the amplitude of TPC2 currents was reduced to 72 ± 17 % by ATP-Mg (n = 3) (**Fig. 12a-b**) and to ~ 100 % by micromolar concentration NED-19 (n = 4) (**Fig. 12c**). These data are comparable with reported previously in other electrophysiological methods such

as modified whole-lysosome patch-clamp (Cang et al., 2013) and artificial lipid bilayer recording (Brailoiu et al., 2010).

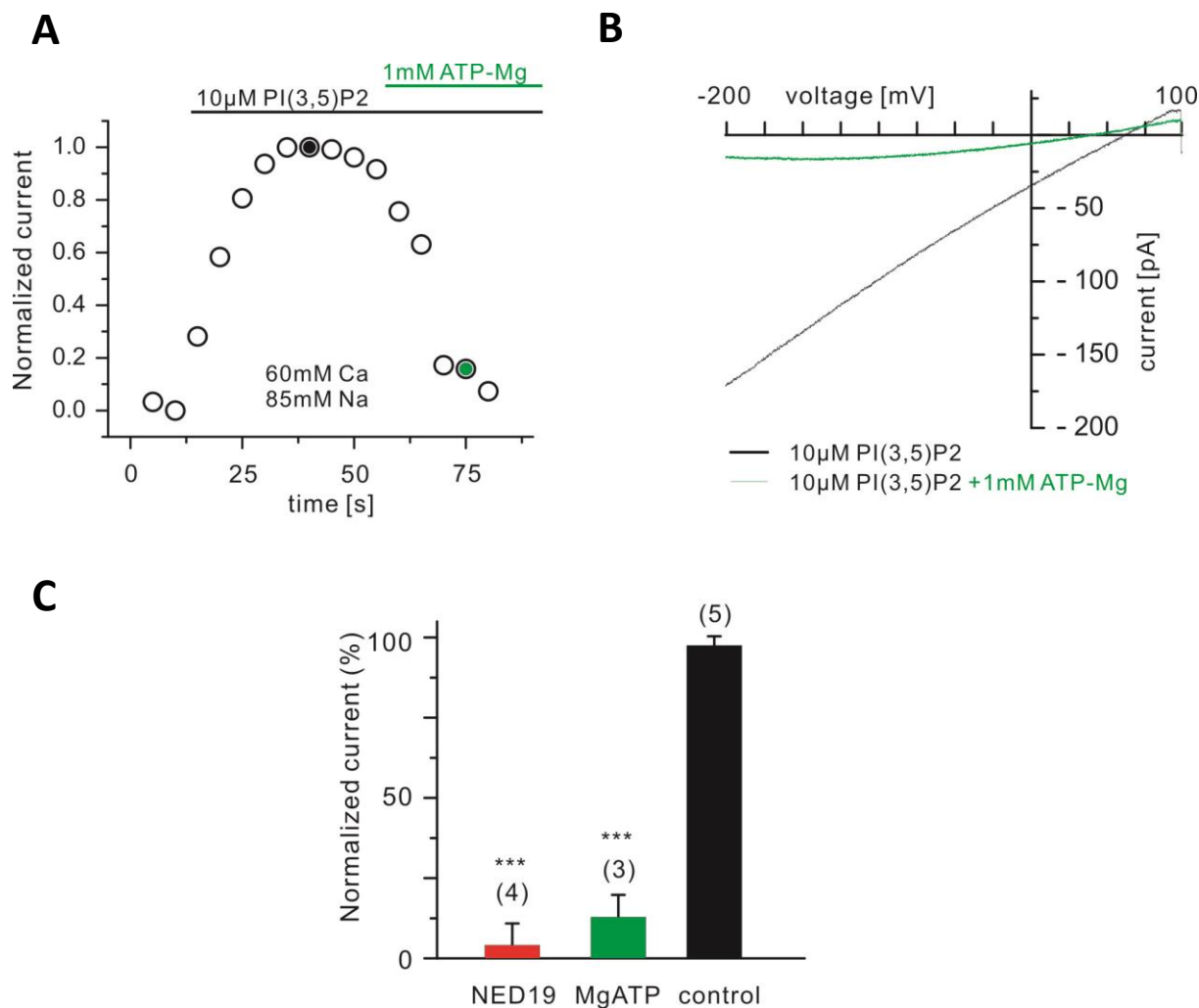


Figure 12: ATP-sensitive currents recorded from TPC2. (A) Representative continuous recordings of isolated lysosomes from TPC2 overexpressing HEK293 cells. Whole-lysosome currents were elicited by repeated voltage ramps (-200 to +100 mV; 500ms) with a 5 second interval between ramps; current amplitudes measured at -200 mV were used to plot the time course of activation. Application of 10 μ M PI(3,5)P2 (black) and 1 mM ATP (green) are indicated by closed bars, respectively. (B) shows representative current-voltage relations of TPC2-mediated whole-lysosome currents before and after ATP extralysosomal application at different time points in the presence of PI(3,5)P2. (C) Comparison of PI(3,5)P2 evoked current amplitudes at -200mV (Fig.9C and Fig.10B) in the presence or absence of NED-19 or ATP. Numbers of lysosomes are in parentheses. Data are presented as mean \pm SEM. *** = $p < 0.001$.

3.1.5. Ion permeability of TPC2

The relative permeability of TPC2 to monovalent and divalent cations was assessed by monitoring shifts in the reversal potential (**Fig. 13**). NAADP evoked TPC2-like current recordings under bi-ionic conditions with luminal 107 mM Ca^{2+} and cytoplasmic 165 mM K^+ or Na^+ revealed that the estimated permeability ratios for $P_{\text{Ca}}/P_{\text{K}}$ and $P_{\text{Ca}}/P_{\text{Na}}$ were about 340 ($n = 8$) and 0.7 ($n = 6$), respectively, which is consistent with previous experiments. These ion substitution analyses demonstrate that TPC2 forms channels which are permeable for highly Ca^{2+} and Na^+ , but not K^+ .

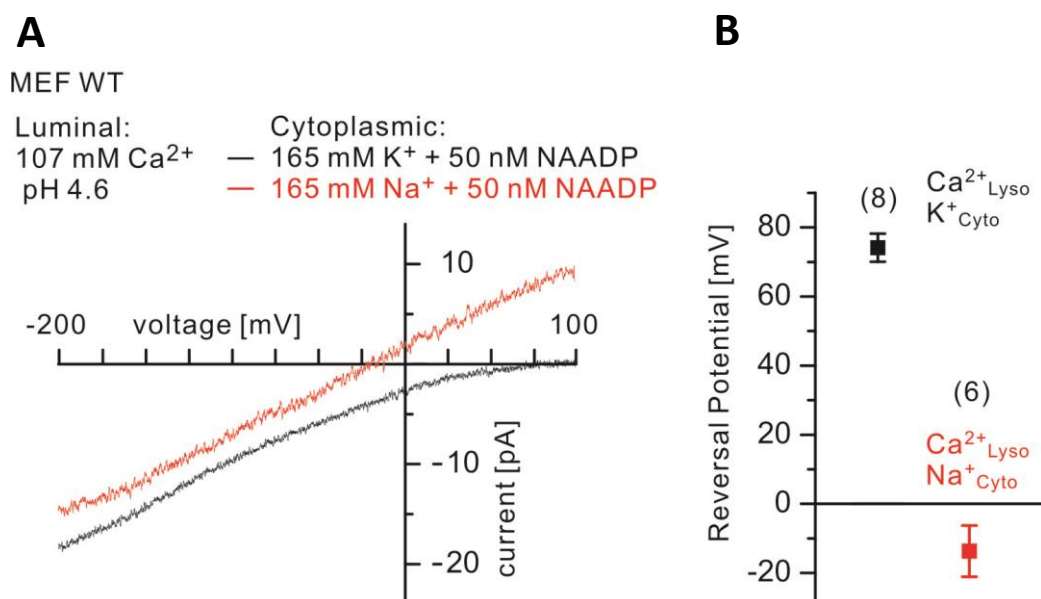


Figure 13: NAADP-activated TPC2 currents are Na^+ and Ca^{2+} permeable. Whole-lysosome recordings of NAADP-evoked TPC2-like currents under bi-ionic conditions with luminal Ca^{2+} , cytoplasmic K^+ and cytoplasmic Na^+ revealed E_{rev} is 77 ± 4 mV ($n=8$) and -14 ± 7 mV ($n=6$), respectively. Data are presented as mean \pm SEM.

3.1.6. Different direct electrophysiological approaches

Breakage of a patch while the pipette is attached to the cell results in whole-cell recordings which are employed when ion channels of the entire cell membrane are measured. This configuration is the most popular patch technique. The main drawback is a possible loss of cytosolic factors and the incapability to change the cytosolic solution during the measurement. Besides, this modified whole-lysosome patch-clamp technique is difficult to apply for intracellular organelles because these organelles are floating around in the bath solution after breaking the cell.

Technically, the major problem preventing the characterization of intracellular ion channels by glass pipette-based patch-clamp measurements has been the maintenance of organelle integrity. The whole-lysosome planar patch-clamp system with the planar glass chip and automatic suction control provides more efficient formation of gigaseals and more stable electrophysiological recordings than the modified whole-lysosome patch-clamp with a semi-automatic manipulator system. Therefore, the following data were collected with the whole-lysosome planar patch-clamp approach.

3.2. Electrophysiological characterization of MLIV causing point mutants of TRPML1

The previous chapter illustrates the whole-lysosome planar patch-clamp electrophysiological approach to characterize the regulation of ionic channels in lysosomes. This electrophysiological approach was applied to characterize novel TRPML1 agonists with the aim to develop a compound to restore function to TRPML1 mutant channels responsible for MLIV.

3.2.1. Subcellular localization of ML IV causing point mutants of TRPML1

Wild-type TRPML1 almost exclusively localizes to lysosomes. To identify the subcellular localization of ML IV causing point mutants of TRPML1 channels, LysoTracker Deep Red was used to visualize lysosomes in murine embryonic fibroblasts (MEF) overexpressing human TRPML1-YFP. This confirmed that LysoTracker substantially colocalizes with TRPML1-YFP. The subcellular localization of several ML IV causing in-frame point mutants described in the literature with either unknown subcellular localization such as R403C, Y436C, V446L, V447P, or S456L (Altarescu et al., 2002; Goldin et al., 2004; Sun et al., 2000; Tüysüz et al., 2009; AlBakheet et al., 2013) or mutant isoforms reported to show partial colocalization with LAMP1, a marker for late endosomes and lysosomes, i.e. F408 Δ and F465L was analyzed systematically (Manzoni et al., 2004; Sun et al., 2000; **Fig. 14a**).

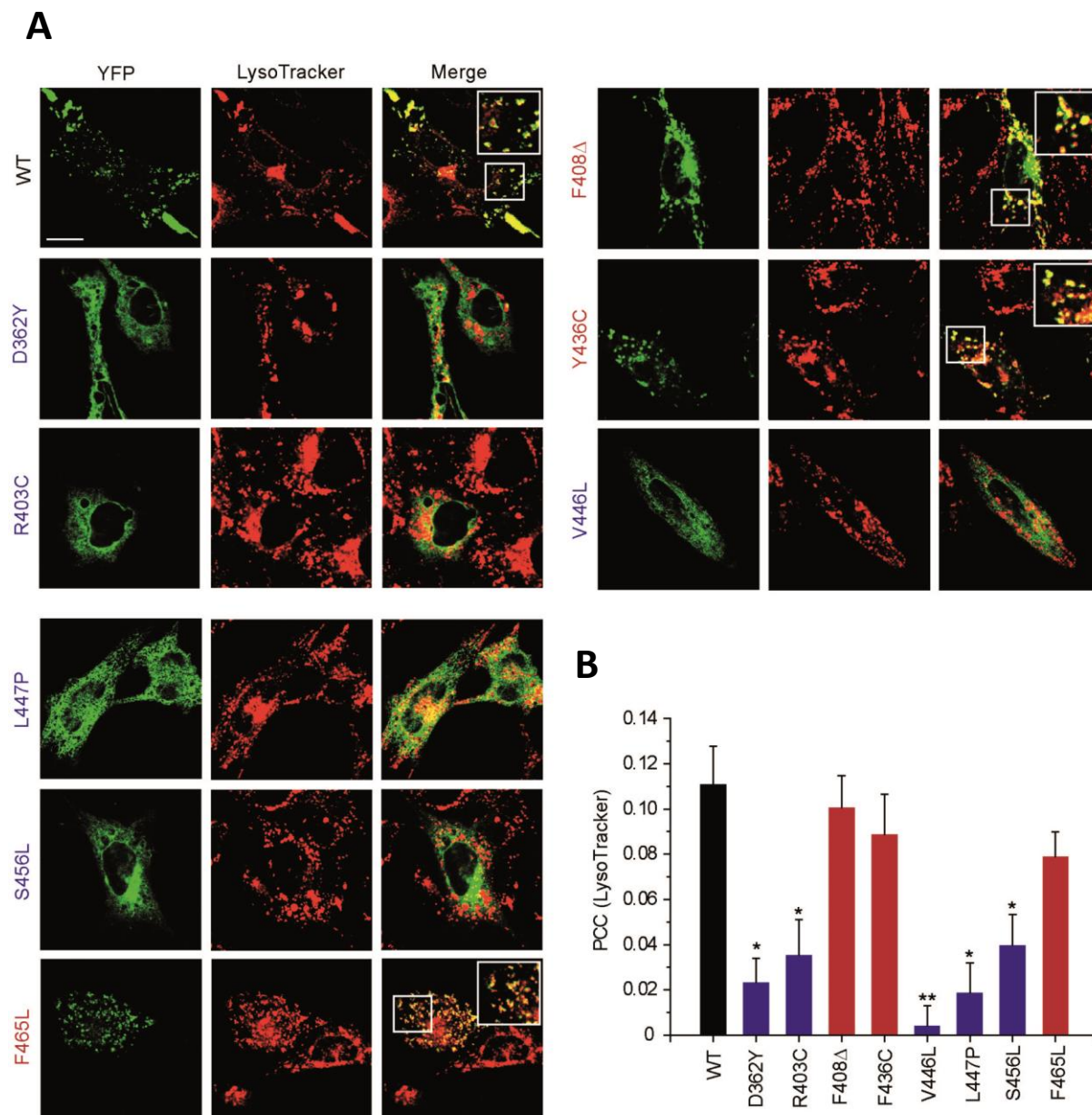


Figure 14: Subcellular localization of ML IV causing point mutants of TRPML1. (A) Representative images of wild-type (WT) and ML IV causing mutant isoforms of human TRPML1 overexpressed in WT fibroblasts. All WT and mutant variants are cloned with YFP in fusion at the C-terminus. Cells were transfected for 24-48 h and incubated with LysoTracker Deep Red (100 nM) for 30 min at 37°C prior to confocal analysis. Scale bar = 20 μ m. (B) Pearson Correlation Coefficients (PCC) to quantify colocalization of TRPML1 WT and mutant isoforms with LysoTracker Deep Red. ImageJ software was used for PCC calculations. Shown are mean PCC values \pm SEM of at least 10 cells.

WT, F408 Δ , Y436C, and F465L showed substantial colocalization with LysoTracker Deep Red (**Fig. 14a**). R403C, V446L, V447P, and S456L did colocalize much less with LysoTracker compared to WT and rather showed an expression pattern similar to L106P or D362Y, reported previously to colocalize with the ER (Kiselyov et al., 2005; Marks et al., 2012). To quantify the relative degree of colocalization

between LysoTracker and TRPML1 or the ML IV mutants, the respective Pearson Correlation Coefficients (PCC) were calculated (**Fig. 14b**). Additionally, unlike mutant isoforms F408 Δ , Y436C, or F465L, R403C or V446L mutant isoforms showed no or less expression on enlarged lysosomes (>5 μ M) as judged by fluorescence imaging compared to WT (**Fig.15**).

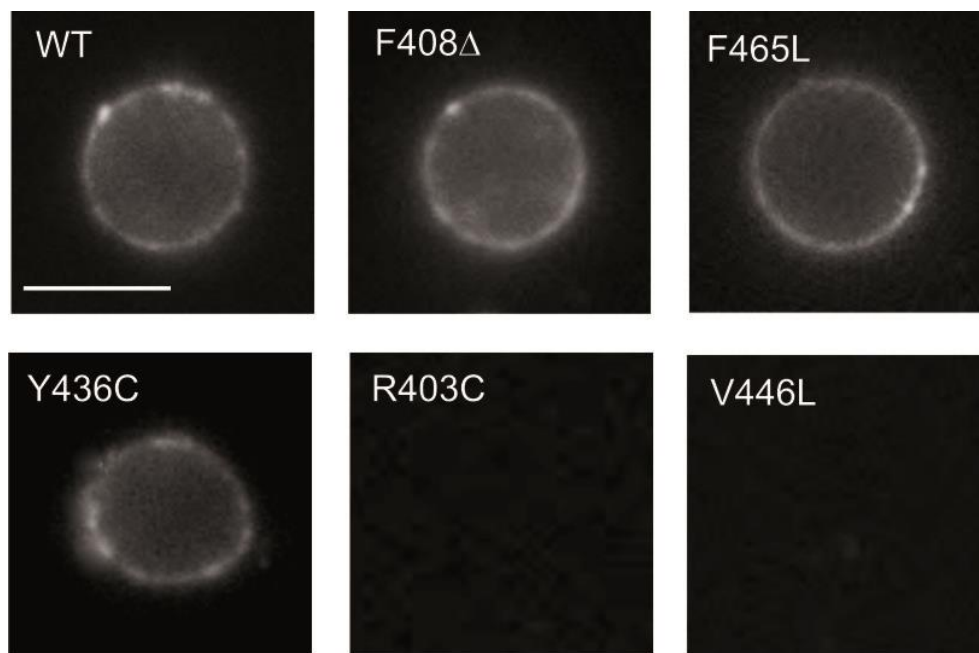


Figure 15: Epifluorescence image of vacuolin-treated lysosomes expressing TRPML1-YFP WT and mutants. Scale bar = 5 μ m.

3.2.2. Small molecule agonists increase channel activity of TRPML1 mutant isoforms

A plasma membrane variant of WT hTRPML1 which lacks the N- and C-terminal lysosomal targeting sequences (TRPML1 Δ NC) can be activated by SF-22 (5-chloro-N-(2-piperidin-1-ylphenyl)thiophene-2-sulfonamide; CID2111037) in single cell calcium imaging experiments as reported previously (Grimm et al., 2010). Here, whole-lysosome planar patch-clamp technique (Schieder et al., 2010a; Schieder et al., 2010b) was used to investigate small molecule activation of WT hTRPML1 and selected mutant isoforms of TRPML1. These results demonstrate that SF-22 elicits inwardly rectifying (from lysosomal lumen to cytosol) currents in lysosomes isolated from a HEK293 cell line stably expressing hTRPML1 (**Fig. 16**). These data also show that PI(3,5)P₂ which has been reported recently to activate TRPML channels (Dong et al., 2010) has a comparable effect on TRPML1 channel activity as SF-22 when applied at a concentration of 10 μ M, respectively (**Fig. 16**). Both, SF-22 and PI(3,5)P₂ evoked currents became smaller when pH was increased (**Fig. 16**) as reported before (Xu et al., 2007; Shen et al., 2012).

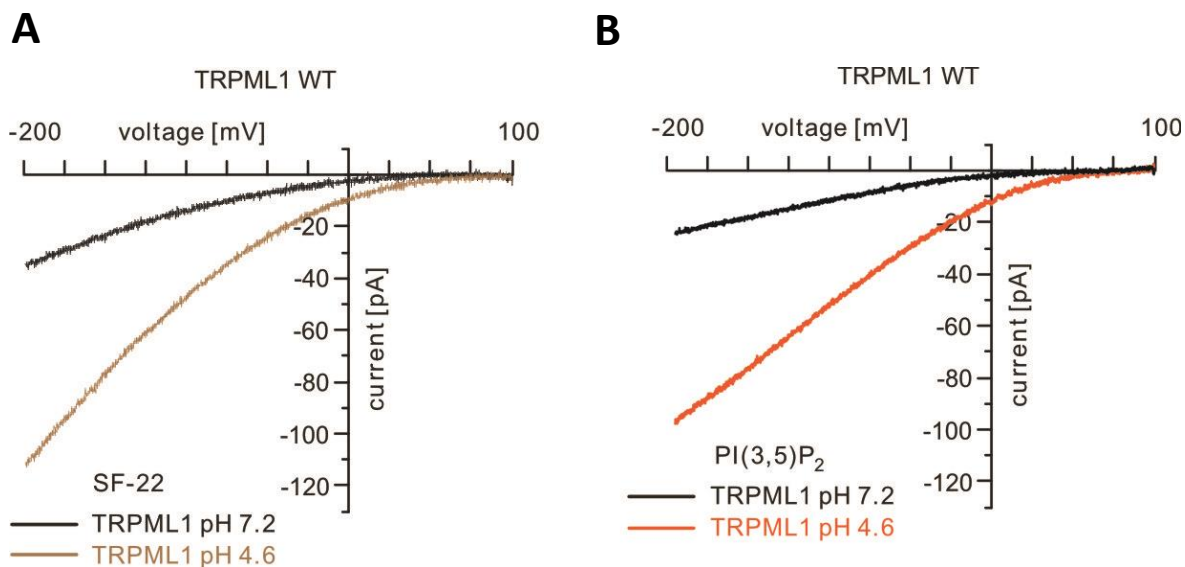


Figure 16: Effect of small molecule activator SF-22 and PI(3,5)P₂ on activation of TRPML1 WT. Current-voltage relations of whole-lysosome planar patch-clamp experiments demonstrating that human TRPML1-YFP is activated by extralysosomal application of SF-22 (10 μ M) (A) and PI(3,5)P₂ (diC8, 10 μ M) (B) when overexpressed in HEK293 cells. Activation was decreased when luminal pH was increased, respectively.

Surprisingly, when PI(3,5)P₂ was applied on lysosomes overexpressing the mutant isoforms F408 Δ , Y436C, or F465L, whole-lysosome planar patch-clamp recordings show that its effect on channel activity was much smaller compared to WT. In contrast, SF-22 evoked channel activity in F408 Δ and F465L lysosomes was 3-4 fold higher compared to PI(3,5)P₂ (Fig. 17). Although Y436C appeared to be present in LysoTracker positive vesicles in intact cells as well as in isolated lysosomes (Fig. 15 and Fig. 17d), no significant channel activation could be detected with SF-22.

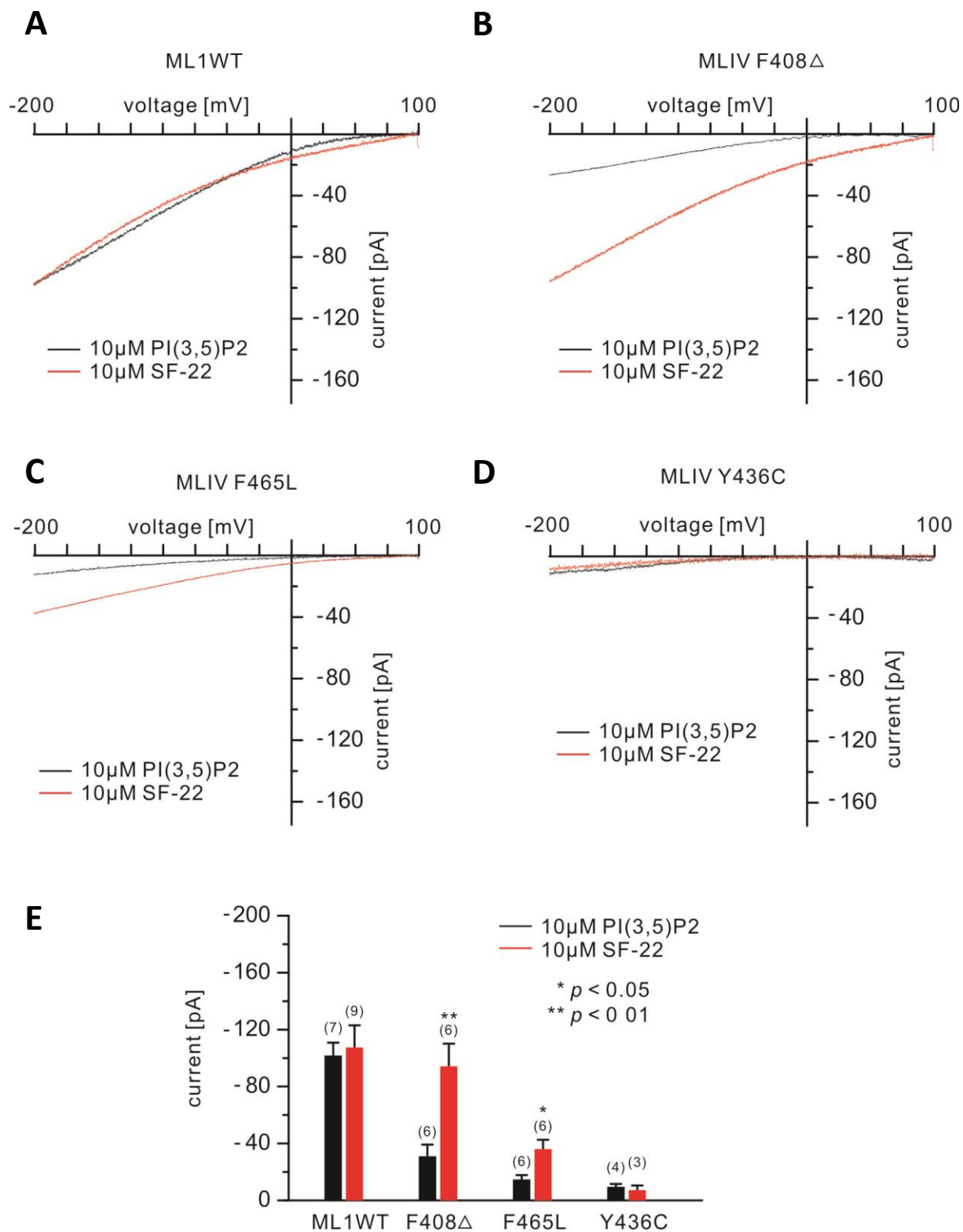


Figure 17: Effect of small molecule activator SF-22 and PI(3,5)P2 on activation of TRPML1 mutant channels. (A-D) Current-voltage relations of whole-lysosome planar patch-clamp experiments demonstrating that the effect of PI(3,5)P2 on the channel activity of TRPML1 mutant isoforms F408 Δ or F465L is significantly smaller than the effect of SF-22. (E) Bar diagram summarizing data at -200 mV from experiments shown in A. Numbers of measured lysosomes are in parentheses. Data are presented as mean \pm SEM.

Dose response measurements with PI(3,5)P₂ revealed a strong decrease in efficacy for both F408Δ and F465L compared to WT while EC₅₀ values (relative potency) were comparable (0.17 ± 0.01 μM for WT TRPML1, 0.27 ± 0.14 μM for F465L, and 0.1 ± 0.03 μM for F408Δ) (**Fig. 18a**). Dose response measurements with SF-22 revealed an EC₅₀ of 0.51 ± 0.05 μM for WT TRPML1, 0.64 ± 0.17 μM for F465L, and 1.41 ± 0.36 μM for F408Δ. While F408Δ showed a significant shift in the dose-response curve affecting potency, the relative efficacy of SF-22 was similar in F408Δ compared to WT. In contrast, it was decreased in F465L (**Fig. 18b**).

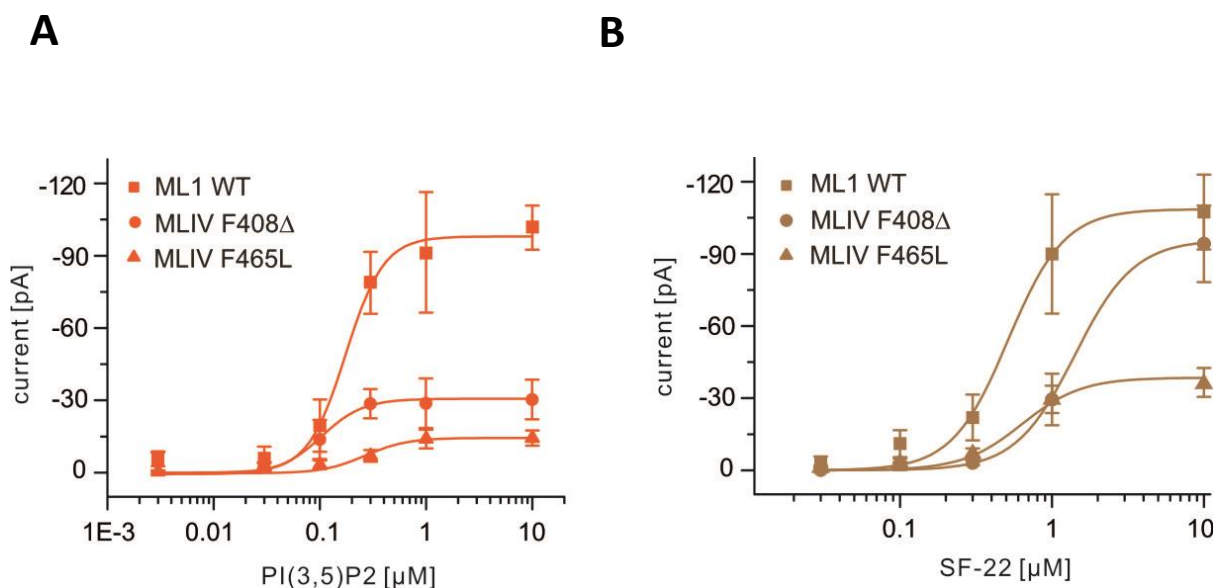


Figure 18: Dose-response curves for the PI(3,5)P₂ and SF22 mediated effects on TRPML1 WT and mutant channels. Dose-response curves determined at extralysosomal 10 μM PI(3,5)P₂ (A) and SF-22 (B) from whole-lysosome planar patch-clamp experiments from HEK293 cells overexpressing TRPML1 and MLIV. Statistics of current amplitudes at -200mV.

3.2.3. Further development of the lead structure SF-22

With the aim to further improve efficacy, and potency of SF-22, several series of chemically modified SF-22 analogues were generated (see Appendix and Chen et al. 2014) and subsequently analysed using single-cell calcium imaging (**Fig. 19**). The SF-22 analogues were designed and synthesized by Dr. Marco Keller and Dr. Annette Wolfgardt under the supervision of Prof. Dr. Franz Bracher at the Department of Pharmacy, LMU Munich. For this purpose systematic modifications have been performed in any structural motif (phenyl ring, thiophene, piperidine, sulfonamide) of the lead structure.

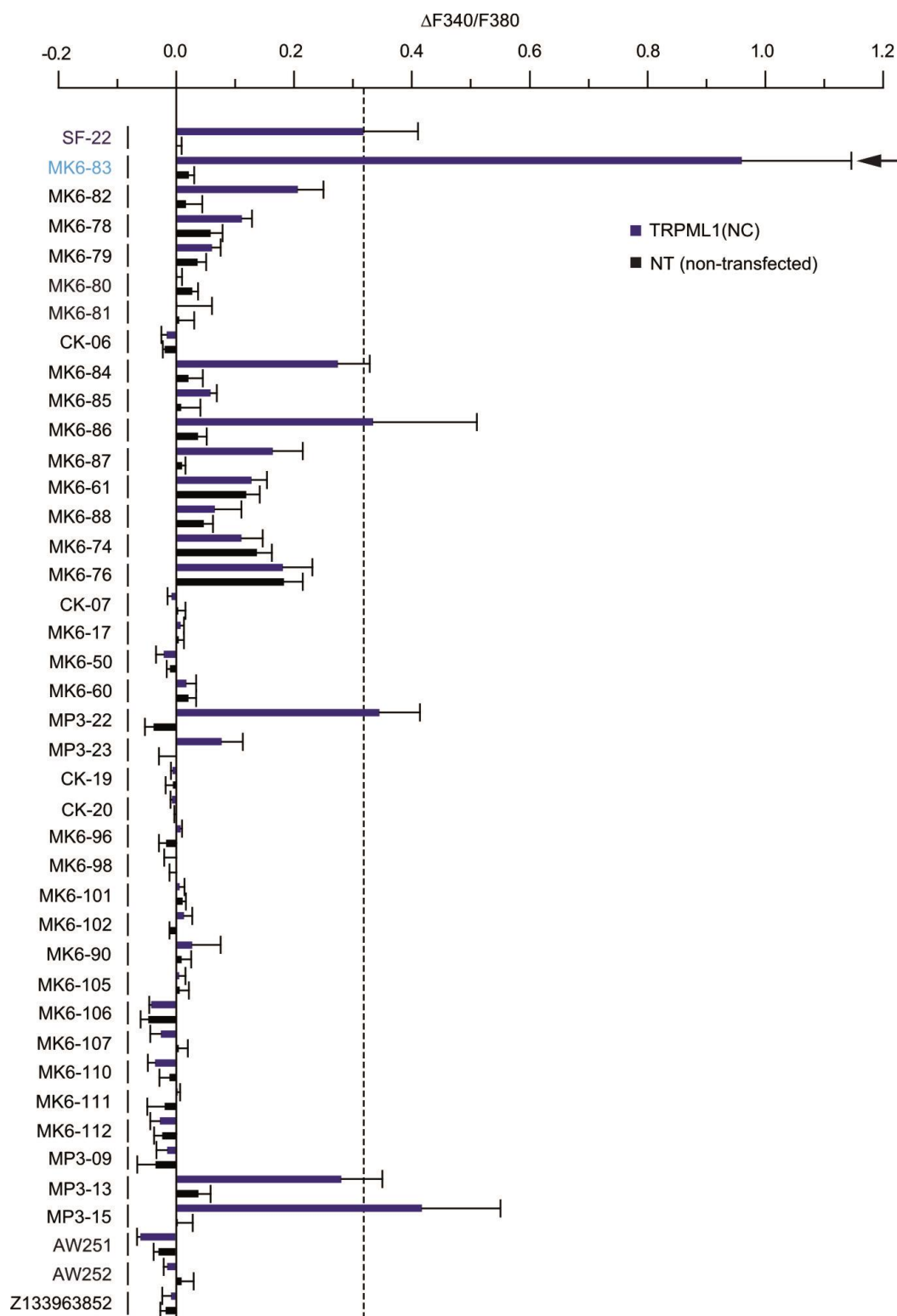


Figure 19: Effects of SF-22 and novel analogues on TRPML1 in calcium imaging experiments. shown are the effects of SF-22 and related compounds on intracellular calcium levels (fura-2 ratios F340/F380) of HEK203 cells transiently transfected with TRPML1(NC)-YFP and loaded with fura-2. Shown are mean values \pm SEM of at least 3 independent experiments with $n = 5-10$ cells, each. (Data were provided by Dr. Christian Grimm)

Interestingly, modifying the thiophene rest by replacing chlorine with a methyl group greatly increased both compound potency and efficacy for TRPML1 (MK6-83, **Fig. 20; Appendix**). Replacing the piperidine (azacyclohexane) rest with different other nitrogen-containing residues such as pyrrolidine (azacyclopentane; MK6-78 – MK6-81), pyrrole (CK-06), azacycloheptane (MK6-84 – MK6-87), cyclohexylamine (MK6-61, MK6-88), aniline (MK6-74, MK6-76), or phenyl (CK-07) led to a complete loss of activation or decreased efficacy for TRPML1. The effect was most prominent with MK6-84 and CK-07. Replacing piperidine in SF-22 with azacyclopentane and, at the same time replacing chlorine at the thiophene ring with a methyl group (MK6-80) led to a compound which greatly increased efficacy for TRPML1. Replacing the thiophene ring with a furan ring or changing the position of sulphur in the thiophene ring was likewise not beneficial (MK6-96, MK6-98, MK6-101, MK6-102). Neither was the replacement of the piperidine with a dimethylamino group (MK6-90) or introduction of a N-methyl group at the sulfonamide rest (Z138963852). Finally, insertion of a methylene group between thiophene and sulfonamide (AW-251, AW-252) lead to a complete loss of TRPML1 activation. In summary, the above described chemical modifications led to a new candidate activator of TRPML1 with improved potency and efficacy: MK6-83.

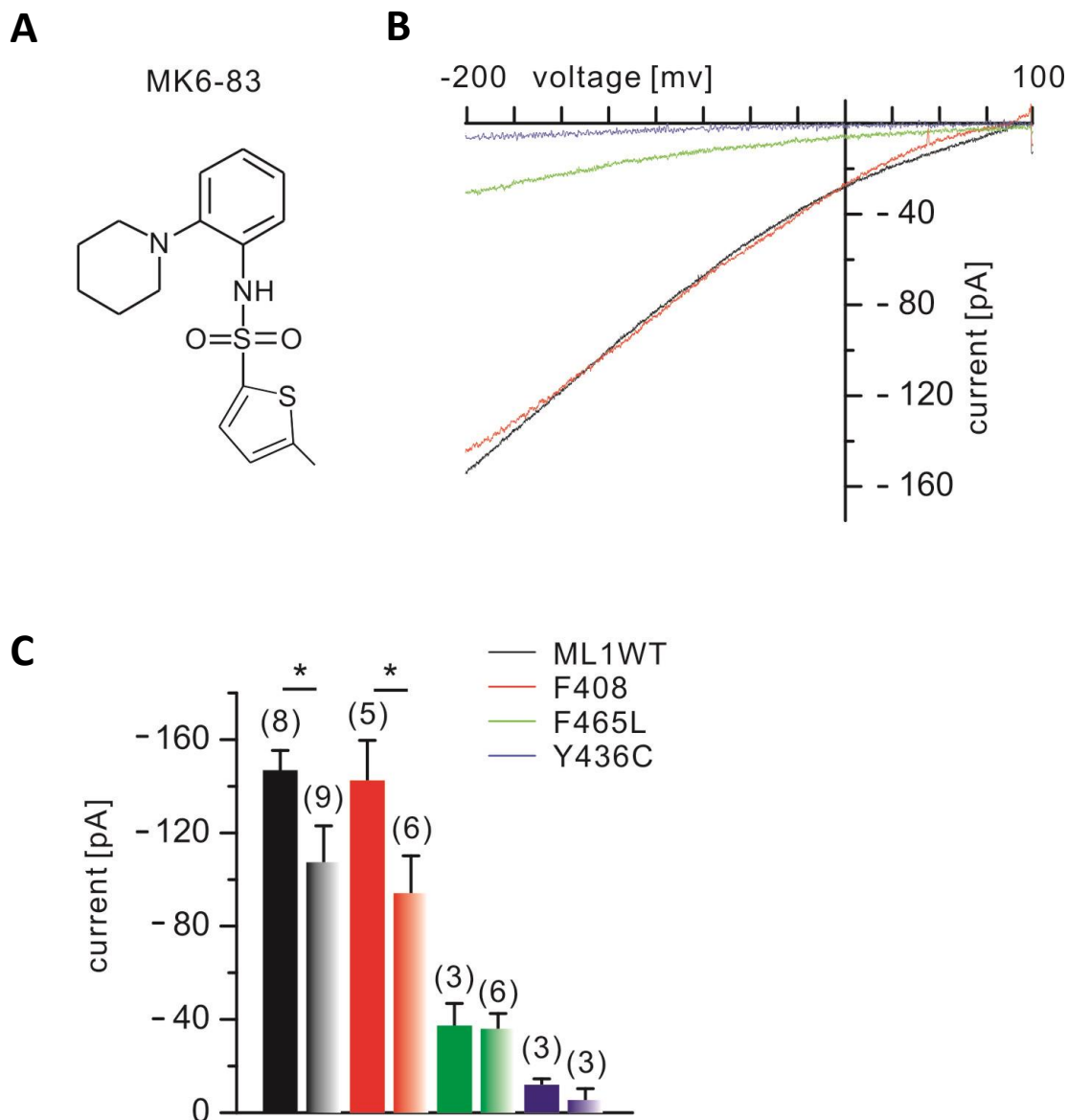


Figure 20: Effect of small molecule activator MK6-83 on activation of TRPML1 WT and mutant channels. (A) Chemical structure of MK6-83. (B) Current-voltage relations of whole-endolysosome planar patch-clamp experiments demonstrating that the effect of MK6-83 on the channel activity of TRPML1 WT or mutant isoforms F408Δ is significantly stronger than the effect SF-22. (C) Bar diagram summarizing data at -200 mV from experiments shown in B. Numbers of lysosomes are in parentheses. Data are presented as mean ± SEM.

In a further set of experiments, whole-lysosome recordings using the planar patch-clamp technique revealed that MK6-83 strongly activates TRPML1 in isolated lysosomes from over expressing HEK293 cells (**Fig. 20**). Compared to SF-22, the efficacy of TRPML1 activation was significantly increased in WT and F408Δ but not in F465L (**Fig. 21**). Likewise, no significant difference was seen for Y436C (**Fig. 20**). Next, dose-response measurements revealed EC_{50} s of $0.11 \pm 0.01 \mu\text{M}$ for WT TRPML1 and $0.1 \pm 0.03 \mu\text{M}$ for F465L when activated with MK6-83 (**Fig. 21**) compared to $0.51 \pm 0.05 \mu\text{M}$ for WT TRPML1 and $0.64 \pm 0.17 \mu\text{M}$ for F465L when activated with SF-22 (**Fig. 18**). The EC_{50} for F408Δ was less significantly

shifted ($1.23 \pm 0.19 \mu\text{M}$ and $1.41 \pm 0.36 \mu\text{M}$, for MK6-83 and SF-22, respectively) (**Fig. 21**). These data show that MK6-83 has a higher efficacy than SF-22 for TRPML1 and some MLIV mutant isoforms.

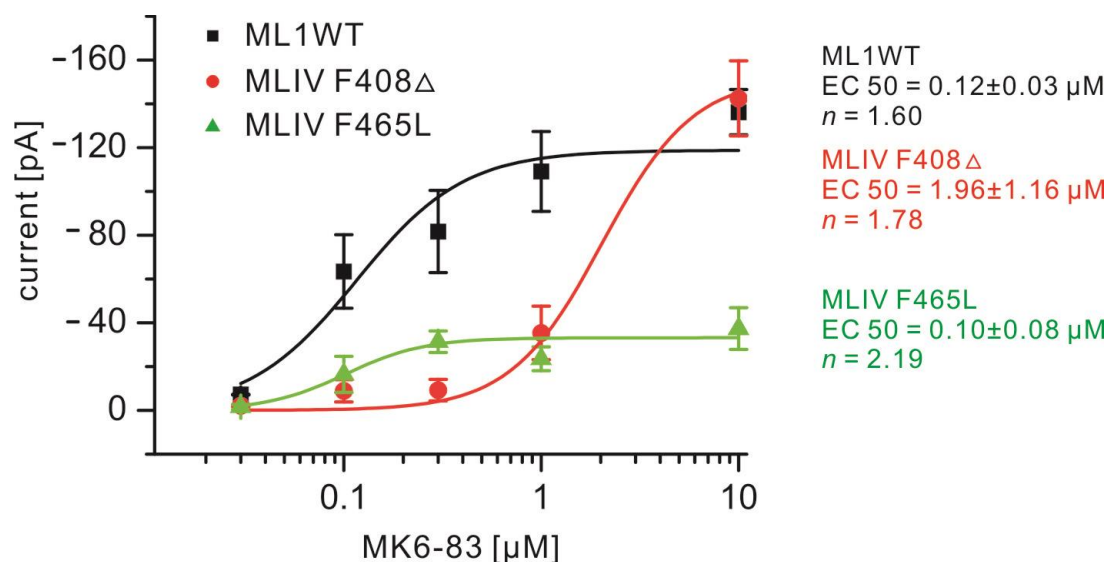


Figure 21: Dose-response curves for MK6-83 effect on TRPML1 WT and mutant channels. Dose-response relationships determined at extralysosomal MK6-83 from whole-lysosome planar patch-clamp experiments from HEK293 cells overexpressing TRPML1 and MLIV mutants. Statistics of current amplitudes at -200mV. Data are presented as mean \pm SEM.

In addition, it was found that F465L has lost its pH sensitivity when activated with SF-22 or MK6-83 in pH 4.6 (luminal) versus pH 7.2 (luminal), while F408Δ showed similar pH sensitivity as WT TRPML1 (**Fig. 22**). Furthermore, the synergistic effect of SF-22 and PI(3,5)P₂ was monitored by recording evoked over-expressing WT TRPML1 with direct whole-lysosome patch-clamp experiments. In contrast, the recordings of SF-22 and MK6-83 show non-synergistic effect, most likely due to competition for the same binding site (**Fig. 23**).

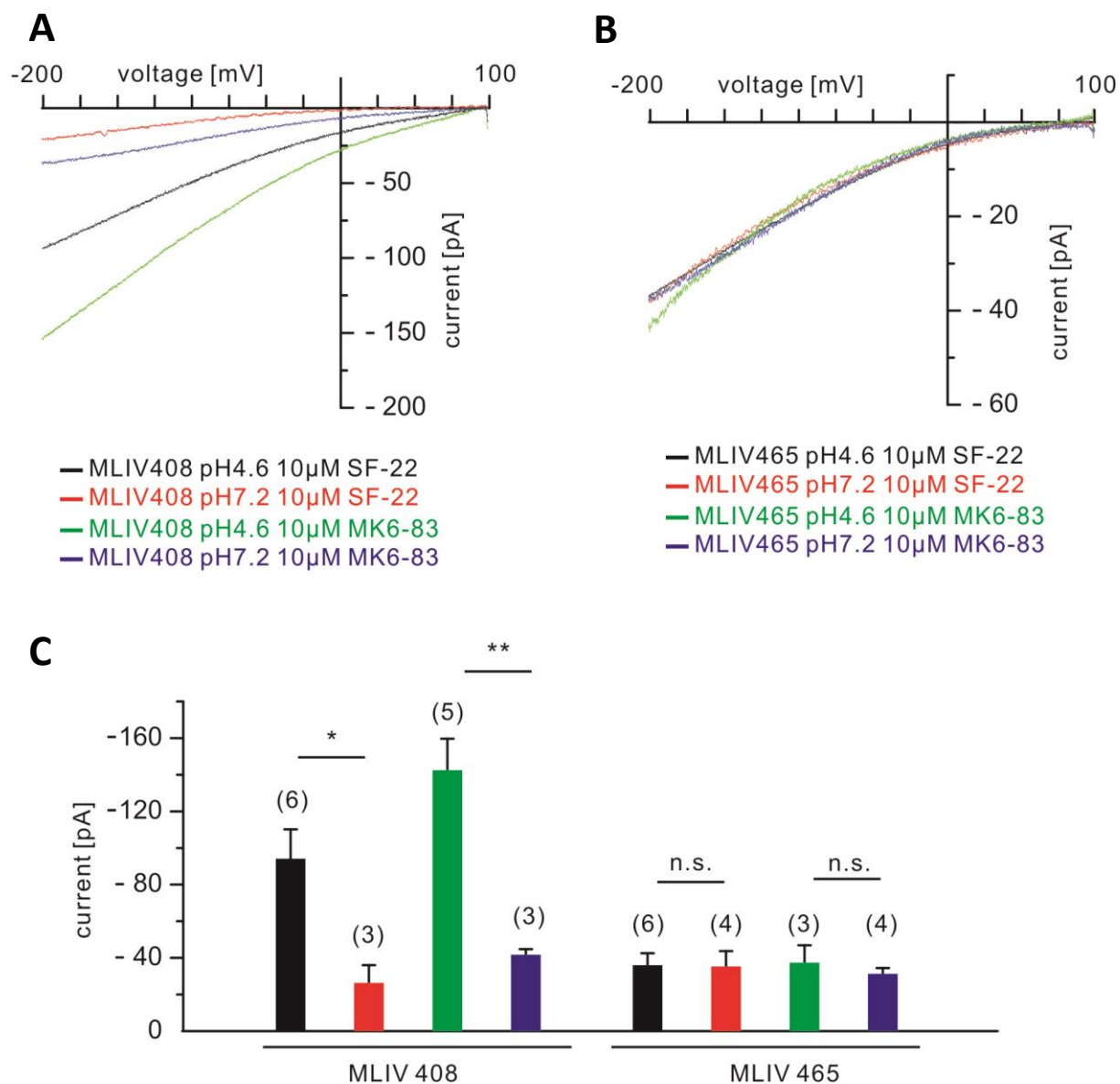
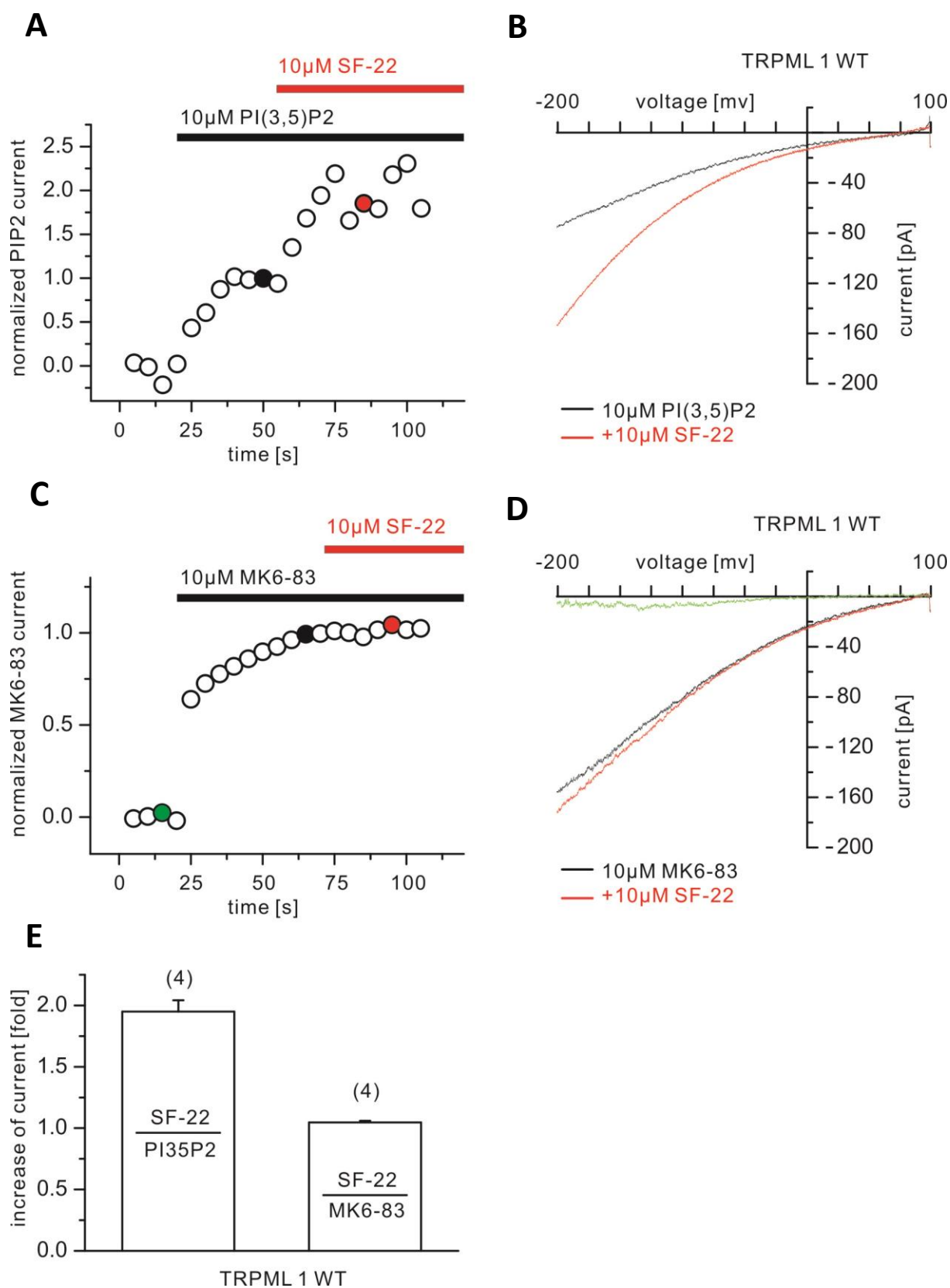


Figure 22: pH sensitivity of TRPML1 mutant channels function. Current-voltage relations of whole-endolysosome planar patch-clamp experiments from HEK293 cells overexpressed TRPML1 and MLIV demonstrating that (A) the effect of MK6-83 and SF-22 on the channel activity of TRPML1 mutant isoform F408 Δ is enhanced by a reduction of pH. (B) No effect of luminal pH on the inward current of F465L. Data are presented as mean \pm SEM. Numbers of lysosomes are in parentheses.



HEK293 overexpressed TRPML1 WT. Currents were measured at -200 mV and normalized to the current before application of 10 μ M SF-22. Application of 10 μ M PI(3,5)P₂ and SF-22 is indicated by black and gray bars, respectively. Recordings at time points (indicated with color) were used for the current-voltage relationship in (B). (C) Application of small molecule activators MK6-83 (10 μ M) and SF-22 (10 μ M) is indicated by blue and light brown bars, respectively. Recordings at time points (indicated with color) were used for the current-voltage relationship in (D). (E) Bar diagram summarizing data. Data are presented as mean \pm SEM. Numbers of lysosomes are in parentheses.

3.2.4. Effect of MK6-83 on channel activity in ML IV patient derived cell lines

To test for in-vivo effects of the TRPML1 activating compounds, lysosomes were isolated from fibroblast cell lines derived from ML IV patients carrying either the F408 Δ , the R403C, or the V446L mutation. Human TRPML1^{+/+} (GM03440) and TRPML1^{-/-} (GM02048) fibroblast cell lines were used as positive and negative control, respectively. In line with the above described results for overexpressing HEK293 cells, lysosomes isolated from TRPML1^{+/+} fibroblasts (WT) were activated by SF-22 and MK6-83. (**Fig. 24a-b**). SF-22 or MK6-83 had no significant effect on lysosomes isolated from TRPML1^{-/-} fibroblasts. The measurements were performed at a luminal pH of 4.6. Lysosomes isolated from R403C or V446L expressing cells showed only little activation by SF-22 or MK6-83 while F408 Δ showed activation similar to WT for both compounds (**Fig. 24c-f**). Notably, MK6-83 appeared to be significantly more efficacious on fibroblasts endogenously expressing R403C and V446L than on those isolated from TRPML1^{-/-} cells (**Fig. 24g**). PI(3,5)P₂ responses were still detectable in TRPML1^{-/-} lysosomes albeit reduced, confirming the presence of other PI(3,5)P₂ sensitive channels such as two-pore channels, in particular TPC2 (Wang et al., 2012) and possibly TRPML2 (**Fig. 24h-i**).

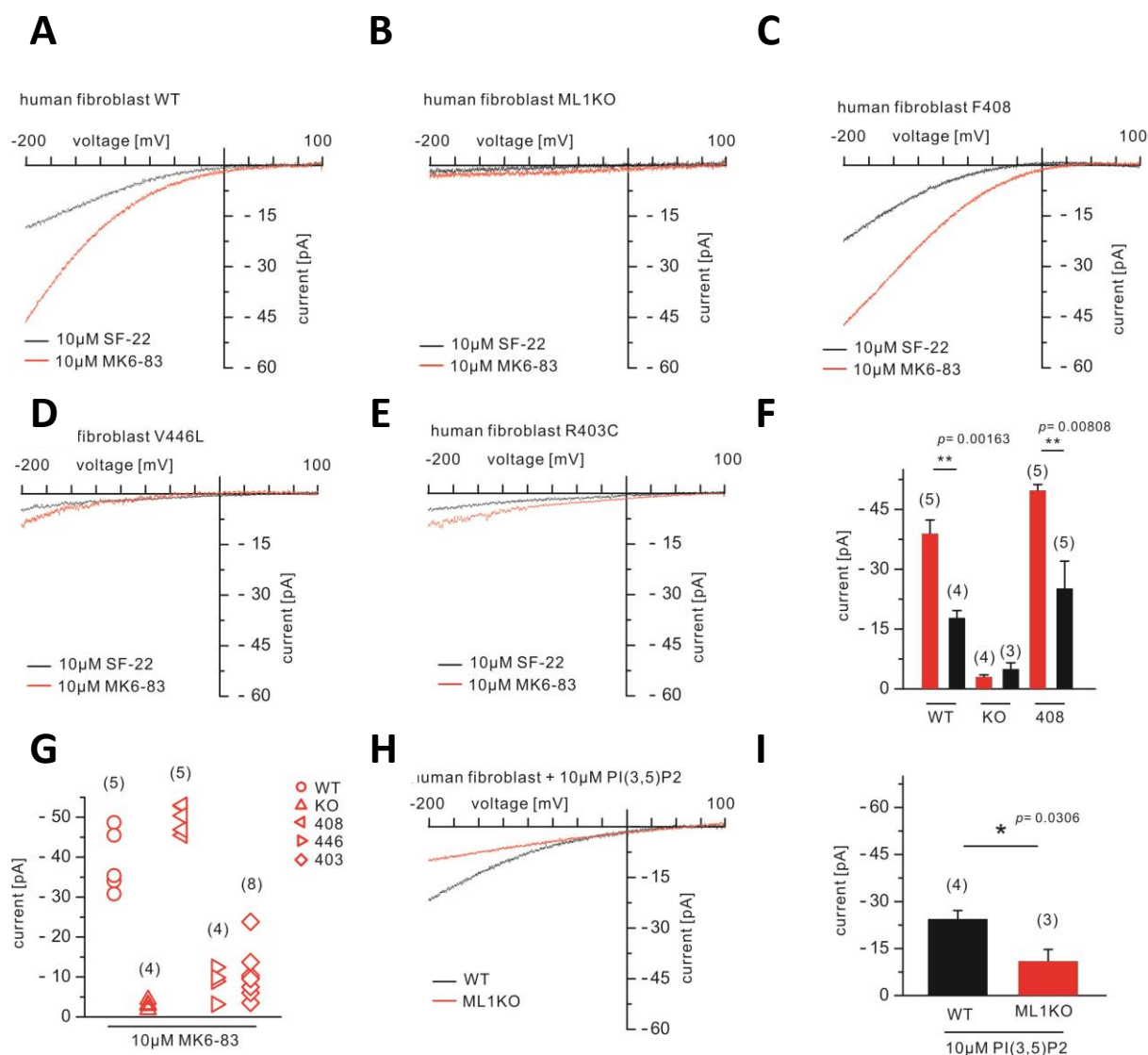


Figure 24: SF-22 and MK6-83 currents in human fibroblasts. Representative currents elicited in lysosomes isolated from human fibroblast cells derived from healthy individuals (A) and individuals with mutations in TRPML1 causing ML IV such as TRPML1^{-/-} (B), F408 Δ (C), V446L (D) and R403C (E). (F) Bar diagram summarizing data at -200 mV from experiments shown in A-C. Recordings show were obtained with 10 μ M SF-22 and 10 μ M MK6-83, respectively. (G) Individual MK6-83 evoked currents are shown in the scatter plot. (H) PI(3,5)P2 evoked TPC2-like non-rectifying currents in endolysosomes isolated from TRPML1^{-/-} human fibroblast cells. (I) Bar diagram summarizing data at -200 mV from experiments shown in H. Data are presented as mean \pm SEM. Numbers of lysosomes are in parentheses.

4. Discussion

4.1. Direct whole-lysosome patch-clamp methods

The aim of this thesis was to investigate the channel activity of TPC2 and TRPML1 *in situ* in the lysosomal membrane via direct whole-lysosome patch-clamp methods. Whilst the channel recordings of native intracellular membranes by patch-clamping had already been published for limited types of intracellular organelles (Dingwall et al., 1992; Kasri et al., 2006; Ionescu et al., 2006; Foskett et al., 2007; Kinnally et al., 1992; Henry et al., 1996; Ballarin et al., 1996; Grigoriev et al., 2004), the presence of an ion channels responsible for releasing cations from the lysosomal system remained quite elusive. This thesis investigated the optimization of whole-lysosome recordings and allowed a direct comparison of two electrophysiological techniques used to measure TPC2 currents: modified whole-lysosome patch-clamp and whole-lysosome planar patch-clamp.

Previous attempts to electrophysiologically study on lysosomal channels have been unsuccessful, mainly because of the vacuole size range is from 0.1 to 1.2 μm . The first direct patch-clamp experiment on endosomes was achieved by introducing a hydrolysis-deficient mutant of SKD1/VPS4B (E235Q) into HEK293 cells (Saito et al., 2007). The initial study of a direct whole-lysosome recording by a modified whole-lysosome patch-clamp technique was the investigation of the iron release channel on late endosomes/lysosomes (Dong et al., 2008). In 2010, Schieder et al demonstrated a novel glass chop-based method to characterize lysosomal ion channels in lysosomes.

The two methodologies used in this thesis to measure currents through lysosomal TPC2 channels gave remarkably similar results. Nevertheless, both techniques show different advantages and disadvantages (**Table 2**).

	<i>Modified Whole-lysosome Patch-clamp</i>	<i>Whole-lysosome Planar Patch-clamp</i>
Average recordings per day	Average 1-2 recordings 5-10 enlarged lysosomes isolated	Average 1-2 recordings 3-5 enlarged lysosomes isolated
Advantages	1. Large amplitudes 2. Fast and visible patch	1. Stable and long-lasting 2. Auto suction patch*
Disadvantages	1. Suspended type of manipulator 2. Fatigued pipette manipulaton	1. Centrifuge-lysoprep (2 hours) 2. High concentration of CaF ₂ is necessary for giga sealing&
Success rate of independent lysosome recordings of TPC2 activation	95% lysosomes (NAADP)# 45% Plasma membrane (NAADP)#	43% lysosomes (NAADP) 84% lysosomes (PI(3,5)P2)

Table 2: Summary of advantages and disadvantages of two direct whole-lysosome recording approaches. *, Port-a-Patch air suction control system (Nanion, Munich, Germany). & refers to Schieder et al., 2010a, # refers to Jha et al., 2014.

From a physiological perspective, both methods preserve all luminal accessory and modulatory proteins until seal formation. Moreover, the complex array of phosphor and glycosphingolipids of lysosomal membranes were also preserved during recordings. Both approaches observed an identical capacitance (~ 1 pF) of enlarged lysosomes in vacuolin-treated cells (Wang et al., 2012; Cang et al., 2013), which corresponds to an enlarged lysosome diameter of 10 - 15 μm , if the lipid unit membrane capacitance is assumed to be 1 microfarad/cm². The results of PI(3,5)P2 evoked TPC2 cation currents from whole-lysosome planar patch-clamp recordings were comparable with modified whole-lysosome recordings. The recording success rate was similar with both methods.

The current amplitudes derived from planar patch-clamp were 1/3 \sim 1/10 smaller than the whole-lysosome recordings in modified whole-lysosome patch-clamp (**Table 3**). This can be attributed to

time-dependent rundowns of channels after the two hour lysosome preparation and multiple fast voltage ramps applied to form sealings, and dissimilar solution compositions.

	Cell type	Cang et al., 2013	Wang et al., 2012	Jha et al., 2014	Planar Patch-clamp [#]
PI(3,5)P2	Stable cells	HEK293	COS-1	COS-1	HEK293
	Blank	100 pA	100 pA		
	TPC2	1200 pA	1400 pA	2000 – 3000 pA **	100 pA
	TPC1	300 pA	1200 pA		
	Native cell				
	Macrophage	300 pA	200 pA		
	Cardiac myocyte	300 pA			
	Hepatocyte	400 pA			
	Fibroblast	150 pA			30 pA
NAADP	Stable TPC2	0*	0	200 pA **	60 pA
	Macrophage	0*			
	Fibroblast				10 pA

Table 3: TPC channel properties. Summary of channel amplitudes at -100 mV from modified whole-lysosome patch-clamp and planar patch-clamp experiments. *, 1 μ m PI(3,5)P2 and 1mM ATP-Mg in bath/cytosolic solutions. **, without Mg²⁺ in both solutions. #, without Mg²⁺_{cyto.}

The greatest drawback of whole-lysosome planar patch-clamp is high luminal calcium and external fluoride which limits the experimental solutions for whole-lysosome recordings. However, less background noise interference has been observed in planar patch-clamp experiments due to the solid-matrix planar glass chip and automatic suction control (Farre et al., 2007). Additionally, planar patch-clamp systems with internal perfusion have been demonstrated to completely exchange intracellular liquids in the whole-cell recording mode and to exchange luminal solutions of intracellular organelles in the whole-lysosome recording mode (Farre et al., 2007; Mergler et al., 2010; Zong et al., 2012). Thus both methodologies have their advantages and disadvantages and to fully understand the biophysical properties of ion channels on intact lysosome, these techniques can be used in parallel.

4.2 Characterization of TPC2 channels

TPC2 has been identified as a NAADP-regulated Ca^{2+} channel on lysosomes (Brailoiu et al., 2009; Calcraft et al., 2009; Zong et al., 2009; Pereira et al., 2011; Brailoiu et al., 2010; Yamaguchi et al. 2011; Pitt et al., 2010; Schieder et al., 2010a; Tugba Durlu-Kandilci et al., 2010). Nevertheless, two recent papers showed that TPC2-mediated currents are induced by PI(3,5)P₂, not NAADP (Wang et al., 2012; Cang et al., 2013). However, the latest findings of direct electrophysiological TPC2 channel studies help to resolve this contradiction by demonstrating NAADP-evoked TPC2 $\text{Ca}^{2+}/\text{Na}^{+}$ inward currents which are inhibited in the presence of Mg^{2+} ($\text{IC}_{50} = 0.13 \text{ mM}$). The inhibition by luminal Mg^{2+} is completely relieved by reducing luminal pH (Jha et al., 2014). All NAADP-evoked TPC2 currents in this thesis were obtained in absence of luminal Mg^{2+} . Another potential complication of this controversy of TPCs being NAADP-independent have recently pointed out by other groups (Morgan et al. 2013; Marchant et al. 2013; Churamani et al. 2013); e.g. TPCs tagged at the N-terminus render some TPC channels insensitive to NAADP. However, it is not obvious whether this modification affects NAADP sensitivity. Further clarification of this issue is required.

Isoform	Technique	Acid Lyso pH	Ca^{2+} $P_{\text{Ca}}/P_{\text{K}}$	K^{+} $P_{\text{K}}/P_{\text{Ca}}$	Na^{+} $P_{\text{Na}}/P_{\text{Ca}}$	Voltage-gated	NAADP-induced	Ref
hTPC1	Bilayer	↑ Po		$(P_{\text{K}}/P_{\text{Ba}}) = 2$		Yes	Yes	1
hTPC1	Bilayer	↑ Po	0.1	9	1	No	Yes	2
hTPC1	Modified Lyso Patch	↓ Po	0.5	2	200	Yes	No	3
hTPC2	Bilayer	↓ Po	3	0.3		No	Yes	4
hTPC2	Plasma membrane targeting		(40 pS)			No	Yes	5
mTPC2	Planar Patch	↑ Po	1000	0.001		No	Yes	6

h/m TPC2	Modified Lyso Patch	No effect	30	0.03	10	No	No	7
hTPC2	Modified Lyso Patch	No effect			(400 pA)	No	Yes	8
Macrophage WT	Modified Lyso Patch				$P_{Na}/P_K = 0.3$ or 9 (PI35P2)			3
MEF WT	Planar Patch		300	0.003	1.5		Yes	

Table 4: Permeability of TPC channel. Summary of TPC channel properties in artificial lipid bilayers, channels inserted into the plasma membrane, modified lysosomal patch-clamp or whole-lysosome planar patch-clamp. Detailed ionic conditions are described in the related references (1. Rybalchenko et al., 2012, 2. Pitt et al., 2014, 3. Cang et al., 2014, 4. Pitt et al., 2010, 5. Brailoiu et al., 2010, 6. Schieder et al., 2010, 7. Wang et al., 2012, 8. Jha et al., 2014).

A methodological complication is that the controversial observations regarding the NAADP effect on TPCs are based on different electrophysiological approaches. Wang et al. (2012) and Cang et al. (2013) showed that TPCs are NAADP-independent channels using the modified whole-lysosome patch-clamp. Most studies indicating that TPCs are NAADP-dependent channels used the planar patch-clamp and bilayer recording techniques (**Table 4**). Modified whole-lysosome patch-clamp and whole-lysosome planar patch-clamp use isolated intact lysosomes, but the whole-lysosome planar patch-clamp technique uses lysosomes isolated by lysosome preparation centrifugation protocol. The lysosome preparation for the whole-lysosome planar patch-clamp and the lysosomal protein purification for bilayer recordings show some common points, the high speed centrifugations (>14000g) and integrated protocols need more than 2 hours at low temperature (4°C). In the whole-lysosome patch-clamp experiment, enlarged lysosomes are isolated and patched beside the host cell (**Fig.5A**). In order to attach and patch lysosomes under steady state conditions, the isolated lysosome still links to the host cell with part of the cytoskeleton such as microtubules and microfilaments (Saito et al. 2007). **Figure 25** illustrates the model of a hypothesis that TPCs show NAADP-dependent gating under different electrophysiological conditions. X as an upstream regulator only exists in the cytoplasm, and has lost the binding with Y under whole-lysosome patch-clamp. Y as an additional regulator which locates on or close to the cytoskeleton or the lysosomal membrane, has lost the effect on TPCs after lysosome preparation or protein purification. That X-Y complexes regulate NAADP modulation of TPCs in vivo would be one of possible explanation for the NAADP modulation issue.

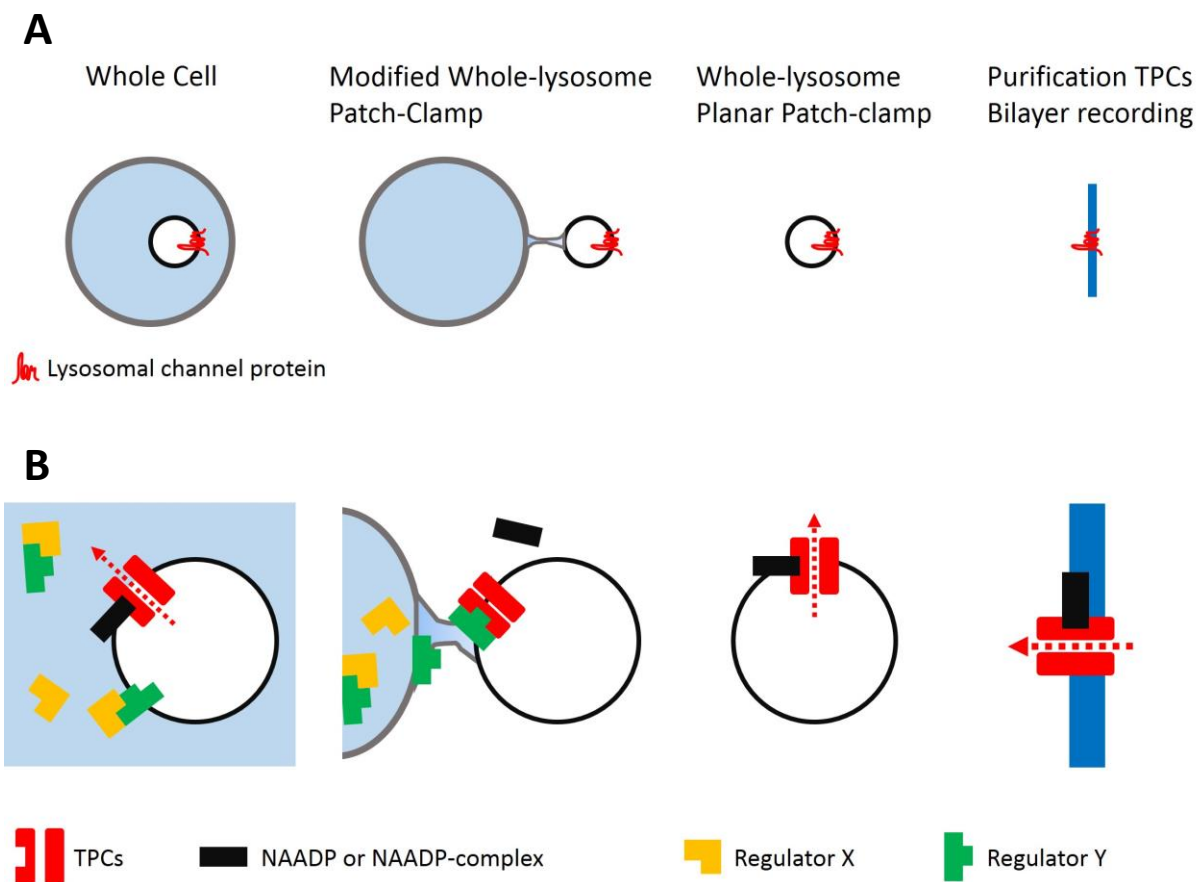


Figure 25: Model of hypothesis of different electrophysiological methods affect NAADP modulation of TPCs channel gating. (A) Three electrophysiological approaches were used to investigate lysosomal channels. Modified whole-lysosome patch-clamp is more direct recording than other methods. Lysosome preparation was applied to isolate pure lysosomes using multiple ultra centrifuge steps under cold temperature for planar patch-clamp. The purification of the recombinant TPC complexes which include multiple high speed centrifuge steps and cold incubation overnight, were applied for subsequent reconstitution into artificial membranes (Pitt et al. 2010; Rybalchenko et al., 2012, 2. Pitt et al., 2014). (B) The regulator X stays inside of host cell. Regulator Y remains on fresh isolated lysosome in modified whole-lysosome patch-clamp and NAADP or NAADP-complex dissociate from TPC channel. After few hours preparation or purification steps, Y doesn't exist in the recording environments of planar patch-clamp or bilayer recording.

Results of this thesis obtained with isolated lysosomes in planar patch-clamp experiments suggest that the binding sites for NAADP may be either on the TPC2 channels themselves or on tightly associated proteins, which is consistent with previous work of other research groups who characterized TPC function in a cellular or lysosomal setting and linked activation of TPCs directly to NAADP (Calcraft et al., 2009; Zong et al., 2009; Zhu et al., 2010; Jiang et al., 2013; Ogunbayo et al., 2011; Tugba Durlu-Kandilci et al., 2010). These data show a bell-shaped activation in response to a narrow nanomolar concentration range of NAADP and inhibition at micromolar concentrations. These data are in agreement with other TPC studies (Morgan et al., 2008; Zong et al., 2009; Schieder et al.,

2010a; Galione et al 2012; Guse et al., 2012; Arndt et al., 2014). Blockade of TPC2 channel activity in the enlarged lysosome was achieved by cytoplasmic application of 10 μ M NED-19 or 1 mM Mg-ATP. The antagonism by NED-19 supports the hypothesis of NAADP binding to TPC or the formation of a NAADP receptor complex with TPC2. Mg²⁺ binds to the ATP phosphate group as an energy carrier and coenzyme in cells (Saylor et al., 1998). The whole-lysosome planar patch-clamp study confirms the inhibition by Mg-ATP and confirming recent findings that TPC2 forms a lysosomal ATP-sensitive channel (Cang et al., 2013). However, TPC2 channels gated by intracellular ligands were not examined systematically under physiological conditions. It remains to be determined whether binding of NAADP and PI(3,5)P2 directly on TPC2 or other tightly associated proteins regulates TPC2 activity.

This thesis also demonstrates that NAADP-evoked TPC2-like currents in lysosomes from MEF WT under bi-ionic conditions results in the following ion permeabilities: $\text{Na}^+ \cong \text{Ca}^{2+} \gg \text{K}^+$. This is in agreement with a strong Ca²⁺-selectivity found by recent electrophysiological studies using the whole-lysosome planar patch-clamp technique in combination with overexpressed TPC2 in HEK293 cells ($P_{\text{Ca}}/P_{\text{K}} = >1000$) (Schieder et al., 2010a) as well as bilayer recordings with artificial lipid membrane systems ($P_{\text{Ca}}/P_{\text{K}} = >33$) (Pitt et al., 2010). Wang et al. recently showed Na⁺-selective TPCs currents in direct whole-lysosome recordings and proposed TPC2 is highly permeable for Na⁺ over K⁺ ($(P_{\text{Na}}/P_{\text{K}} = >33)$), relatively selective for Na⁺ over Ca²⁺ ($P_{\text{Ca}}/P_{\text{Na}} = 0.1$) and slightly selective for Ca²⁺ over K⁺ ($P_{\text{Ca}}/P_{\text{K}} = \{P_{\text{Ca}}/P_{\text{Na}}\} * \{P_{\text{Na}}/P_{\text{K}}\} = >3.3$) when overexpressed in COS cells (Wang et al., 2012) (**Table 4**). However, reportedly different expression levels may critically impact channel regulation, oligomerization states, and ion selectivity of e.g. TRP or Orai channels (Putney Jr. 2004, Thompson and Shuttleworth 2013). It is unclear whether heterologous over-expression systems truly replicate the properties of endogenous TPCs. The whole-lysosome recordings from MEF WT cells suggest that the endogenously expressed TPC2 channel is highly permeable for Na⁺ and Ca²⁺, and less for K⁺. Jha et al. recently proposed NAADP-mediated TPC2 is Na⁺ permeable and inhibited by Mg²⁺ (Jha et al., 2014). Further electrophysiological studies will be necessary to clarify these issues.

4.3 Towards a treatment for MLIV disease

The whole-lysosome planar patch-clamp approach was applied in this study to demonstrate the effect of mucopolipidosis type IV causing mutations on TRPML1 channel activity. Overexpressing mutant isoforms F408 Δ , F465L, and Y436C in HEK293 cells show predominant colocalization with lysosomal marker. Endogenous phosphoinositide PI(3,5)P2 evoked inward currents in lysosomes overexpressing WT TRPML1 are significantly smaller in lysosomes overexpressing the mutant isoforms F408 Δ and F465L. Slightly larger PI(3,5)P2 evoked inward currents were detected for the

mutant isoform F408 Δ . Patients carrying the F408 Δ mutation also have a relatively mild phenotype (Altarescu et al., 2002; Bargal et al., 2002). On the other hand, the Y436C mutation showed almost no response, although the subcellular localization pattern of this mutant was similar to F408 Δ and F465L or even WT TRPML1. However, patients carrying the Y436C mutation were reported to have a severe phenotype which would be in line with these findings (AlBakheet et al., 2013). Taken together, these results suggest that MLIV mutations significantly impair the channel gating of TRPML1. The degree of the impaired channel activity highly correlates with disease severity observed in MLIV patients.

F408 is predicted to reside at the lower end of TMD4 or shortly after TMD4. F465 resides in the highly conserved pore helix region. The potency and efficacy data from dose-response relationships indicate that loss of phenylalanine at position F408 has an effect on the binding affinity of small chemical compounds: SF22 and MK6-83. F465L shows a similar potency of the small chemical agonists compared with WT but a lower efficacy, which suggests that F465L causes severe alterations in the pore region of the channel. Furthermore, F465L shows a loss of the pH sensitivity, which is in line with previous studies on TRP channels suggesting residues of the pore region are critical for pH activation/potentialiation (Jordt et al., 2000; Ryu et al., 2007; Aneiros et al., 2011). The cytoplasmic N terminus of TRPML1 contains a poly-basic region and clusters of positively charged amino-acid residues were suggested as a potential PI(3,5)P₂-binding site (Dong et al., 2010). Interestingly, the dose-response curves of F408 Δ , F465L and WT show similar potencies for PI(3,5)P₂, which further confirms that the PI(3,5)P₂ binding position might reside away from the pore region. These results are also in accordance with the synergistic effect seen with small molecule activators and PI(3,5)P₂.

Y436C is located in the center of TMD5 of TRPML1. Recent studies have shown that TMD5 mutations in TRPML channels have a critical impact on channel gating (varitint-waddler mutant isoforms and analogues). Mutation of V432 to proline in TRPML1 results in a strong constitutive activity (Grimm et al., 2007; Dong et al., 2009). Moreover, C430 and C431 when mutated to proline were found to be constitutively active. In contrast, V432P rendered the channel inactive (Dong et al., 2009). Similarly, Y436C may render the channel inactive by a mechanism which cannot be overcome by compounds of the SF-22 type.

Direct whole-lysosome recordings from patient fibroblasts indicate that MK6-83 has effects not only on F408 Δ but also slight effects on R403C or V446L expressing fibroblasts. Amplitudes of inwardly rectifying TRPML-like currents higher than 10 pA were recorded in 2 out of 4 lysosomes from V446L, and in 3 out of 8 lysosomes from R403C. The effect on the mutant isoforms R403C and V446L was unexpected since after overexpression these two mutants were barely detectable in isolated lysosomes as outlined above. However, as expected no MK6-83 evoked inward currents could be observed in lysosomes isolated from TRPML1^{-/-} fibroblasts. These data imply MK6-83 can possibly

also be considered as a potential compound for the treatment of different MLIV mutant carriers in the future. The TRPML1 activators of the SF-22 type are thus remarkable candidates to restore channel activity of certain MLIV mutants.

5. Summary

This thesis demonstrates and modifies the first successful application of two novel electrophysiological techniques to investigate the *in situ* properties of lysosomal ion channels in whole lysosomes worldwide. This thesis draws a parallel between the modified whole-lysosome patch-clamp and whole-lysosome planar patch-clamp methods. Both methodologies are access to characterize the biophysical properties of lysosomal ion channels efficiently.

The major focus of this thesis was to study the channel properties of TPC2 and TRPML1 in lysosomes. These two channels belong to a superfamily of transient receptor potential channels and are expressed in the endolysosomal system. The TPC2 channel was recorded and functionally characterized as a NAADP-dependent cation permeable channel which showed high sodium and partial calcium selectivity. A bell-shaped dose-response relationship of the NAADP-evoked TPC2-like currents in lysosomes from native mouse embryonic fibroblasts was found.

The endolysosome-located lipid phosphatidylinositol 3,5-bisphosphate [PI(3,5)P₂] activated both TPC2 and TRPML1. Furthermore, TRPML1 currents were also activated by synthetic ligands in a pH dependent manner with maximal current amplitude at pH 4.6 in isolated enlarged lysosomes. Mutations in the TRPML1 gene are causative for MLIV which is an autosomal recessive lysosomal storage disorder. Using the whole-lysosome planar patch-clamp technique, activation of MLIV mutant isoforms by the endogenous ligand PI(3,5)P₂ is strongly reduced, while activity can be increased using synthetic ligands such as SF-22 and MK6-83. These data also suggest that the F465L mutation of TRPML1 renders pH insensitive, while F408Δ impacts synthetic ligand binding. These results demonstrate that small molecules can be used to restore channel function and rescue disease associated abnormalities in patient cells expressing specific MLIV point mutations.

6. Literature

- AlBakheet A, Qari A, Colak D, Rasheed A, Kaya N, Al-Sayed M. A novel mutation in a large family causes a unique phenotype of Mucopolysaccharidosis IV. *Gene*. 2013 Sep 10;526(2):464-6.
- Altarescu G, Sun M, Moore DF, Smith JA, Wiggs EA, Solomon BI, Patronas NJ, Frei KP, Gupta S, Kaneski CR, Quarrell OW, Slaugenhaupt SA, Goldin E, Schiffmann R. The neurogenetics of mucopolysaccharidosis type IV. *Neurology*. 2002 Aug 13;59(3):306-13.
- Aneiros E, Cao L, Papakosta M, Stevens EB, Phillips S, Grimm C. The biophysical and molecular basis of TRPV1 proton gating. *EMBO J*. 2011 Mar 16;30(6):994-1002.
- Anzai K, Masumi M, Kawasaki K, Kirino Y. Frequent fusion of liposomes to a positively charged planar bilayer without calcium ions. *J Biochem*. 1993 Oct;114(4):487-91.
- Arndt L, Castonguay J, Arlt E, Meyer D, Hassan S, Borth H, Zierler S, Wennemuth G, Breit A, Biel M, Wahl-Schott C, Gudermann T, Klugbauer N, Boehhoff I. NAADP and the two-pore channel protein 1 participate in the acrosome reaction in mammalian spermatozoa. *Mol Biol Cell*. 2014 Mar;25(6):948-64.
- Ballarin C, Sorgato MC. Anion channels of the inner membrane of mammalian and yeast mitochondria. *J Bioenerg Biomembr*. 1996 Apr;28(2):125-30.
- Bargal R, Avidan N, Ben-Asher E, Olender Z, Zeigler M, Frumkin A, Raas-Rothschild A, Glusman G, Lancet D, Bach G. Identification of the gene causing mucopolysaccharidosis type IV. *Nat Genet*. 2000 Sep;26(1):118-23.
- Bassi MT, Manzoni M, Monti E, Pizzo MT, Ballabio A, Borsani G. Cloning of the gene encoding a novel integral membrane protein, mucopolysaccharidin-IV and identification of the two major founder mutations causing mucopolysaccharidosis type IV. *Am J Hum Genet*. 2000 Nov;67(5):1110-20.
- Beck A, Kolisek M, Bagley LA, Fleig A, Penner R. Nicotinic acid adenine dinucleotide phosphate and cyclic ADP-ribose regulate TRPM2 channels in T lymphocytes. *FASEB J*. 2006 May;20(7):962-4.
- Berridge G, Dickinson G, Parrington J, Galione A, Patel S. Solubilization of receptors for the novel Ca²⁺-mobilizing messenger, nicotinic acid adenine dinucleotide phosphate. *J Biol Chem*. 2002 Nov 15;277(46):43717-23.
- Berridge MJ, Lipp P, Bootman MD. Signal transduction. The calcium entry pas de deux. *Science*. 2000 Mar 3;287(5458):1604-5.
- Berridge MJ, Bootman MD, Roderick HL. Calcium signalling: dynamics, homeostasis and remodelling. *Nat Rev Mol Cell Biol*. 2003 Jul;4(7):517-29.
- Bertl A, Gradmann D, Slayman CL. Calcium- and voltage-dependent ion channels in *Saccharomyces cerevisiae*. *Philos Trans R Soc Lond B Biol Sci*. 1992 Oct 29;338(1283):63-72.
- Bonangelino CJ, Nau JJ, Duex JE, Brinkman M, Wurmser AE, Gary JD, Emr SD, Weisman LS. Osmotic stress-induced increase of phosphatidylinositol 3,5-bisphosphate requires Vac14p, an activator of the lipid kinase Fab1p. *J Cell Biol*. 2002 Mar 18;156(6):1015-28.
- Bonner OD. Study of methanesulfonates and trifluoromethanesulfonates. Evidence for hydrogen bonding to the trifluoro group. *J. Am. Chem. Soc.*, 1981, 103 (12), 3262–3265

Bonifacino JS, Dell'Angelica EC. Molecular bases for the recognition of tyrosine-based sorting signals. *J Cell Biol.* 1999 May 31;145(5):923-6.

Bonifacino JS, Traub LM. Signals for sorting of transmembrane proteins to endosomes and lysosomes. *Annu Rev Biochem.* 2003;72:395-447.

Botelho RJ, Efe JA, Teis D, Emr SD. Assembly of a Fab1 phosphoinositide kinase signaling complex requires the Fig4 phosphoinositide phosphatase. *Mol Biol Cell.* 2008 Oct;19(10):4273-86.

Brailoiu E, Hooper R, Cai X, Brailoiu GC, Keebler MV, Dun NJ, Marchant JS, Patel S. An ancestral deuterostome family of two-pore channels mediates nicotinic acid adenine dinucleotide phosphate-dependent calcium release from acidic organelles. *J Biol Chem.* 2010 Jan 29;285(5):2897-901.

Brailoiu E, Churamani D, Cai X, Schrlau MG, Brailoiu GC, Gao X, Hooper R, Boulware MJ, Dun NJ, Marchant JS, Patel S. Essential requirement for two-pore channel 1 in NAADP-mediated calcium signaling. *J Cell Biol.* 2009 Jul 27;186(2):201-9.

Brailoiu E, Rahman T, Churamani D, Prole DL, Brailoiu GC, Hooper R, Taylor CW, Patel S. An NAADP-gated two-pore channel targeted to the plasma membrane uncouples triggering from amplifying Ca²⁺ signals. *J Biol Chem.* 2010 Dec 3;285(49):38511-6.

Cai X, Patel S. Degeneration of an intracellular ion channel in the primate lineage by relaxation of selective constraints. *Mol Biol Evol.* 2010 Oct;27(10):2352-9.

Calcraft PJ, Ruas M, Pan Z, Cheng X, Arredouani A, Hao X, Tang J, Rietdorf K, Teboul L, Chuang KT, Lin P, Xiao R, Wang C, Zhu Y, Lin Y, Wyatt CN, Parrington J, Ma J, Evans AM, Galione A, Zhu MX. NAADP mobilizes calcium from acidic organelles through two-pore channels. *Nature.* 2009 May 28;459(7246):596-600.

Cancela JM, Churchill GC, Galione A. Coordination of agonist-induced Ca²⁺-signalling patterns by NAADP in pancreatic acinar cells. *Nature.* 1999 Mar 4;398(6722):74-6.

Cang C, Zhou Y, Navarro B, Seo YJ, Aranda K, Shi L, Battaglia-Hsu S, Nissim I, Clapham DE, Ren D. mTOR regulates lysosomal ATP-sensitive two-pore Na⁽⁺⁾ channels to adapt to metabolic state. *Cell.* 2013 Feb 14;152(4):778-90.

Cantiello HF, Montalbetti N, Goldmann WH, Raychowdhury MK, González-Perrett S, Timpanaro GA, Chasan B. Cation channel activity of mucolipin-1: the effect of calcium. *Pflugers Arch.* 2005 Oct;451(1):304-12. Epub 2005 Aug 23.

Carafoli E, Santella L, Branca D, Brini M. Generation, control, and processing of cellular calcium signals. *Crit Rev Biochem Mol Biol.* 2001 Apr;36(2):107-260.

C.-C. Chen, M. Keller, M. Hess, R. Schiffmann, N. Urban, Michael Schaefer, F. Bracher, M. Biel, C. A. Wahl-Schott, and C. Grimm. A small molecule to restore function of TRPML1 mutant isoforms causing mucopolipidosis type IV. *Nature Communication* 2014 Aug;14;5:4681.

Chen CS, Bach G, Pagano RE. Abnormal transport along the lysosomal pathway in mucopolipidosis, type IV disease. *Proc Natl Acad Sci U S A.* 1998 May 26;95(11):6373-8.

- Cheng X, Shen D, Samie M, Xu H. Mucopolipins: Intracellular TRPML1-3 channels. *FEBS Lett.* 2010 May 17;584(10):2013-21.
- Chow CY, Zhang Y, Dowling JJ, Jin N, Adamska M, Shiga K, Szigeti K, Shy ME, Li J, Zhang X, Lupski JR, Weisman LS, Meisler MH. Mutation of FIG4 causes neurodegeneration in the pale tremor mouse and patients with CMT4J. *Nature.* 2007 Jul 5;448(7149):68-72.
- Christensen KA, Myers JT, Swanson JA. pH-dependent regulation of lysosomal calcium in macrophages. *J Cell Sci.* 2002 Feb 1;115(Pt 3):599-607.
- Churamani D, Hooper R, Rahman T, Brailoiu E, Patel S. The N-terminal region of two-pore channel 1 regulates trafficking and activation by NAADP. *Biochem J.* 2013 Jul 1;453(1):147-51.
- Clapham DE. Calcium signaling. *Cell.* 2007 Dec 14;131(6):1047-58.
- Cohn DV, Bawdon R, Newman RR, Hamilton JW. Effect of calcium chelation on the ion content of liver mitochondria in carbon tetrachloride-poisoned rats. *J Biol Chem.* 1968 Mar 25;243(6):1089-95.
- Dani JA, Sanchez JA, Hille B. Lyotropic anions. Na channel gating and Ca electrode response. *J Gen Physiol.* 1983 Feb;81(2):255-81.
- Davis LC, Morgan AJ, Chen JL, Snead CM, Bloor-Young D, Shenderov E, Stanton-Humphreys MN, Conway SJ, Churchill GC, Parrington J, Cerundolo V, Galione A. NAADP activates two-pore channels on T cell cytolytic granules to stimulate exocytosis and killing. *Curr Biol.* 2012 Dec 18;22(24):2331-7.
- de Duve C, Pressman BC, Gianetto R, Wattiaux R, and Appelmans F. Tissue fractionation studies. 6. Intracellular distribution patterns of enzymes in rat-liver tissue. *Biochem J.* 1955 Aug;60(4):604-17.
- de Duve C. The lysosome. *Sci Am.* 1963 May;208:64-72.
- de Duve C. The lysosome turns fifty. *Nat Cell Biol.* 2005 Sep;7(9):847-9.
- Di Palma F, Belyantseva IA, Kim HJ, Vogt TF, Kachar B, Noben-Trauth K. Mutations in Mcoln3 associated with deafness and pigmentation defects in varitint-waddler (Va) mice. *Proc Natl Acad Sci U S A.* 2002 Nov 12;99(23):14994-9.
- Di Paolo G, De Camilli P. Phosphoinositides in cell regulation and membrane dynamics. *Nature.* 2006 Oct 12;443(7112):651-7.
- Dingwall C, Laskey R. The nuclear membrane. *Science.* 1992 Nov 6;258(5084):942-7.
- Dionisio N, Albarrán L, López JJ, Berna-Erro A, Salido GM, Bobe R, Rosado JA. Acidic NAADP-releasable Ca(2+) compartments in the megakaryoblastic cell line MEG01. *Biochim Biophys Acta.* 2011 Aug;1813(8):1483-94.
- Dong XP, Cheng X, Mills E, Delling M, Wang F, Kurz T, Xu H. The type IV mucopolipidosis-associated protein TRPML1 is an endolysosomal iron release channel. *Nature.* 2008 Oct 16;455(7215):992-6.
- Dong XP, Wang X, Shen D, Chen S, Liu M, Wang Y, Mills E, Cheng X, Delling M, Xu H. Activating mutations of the TRPML1 channel revealed by proline-scanning mutagenesis. *J Biol Chem.* 2009 Nov 13;284(46):32040-52.

Dong XP, Shen D, Wang X, Dawson T, Li X, Zhang Q, Cheng X, Zhang Y, Weisman LS, Delling M, Xu H. PI(3,5)P₂ controls membrane trafficking by direct activation of mucolipin Ca²⁺ release channels in the endolysosome. *Nat Commun.* 2010 Jul 13;1:38.

Dove SK, Michell RH. Inositol lipid-dependent functions in *Saccharomyces cerevisiae*: analysis of phosphatidylinositol phosphates. *Methods Mol Biol.* 2009;462:59-74.

Duex JE, Tang F, Weisman LS. The Vac14p-Fig4p complex acts independently of Vac7p and couples PI₃,5P₂ synthesis and turnover. *J Cell Biol.* 2006 Feb 27;172(5):693-704.

Duex JE, Nau JJ, Kauffman EJ, Weisman LS. Phosphoinositide 5-phosphatase Fig 4p is required for both acute rise and subsequent fall in stress-induced phosphatidylinositol 3,5-bisphosphate levels. *Eukaryot Cell.* 2006 Apr;5(4):723-31.

Eder P, Schindl R, Romanin C, Groschner K. Protein-Protein Interactions in TRPC Channel Complexes. In: Liedtke WB, Heller S, editors. *TRP Ion Channel Function in Sensory Transduction and Cellular Signaling Cascades*. Boca Raton (FL): CRC Press; 2007. Chapter 24.

Eichelsdoerfer JL, Evans JA, Slaugenhaupt SA, Cuajungco MP. Zinc dyshomeostasis is linked with the loss of mucopolidosis IV-associated TRPML1 ion channel. *J Biol Chem.* 2010 Nov 5;285(45):34304-8.

Erler I, Hirnet D, Wissenbach U, Flockerzi V, Niemeyer BA. Ca²⁺-selective transient receptor potential V channel architecture and function require a specific ankyrin repeat. *J Biol Chem.* 2004 Aug 13;279(33):34456-63.

Eskelinen EL, Tanaka Y, Saftig P. At the acidic edge: emerging functions for lysosomal membrane proteins. *Trends Cell Biol.* 2003 Mar;13(3):137-45.

Farre C, Stoelzle S, Haarmann C, George M, Brüggemann A, Fertig N. Automated ion channel screening: patch-clamping made easy. *Expert Opin Ther Targets.* 2007 Apr;11(4):557-65.

FATT P, GINSBORG BL. The ionic requirements for the production of action potentials in crustacean muscle fibres. *J Physiol.* 1958 Aug 6;142(3):516-43.

Favre I, Moczydlowski E. Simultaneous binding of basic peptides at intracellular sites on a large conductance Ca²⁺-activated K⁺ channel. Equilibrium and kinetic basis of negatively coupled ligand interactions. *J Gen Physiol.* 1999 Feb;113(2):295-320.

Foskett JK, White C, Cheung KH, Mak DO. Inositol trisphosphate receptor Ca²⁺ release channels. *Physiol Rev.* 2007 Apr;87(2):593-658.

Galione A, Evans AM, Ma J, Parrington J, Arredouani A, Cheng X, Zhu MX. The acid test: the discovery of two-pore channels (TPCs) as NAADP-gated endolysosomal Ca²⁺ release channels. *Pflugers Arch.* 2009 Sep;458(5):869-76.

Genazzani AA, Galione A. A Ca²⁺ release mechanism gated by the novel pyridine nucleotide, NAADP. *Trends Pharmacol Sci.* 1997 Apr;18(4):108-10.

Gerasimenko JV, Tepikin AV, Petersen OH, Gerasimenko OV. Calcium uptake via endocytosis with rapid release from acidifying endosomes. *Curr Biol.* 1998 Dec 3;8(24):1335-8.

Goldin E, Stahl S, Cooney AM, Kaneski CR, Gupta S, Brady RO, Ellis JR, Schiffmann R. Transfer of a mitochondrial DNA fragment to MCOLN1 causes an inherited case of mucopolipidosis IV. *Hum Mutat.* 2004 Dec;24(6):460-5.

Grabe M, Oster G. Regulation of organelle acidity. *J Gen Physiol.* 2001 Apr;117(4):329-44.

Grigoriev SM, Muro C, Dejean LM, Campo ML, Martinez-Caballero S, Kinnally KW. Electrophysiological approaches to the study of protein translocation in mitochondria. *Int Rev Cytol.* 2004;238:227-74.

Grimm C, Hassan S, Wahl-Schott C, Biel M. Role of TRPML and two-pore channels in endolysosomal cation homeostasis. *J Pharmacol Exp Ther.* 2012 Aug;342(2):236-44.

Grimm C, Barthmes M, Wahl-Schott C. TRPML3. *Handb Exp Pharmacol.* 2014;222:659-74.

Grimm C, Cuajungco MP, van Aken AF, Schnee M, Jörs S, Kros CJ, Ricci AJ, Heller S. A helix-breaking mutation in TRPML3 leads to constitutive activity underlying deafness in the varitint-waddler mouse. *Proc Natl Acad Sci U S A.* 2007 Dec 4;104(49):19583-8.

Grimm C, Jörs S, Saldanha SA, Obukhov AG, Pan B, Oshima K, Cuajungco MP, Chase P, Hodder P, Heller S. Small molecule activators of TRPML3. *Chem Biol.* 2010 Feb 26;17(2):135-48.

Haller T, Völkl H, Deetjen P, Dietl P. The lysosomal Ca²⁺ pool in MDCK cells can be released by ins(1,4,5)P₃-dependent hormones or thapsigargin but does not activate store-operated Ca²⁺ entry. *Biochem J.* 1996 Nov 1;319 (Pt 3):909-12.

Hay JC. Calcium: a fundamental regulator of intracellular membrane fusion? *EMBO Rep.* 2007 Mar;8(3):236-40.

Henry JP, Juin P, Vallette F, Thieffry M. Characterization and function of the mitochondrial outer membrane peptide-sensitive channel. *J Bioenerg Biomembr.* 1996 Apr;28(2):101-8.

Hentze MW, Muckenthaler MU, Andrews NC. Balancing acts: molecular control of mammalian iron metabolism. *Cell.* 2004 Apr 30;117(3):285-97.

Ho CY, Alghamdi TA, Botelho RJ. Phosphatidylinositol-3,5-bisphosphate: no longer the poor PIP₂. *Traffic.* 2012 Jan;13(1):1-8.

Holtzman E, Teichberg S, Abrahams SJ, Citkowitz E, Crain SM, Kawai N, Peterson ER. Notes on synaptic vesicles and related structures, endoplasmic reticulum, lysosomes and peroxisomes in nervous tissue and the adrenal medulla. *J Histochem Cytochem.* 1973 Apr;21(4):349-85.

Hooper R, Churamani D, Brailoiu E, Taylor CW, Patel S. Membrane topology of NAADP-sensitive two-pore channels and their regulation by N-linked glycosylation. *J Biol Chem.* 2011 Mar 18;286(11):9141-9.

Huang P, Zou Y, Zhong XZ, Cao Q, Zhao K, Zhu MX, Murrell-Lagnado R, Dong XP. P2X₄ Forms Functional ATP-activated Cation Channels on Lysosomal Membranes Regulated by Luminal pH. *J Biol Chem.* 2014 Jun 20;289(25):17658-17667.

Huynh C, Andrews NW. The small chemical vacuolin-1 alters the morphology of lysosomes without inhibiting Ca²⁺-regulated exocytosis. *EMBO Rep.* 2005 Sep;6(9):843-7.

Ikonomov OC, Sbrissa D, Delvecchio K, Xie Y, Jin JP, Rappolee D, Shisheva A. The phosphoinositide kinase PIKfyve is vital in early embryonic development: preimplantation lethality of PIKfyve^{-/-} embryos but normality of PIKfyve^{+/-} mice. *J Biol Chem.* 2011 Apr 15;286(15):13404-13.

Ionescu L, Cheung KH, Vais H, Mak DO, White C, Foskett JK. Graded recruitment and inactivation of single InsP3 receptor Ca²⁺-release channels: implications for quantal Ca²⁺ release. *J Physiol.* 2006 Jun 15;573(Pt 3):645-62.

Jat PS, Sharp PA. Large T antigens of simian virus 40 and polyomavirus efficiently establish primary fibroblasts. *J Virol.* 1986 Sep;59(3):746-50.

Jentsch TJ, Neagoe I, Scheel O. CLC chloride channels and transporters. *Curr Opin Neurobiol.* 2005 Jun;15(3):319-25.

Jha A, Ahuja M, Patel S, Brailoiu E, Muallem S. Convergent regulation of the lysosomal two-pore channel-2 by Mg²⁺, NAADP, PI(3,5)P₂ and multiple protein kinases. *EMBO J.* 2014 Mar 3;33(5):501-11.

Jiang YL, Lin AH, Xia Y, Lee S, Paudel O, Sun H, Yang XR, Ran P, Sham JS. Nicotinic acid adenine dinucleotide phosphate (NAADP) activates global and heterogeneous local Ca²⁺ signals from NAADP- and ryanodine receptor-gated Ca²⁺ stores in pulmonary arterial myocytes. *J Biol Chem.* 2013 Apr 12;288(15):10381-94.

Jordt SE, Tominaga M, Julius D. Acid potentiation of the capsaicin receptor determined by a key extracellular site. *Proc Natl Acad Sci U S A.* 2000 Jul 5;97(14):8134-9.

Kasri NN, Kocks SL, Verbert L, Hébert SS, Callewaert G, Parys JB, Missiaen L, De Smedt H. Up-regulation of inositol 1,4,5-trisphosphate receptor type 1 is responsible for a decreased endoplasmic-reticulum Ca²⁺ content in presenilin double knock-out cells. *Cell Calcium.* 2006 Jul;40(1):41-51.

Kerr MC, Wang JT, Castro NA, Hamilton NA, Town L, Brown DL, Meunier FA, Brown NF, Stow JL, Teasdale RD. Inhibition of the PtdIns(5) kinase PIKfyve disrupts intracellular replication of Salmonella. *EMBO J.* 2010 Apr 21;29(8):1331-47.

Kidane TZ, Sauble E, Linder MC. Release of iron from ferritin requires lysosomal activity. *Am J Physiol Cell Physiol.* 2006 Sep;291(3):C445-55.

Kim C. TRPV Family Ion Channels and Other Molecular Components Required for Hearing and Proprioception in *Drosophila*. In: Liedtke WB, Heller S, editors. *TRP Ion Channel Function in Sensory Transduction and Cellular Signaling Cascades*. Boca Raton (FL): CRC Press; 2007. Chapter 17.

Kim HJ, Yamaguchi S, Li Q, So I, Muallem S. Properties of the TRPML3 channel pore and its stable expansion by the Varitint-Waddler-causing mutation. *J Biol Chem.* 2010 May 28;285(22):16513-20.

Kim HJ, Soyombo AA, Tjon-Kon-Sang S, So I, Muallem S. The Ca²⁺ channel TRPML3 regulates membrane trafficking and autophagy. *Traffic.* 2009 Aug;10(8):1157-67.

Kinnally KW, Antonenko YN, Zorov DB. Modulation of inner mitochondrial membrane channel activity. *J Bioenerg Biomembr.* 1992 Feb;24(1):99-110.

Kiselyov K, Chen J, Rbaibi Y, Oberdick D, Tjon-Kon-Sang S, Shcheynikov N, Muallem S, Soyombo A. TRP-ML1 is a lysosomal monovalent cation channel that undergoes proteolytic cleavage. *J Biol Chem.* 2005 Dec 30;280(52):43218-23.

Kiselyov KK, Ahuja M, Rybalchenko V, Patel S, Muallem S. The intracellular Ca²⁺ channels of membrane traffic. *Channels (Austin).* 2012 Sep-Oct;6(5):344-51.

Koivusalo M, Steinberg BE, Mason D, Grinstein S. In situ measurement of the electrical potential across the lysosomal membrane using FRET. *Traffic.* 2011 Aug;12(8):972-82.

Korolchuk VI, Menzies FM, Rubinsztein DC. Mechanisms of cross-talk between the ubiquitin-proteasome and autophagy-lysosome systems. *FEBS Lett.* 2010 Apr 2;584(7):1393-8.

Kostyuk PG, Krishtal OA, Pidoplichko VI. Effect of internal fluoride and phosphate on membrane currents during intracellular dialysis of nerve cells. *Nature.* 1975 Oct 23;257(5528):691-3.

Ktistakis NT, Tooze SA. PIPing on lysosome tubes. *EMBO J.* 2013 Feb 6;32(3):315-7.

Kukic I, Lee JK, Coblenz J, Kelleher SL, Kiselyov K. Zinc-dependent lysosomal enlargement in TRPML1-deficient cells involves MTF-1 transcription factor and ZnT4 (Slc30a4) transporter. *Biochem J.* 2013 Apr 15;451(2):155-63.

Lange I, Penner R, Fleig A, Beck A. Synergistic regulation of endogenous TRPM2 channels by adenine dinucleotides in primary human neutrophils. *Cell Calcium.* 2008 Dec;44(6):604-15.

LaPlante JM, Falardeau J, Sun M, Kanazirska M, Brown EM, Slaugenhaupt SA, Vassilev PM. Identification and characterization of the single channel function of human mucolipin-1 implicated in mucopolipidosis type IV, a disorder affecting the lysosomal pathway. *FEBS Lett.* 2002 Dec 4;532(1-2):183-7.

LaPlante JM, Ye CP, Quinn SJ, Goldin E, Brown EM, Slaugenhaupt SA, Vassilev PM. Functional links between mucolipin-1 and Ca²⁺-dependent membrane trafficking in mucopolipidosis IV. *Biochem Biophys Res Commun.* 2004 Oct 1;322(4):1384-91.

Leanza L, Biasutto L, Managò A, Gulbins E, Zoratti M, Szabò I. Intracellular ion channels and cancer. *Front Physiol.* 2013 Sep 3;4:227

Lee HC. Cyclic ADP-ribose and nicotinic acid adenine dinucleotide phosphate (NAADP) as messengers for calcium mobilization. *J Biol Chem.* 2012 Sep 14;287(38):31633-40.

Lee JH, Yu WH, Kumar A, Lee S, Mohan PS, Peterhoff CM, Wolfe DM, Martinez-Vicente M, Massey AC, Sovak G, Uchiyama Y, Westaway D, Cuervo AM, Nixon RA. Lysosomal proteolysis and autophagy require presenilin 1 and are disrupted by Alzheimer-related PS1 mutations. *Cell.* 2010 Jun 25;141(7):1146-58.

Lev S, Zeevi DA, Frumkin A, Offen-Glasner V, Bach G, Minke B. Constitutive activity of the human TRPML2 channel induces cell degeneration. *J Biol Chem.* 2010 Jan 22;285(4):2771-82.

Li M, Yu Y, Yang J. Structural biology of TRP channels. *Adv Exp Med Biol.* 2011;704:1-23.

Li S, Nai Q, Lipina TV, Roder JC, Liu F. $\alpha 7$ nAChR/NMDAR coupling affects NMDAR function and object recognition. *Mol Brain*. 2013 Dec 20;6:58.

Li X, Wang X, Zhang X, Zhao M, Tsang WL, Zhang Y, Yau RG, Weisman LS, Xu H. Genetically encoded fluorescent probe to visualize intracellular phosphatidylinositol 3,5-bisphosphate localization and dynamics. *Proc Natl Acad Sci U S A*. 2013 Dec 24;110(52):21165-70.

Lin-Moshier Y, Walseth TF, Churamani D, Davidson SM, Slama JT, Hooper R, Brailoiu E, Patel S, Marchant JS. Photoaffinity labeling of nicotinic acid adenine dinucleotide phosphate (NAADP) targets in mammalian cells. *J Biol Chem*. 2012 Jan 20;287(4):2296-307.

Lloyd-Evans E, Morgan AJ, He X, Smith DA, Elliot-Smith E, Sillence DJ, Churchill GC, Schuchman EH, Galione A, Platt FM. Niemann-Pick disease type C1 is a sphingosine storage disease that causes deregulation of lysosomal calcium. *Nat Med*. 2008 Nov;14(11):1247-55.

Lloyd-Evans E, Waller-Evans H, Peterneva K, Platt FM. Endolysosomal calcium regulation and disease. *Biochem Soc Trans*. 2010 Dec;38(6):1458-64.

Luzio JP, Pryor PR, Bright NA. Lysosomes: fusion and function. *Nat Rev Mol Cell Biol*. 2007 Aug;8(8):622-32.

Mándi M, Tóth B, Timár G, Bak J. Ca^{2+} release triggered by NAADP in hepatocyte microsomes. *Biochem J*. 2006 Apr 15;395(2):233-8.

Manzoni M, Monti E, Bresciani R, Bozzato A, Barlati S, Bassi MT, Borsani G. Overexpression of wild-type and mutant mucopolin proteins in mammalian cells: effects on the late endocytic compartment organization. *FEBS Lett*. 2004 Jun 4;567(2-3):219-24.

Marchant JS, Patel S. Questioning regulation of two-pore channels by NAADP. *Messenger (Los Angel)*. 2013 Jun 1;2(2):113-119.

Marks DL, Holicky EL, Wheatley CL, Frumkin A, Bach G, Pagano RE. Role of protein kinase d in Golgi exit and lysosomal targeting of the transmembrane protein, Mcoln1. *Traffic*. 2012 Apr;13(4):565-75.

Masgrau R, Churchill GC, Morgan AJ, Ashcroft SJ, Galione A. NAADP: a new second messenger for glucose-induced Ca^{2+} responses in clonal pancreatic beta cells. *Curr Biol*. 2003 Feb 4;13(3):247-51.

Matsuzawa T, Hatano S, Ishiguro T, Kumamoto K, Baba H, Kumagai Y, Ishibashi K, Takeuchi I, Inokuma S, Ishida H. Strategy for surgery in familial adenomatous polyposis patients with invasive colorectal cancer. *Gan To Kagaku Ryoho*. 2013 Nov;40(12):2050-2. Japanese.

Mellman I. Organelles observed: lysosomes. *Science*. 1989 May 19;244(4906):853-4.

Mellman I, Fuchs R, Helenius A. Acidification of the endocytic and exocytic pathways. *Annu Rev Biochem*. 1986;55:663-700.

Mergler S, Valtink M, Coulson-Thomas VJ, Lindemann D, Reinach PS, Engelmann K, Pleyer U. TRPV channels mediate temperature-sensing in human corneal endothelial cells. *Exp Eye Res*. 2010 Jun;90(6):758-70.

- Merz AJ, Wickner WT. Trans-SNARE interactions elicit Ca²⁺ efflux from the yeast vacuole lumen. *J Cell Biol.* 2004 Jan 19;164(2):195-206.
- Michell RH, Heath VL, Lemmon MA, Dove SK. Phosphatidylinositol 3,5-bisphosphate: metabolism and cellular functions. *Trends Biochem Sci.* 2006 Jan;31(1):52-63.
- Miedel MT, Weixel KM, Bruns JR, Traub LM, Weisz OA. Posttranslational cleavage and adaptor protein complex-dependent trafficking of mucolipin-1. *J Biol Chem.* 2006 May 5;281(18):12751-9.
- Miedel MT, Rbaibi Y, Guerriero CJ, Colletti G, Weixel KM, Weisz OA, Kiselyov K. Membrane traffic and turnover in TRP-ML1-deficient cells: a revised model for mucopolipidosis type IV pathogenesis. *J Exp Med.* 2008 Jun 9;205(6):1477-90.
- Milton RL, Caldwell JH. Na current in membrane blebs: implications for channel mobility and patch-clamp recording. *J Neurosci.* 1990 Mar;10(3):885-93.
- Montal M, Mueller P. Formation of bimolecular membranes from lipid monolayers and a study of their electrical properties. *Proc Natl Acad Sci U S A.* 1972 Dec;69(12):3561-6.
- Morgan AJ, Platt FM, Lloyd-Evans E, Galione A. Molecular mechanisms of endolysosomal Ca²⁺ signalling in health and disease. *Biochem J.* 2011 Nov 1;439(3):349-74.
- Morgan AJ, Galione A. Two-pore channels (TPCs): current controversies. *Bioessays.* 2014 Feb;36(2):173-83.
- Nagata K, Zheng L, Madathany T, Castiglioni AJ, Bartles JR, García-Añoveros J. The varitint-waddler (Va) deafness mutation in TRPML3 generates constitutive, inward rectifying currents and causes cell degeneration. *Proc Natl Acad Sci U S A.* 2008 Jan 8;105(1):353-8.
- Naylor E, Arredouani A, Vasudevan SR, Lewis AM, Parkesh R, Mizote A, Rosen D, Thomas JM, Izumi M, Ganesan A, Galione A, Churchill GC. Identification of a chemical probe for NAADP by virtual screening. *Nat Chem Biol.* 2009 Apr;5(4):220-6.
- Neher E, Sakmann B. Single-channel currents recorded from membrane of denervated frog muscle fibres. *Nature.* 1976 Apr 29;260(5554):799-802.
- Neher E. Nobel lecture. Ion channels for communication between and within cells. *EMBO J.* 1992 May;11(5):1672-9.
- Nilius B. Transient receptor potential (TRP) cation channels: rewarding unique proteins. *Bull Mem Acad R Med Belg.* 2007;162(3-4):244-53.
- Nilius B, Mahieu F, Karashima Y, Voets T. Regulation of TRP channels: a voltage-lipid connection. *Biochem Soc Trans.* 2007 Feb;35(Pt 1):105-8.
- Novarino G, Weinert S, Rickheit G, Jentsch TJ. Endosomal chloride-proton exchange rather than chloride conductance is crucial for renal endocytosis. *Science.* 2010 Jun 11;328(5984):1398-401.
- Ogunbayo OA, Zhu Y, Rossi D, Sorrentino V, Ma J, Zhu MX, Evans AM. Cyclic adenosine diphosphate ribose activates ryanodine receptors, whereas NAADP activates two-pore domain channels. *J Biol Chem.* 2011 Mar 18;286(11):9136-40.

Owsianik G, D'hoedt D, Voets T, Nilius B. Structure-function relationship of the TRP channel superfamily. *Rev Physiol Biochem Pharmacol*. 2006;156:61-90.

Parkinson-Lawrence EJ, Shandala T, Prodoehl M, Plew R, Borlace GN, Brooks DA. Lysosomal storage disease: revealing lysosomal function and physiology. *Physiology (Bethesda)*. 2010 Apr;25(2):102-15.

Parnas H, Segel L, Dudel J, Parnas I. Autoreceptors, membrane potential and the regulation of transmitter release. *Trends Neurosci*. 2000 Feb;23(2):60-8.

Patel S, Muallem S. Acidic Ca(2+) stores come to the fore. *Cell Calcium*. 2011 Aug;50(2):109-12.

Peiter E, Maathuis FJ, Mills LN, Knight H, Pelloux J, Hetherington AM, Sanders D. The vacuolar Ca²⁺-activated channel TPC1 regulates germination and stomatal movement. *Nature*. 2005 Mar 17;434(7031):404-8.

Pereira GJ, Hirata H, Fimia GM, do Carmo LG, Bincoletto C, Han SW, Stilhano RS, Ureshino RP, Bloor-Young D, Churchill G, Piacentini M, Patel S, Smaili SS. Nicotinic acid adenine dinucleotide phosphate (NAADP) regulates autophagy in cultured astrocytes. *J Biol Chem*. 2011 Aug 12;286(32):27875-81.

Peters C, Mayer A. Ca²⁺/calmodulin signals the completion of docking and triggers a late step of vacuole fusion. *Nature*. 1998 Dec 10;396(6711):575-80

Pitt SJ, Funnell TM, Sitsapesan M, Venturi E, Rietdorf K, Ruas M, Ganesan A, Gosain R, Churchill GC, Zhu MX, Parrington J, Galione A, Sitsapesan R. TPC2 is a novel NAADP-sensitive Ca²⁺ release channel, operating as a dual sensor of luminal pH and Ca²⁺. *J Biol Chem*. 2010 Nov 5;285(45):35039-46.

Poccia D, Larijani B. Phosphatidylinositol metabolism and membrane fusion. *Biochem J*. 2009 Mar 1;418(2):233-46.

Pryor PR, Reimann F, Gribble FM, Luzio JP. Mucolipin-1 is a lysosomal membrane protein required for intracellular lactosylceramide traffic. *Traffic*. 2006 Oct;7(10):1388-98.

Puertollano R, Kiselyov K. TRPMLs: in sickness and in health. *Am J Physiol Renal Physiol*. 2009 Jun;296(6):F1245-54.

Putney JW Jr. The enigmatic TRPCs: multifunctional cation channels. *Trends Cell Biol*. 2004 Jun;14(6):282-6.

Qian A, Johnson JW. Permeant ion effects on external Mg²⁺ block of NR1/2D NMDA receptors. *J Neurosci*. 2006 Oct 18;26(42):10899-910.

Ramsey IS, Delling M, Clapham DE. An introduction to TRP channels. *Annu Rev Physiol*. 2006;68:619-47.

Raychowdhury MK, González-Perrett S, Montalbetti N, Timpanaro GA, Chasan B, Goldmann WH, Stahl S, Cooney A, Goldin E, Cantiello HF. Molecular pathophysiology of mucopolipidosis type IV: pH dysregulation of the mucolipin-1 cation channel. *Hum Mol Genet*. 2004 Mar 15;13(6):617-27.

Rietdorf K, Funnell TM, Ruas M, Heinemann J, Parrington J, Galione A. Two-pore channels form homo- and heterodimers. *J Biol Chem*. 2011 Oct 28;286(43):37058-62.

Robinson RA, Stokes RH. *Electrolyte Solutions: Second Revised Edition*. Courier Dover Publications. 2002

Rosen D, Lewis AM, Mizote A, Thomas JM, Aley PK, Vasudevan SR, Parkesh R, Galione A, Izumi M, Ganesan A, Churchill GC. Analogues of the nicotinic acid adenine dinucleotide phosphate (NAADP) antagonist Ned-19 indicate two binding sites on the NAADP receptor. *J Biol Chem.* 2009 Dec 11;284(50):34930-4.

Ruas M, Rietdorf K, Arredouani A, Davis LC, Lloyd-Evans E, Koegel H, Funnell TM, Morgan AJ, Ward JA, Watanabe K, Cheng X, Churchill GC, Zhu MX, Platt FM, Wessel GM, Parrington J, Galione A. Purified TPC isoforms form NAADP receptors with distinct roles for Ca²⁺ signaling and endolysosomal trafficking. *Curr Biol.* 2010 Apr 27;20(8):703-9.

Rybalchenko V, Ahuja M, Coblenz J, Churamani D, Patel S, Kiselyov K, Muallem S. Membrane potential regulates nicotinic acid adenine dinucleotide phosphate (NAADP) dependence of the pH- and Ca²⁺-sensitive organellar two-pore channel TPC1. *J Biol Chem.* 2012 Jun 8;287(24):20407-16.

Ryu S, Liu B, Yao J, Fu Q, Qin F. Uncoupling proton activation of vanilloid receptor TRPV1. *J Neurosci.* 2007 Nov 21;27(47):12797-807.

Saftig P, Klumperman J. Lysosome biogenesis and lysosomal membrane proteins: trafficking meets function. *Nat Rev Mol Cell Biol.* 2009 Sep;10(9):623-35.

Saito M, Hanson PI, Schlesinger P. Luminal chloride-dependent activation of endosome calcium channels: patch-clamp study of enlarged endosomes. *J Biol Chem.* 2007 Sep 14;282(37):27327-33.

Sakmann B. Nobel Lecture. Elementary steps in synaptic transmission revealed by currents through single ion channels. *Neuron.* 1992 Apr;8(4):613-29.

Samie MA, Xu H. Lysosomal exocytosis and lipid storage disorders. *J Lipid Res.* 2014 Mar 25;55(6):995-1009.

Samie MA, Grimm C, Evans JA, Curcio-Morelli C, Heller S, Slaugenhaupt SA, Cuajungco MP. The tissue-specific expression of TRPML2 (MCOLN-2) gene is influenced by the presence of TRPML1. *Pflugers Arch.* 2009 Nov;459(1):79-91.

Sandoval IV, Bakke O. Targeting of membrane proteins to endosomes and lysosomes. *Trends Cell Biol.* 1994 Aug;4(8):292-7.

Saylor P, Wang C, Hirai TJ, Adams JA. A second magnesium ion is critical for ATP binding in the kinase domain of the oncoprotein v-Fps. *Biochemistry.* 1998 Sep 8;37(36):12624-30.

Schaefer M. Homo- and heteromeric assembly of TRP channel subunits. *Pflugers Arch.* 2005 Oct;451(1):35-42. Epub 2005 Jun 22.

Schiaffino S, Hanzlíková V. Autophagic degradation of glycogen in skeletal muscles of the newborn rat. *J Cell Biol.* 1972 Jan;52(1):41-51.

Schieder M, Rötzer K, Brüggemann A, Biel M, Wahl-Schott CA. Characterization of two-pore channel 2 (TPCN2)-mediated Ca²⁺ currents in isolated lysosomes. *J Biol Chem.* 2010 Jul 9;285(28):21219-22.

Schieder M, Rötzer K, Brüggemann A, Biel M, Wahl-Schott C. Planar patch-clamp approach to characterize ionic currents from intact lysosomes. *Sci Signal.* 2010 Dec 7;3(151):pl3.

Schmidt R, Zimmermann H, Whittaker VP. Metal ion content of cholinergic synaptic vesicles isolated from the electric organ of *Torpedo*: effect of stimulation-induced transmitter release. *Neuroscience*. 1980;5(3):625-38.

Schöpfer K, Miebach E, Beck M, Pitz S. Lysosomal storage diseases - update and new therapeutic options. *Klin Monbl Augenheilkd*. 2011 Feb;228(2):144-60.

Shaughnessy LM, Swanson JA. The role of the activated macrophage in clearing *Listeria monocytogenes* infection. *Front Biosci*. 2007 Jan 1;12:2683-92.

Shen D, Wang X, Li X, Zhang X, Yao Z, Dibble S, Dong XP, Yu T, Lieberman AP, Showalter HD, Xu H. Lipid storage disorders block lysosomal trafficking by inhibiting a TRP channel and lysosomal calcium release. *Nat Commun*. 2012 Mar 13;3:731.

Shen D, Wang X, Xu H. Pairing phosphoinositides with calcium ions in endolysosomal dynamics: phosphoinositides control the direction and specificity of membrane trafficking by regulating the activity of calcium channels in the endolysosomes. *Bioessays*. 2011 Jun;33(6):448-57.

Sitsapesan R, Montgomery RA, MacLeod KT, Williams AJ. Sheep cardiac sarcoplasmic reticulum calcium-release channels: modification of conductance and gating by temperature. *J Physiol*. 1991 Mar;434:469-88.

Soyombo AA, Tjon-Kon-Sang S, Rbaibi Y, Bashllari E, Bisceglia J, Muallem S, Kiselyov K. TRP-ML1 regulates lysosomal pH and acidic lysosomal lipid hydrolytic activity. *J Biol Chem*. 2006 Mar 17;281(11):7294-301.

Sridhar S, Patel B, Aphkhasava D, Macian F, Santambrogio L, Shields D, Cuervo AM. The lipid kinase PI4KIII β preserves lysosomal identity. *EMBO J*. 2013 Feb 6;32(3):324-39.

Steinberg BE, Huynh KK, Brodovitch A, Jabs S, Stauber T, Jentsch TJ, Grinstein S. A cation counterflux supports lysosomal acidification. *J Cell Biol*. 2010 Jun 28;189(7):1171-86.

Sulem P, Gudbjartsson DF, Stacey SN, Helgason A, Rafnar T, Jakobsdottir M, Steinberg S, Gudjonsson SA, Palsson A, Thorleifsson G, Pálsson S, Sigurgeirsson B, Thorisdottir K, Ragnarsson R, Benediksdottir KR, Aben KK, Vermeulen SH, Goldstein AM, Tucker MA, Kiemenev LA, Olafsson JH, Gulcher J, et al. Two newly identified genetic determinants of pigmentation in Europeans. *Nat Genet*. 2008 Jul;40(7):835-7.

Sun M, Goldin E, Stahl S, Falardeau JL, Kennedy JC, Acierno JS Jr, Bove C, Kaneski CR, Nagle J, Bromley MC, Colman M, Schiffmann R, Slaugenhaupt SA. Mucopolipidosis type IV is caused by mutations in a gene encoding a novel transient receptor potential channel. *Hum Mol Genet*. 2000 Oct 12;9(17):2471-8.

Südhof TC. Neurotransmitter release. *Handb Exp Pharmacol*. 2008;(184):1-21.

Tank DW, Miller C, Webb WW. Isolated-patch recording from liposomes containing functionally reconstituted chloride channels from *Torpedo* electroplax. *Proc Natl Acad Sci U S A*. 1982 Dec;79(24):7749-53.

- Thompson JL, Shuttleworth TJ. How many Orai's does it take to make a CRAC channel? *Sci Rep*. 2013;3:1961.
- Treusch S, Knuth S, Slaugenhaupt SA, Goldin E, Grant BD, Fares H. *Caenorhabditis elegans* functional orthologue of human protein h-mucolipin-1 is required for lysosome biogenesis. *Proc Natl Acad Sci U S A*. 2004 Mar 30;101(13):4483-8.
- Trowbridge IS, Collawn JF, Hopkins CR. Signal-dependent membrane protein trafficking in the endocytic pathway. *Annu Rev Cell Biol*. 1993;9:129-61.
- Tugba Durlu-Kandilci N, Ruas M, Chuang KT, Brading A, Parrington J, Galione A. TPC2 proteins mediate nicotinic acid adenine dinucleotide phosphate (NAADP)-and agonist-evoked contractions of smooth muscle. *J Biol Chem*. 2010 Aug 6;285(32):24925-32.
- Tüysüz B, Goldin E, Metin B, Korkmaz B, Yalçinkaya C. Mucopolidosis type IV in a Turkish boy associated with a novel MCOLN1 mutation. *Brain Dev*. 2009 Oct;31(9):702-5.
- Valenzano KJ, Khanna R, Powe AC, Boyd R, Lee G, Flanagan JJ, Benjamin ER. Identification and characterization of pharmacological chaperones to correct enzyme deficiencies in lysosomal storage disorders. *Assay Drug Dev Technol*. 2011 Jun;9(3):213-35.
- Venkatachalam K, Montell C. TRP channels. *Annu Rev Biochem*. 2007;76:387-417.
- Venkatachalam K, Hofmann T, Montell C. Lysosomal localization of TRPML3 depends on TRPML2 and the mucopolidosis-associated protein TRPML1. *J Biol Chem*. 2006 Jun 23;281(25):17517-27.
- Vergarajauregui S, Puertollano R. Two di-leucine motifs regulate trafficking of mucolipin-1 to lysosomes. *Traffic*. 2006 Mar;7(3):337-53.
- Vergarajauregui S, Connelly PS, Daniels MP, Puertollano R. Autophagic dysfunction in mucopolidosis type IV patients. *Hum Mol Genet*. 2008 Sep 1;17(17):2723-37.
- Walseth TF, Lin-Moshier Y, Jain P, Ruas M, Parrington J, Galione A, Marchant JS, Slama JT. Photoaffinity labeling of high affinity nicotinic acid adenine dinucleotide phosphate (NAADP)-binding proteins in sea urchin egg. *J Biol Chem*. 2012 Jan 20;287(4):2308-15.
- Walseth TF, Lin-Moshier Y, Weber K, Marchant JS, Slama JT, Guse AH. Nicotinic Acid Adenine Dinucleotide 2'-Phosphate (NAADP) Binding Proteins in T-Lymphocytes. *Messenger (Los Angel)*. 2012 Jun 1;1(1):86-94.
- Wang X, Zhang X, Dong XP, Samie M, Li X, Cheng X, Goschka A, Shen D, Zhou Y, Harlow J, Zhu MX, Clapham DE, Ren D, Xu H. TPC proteins are phosphoinositide- activated sodium-selective ion channels in endosomes and lysosomes. *Cell*. 2012 Oct 12;151(2):372-83.
- Xu H, Delling M, Li L, Dong X, Clapham DE. Activating mutation in a mucolipin transient receptor potential channel leads to melanocyte loss in varitint-waddler mice. *Proc Natl Acad Sci U S A*. 2007 Nov 13;104(46):18321-6.
- Xu H, Jin J, DeFelice LJ, Andrews NC, Clapham DE. A spontaneous, recurrent mutation in divalent metal transporter-1 exposes a calcium entry pathway. *PLoS Biol*. 2004 Mar;2(3):E50.

- Yamaguchi S, Jha A, Li Q, Soyombo AA, Dickinson GD, Churamani D, Brailoiu E, Patel S, Muallem S. Transient receptor potential mucolipin 1 (TRPML1) and two-pore channels are functionally independent organellar ion channels. *J Biol Chem*. 2011 Jul 1;286(26):22934-42.
- Zeevi DA, Frumkin A, Offen-Glasner V, Kogot-Levin A, Bach G. A potentially dynamic lysosomal role for the endogenous TRPML proteins. *J Pathol*. 2009 Oct;219(2):153-62.
- Zhang F, Jin S, Yi F, Li PL. TRP-ML1 functions as a lysosomal NAADP-sensitive Ca²⁺ release channel in coronary arterial myocytes. *J Cell Mol Med*. 2009 Sep;13(9B):3174-85.
- Zhang F, Li PL. Reconstitution and characterization of a nicotinic acid adenine dinucleotide phosphate (NAADP)-sensitive Ca²⁺ release channel from liver lysosomes of rats. *J Biol Chem*. 2007 Aug 31;282(35):25259-69.
- Zhang H, Xu Y, Markadieu N, Beauwens R, Erneux C, Prestwich GD. Synthesis and biological activity of phosphatidylinositol-3,4,5-trisphosphorothioate. *Bioorg Med Chem Lett*. 2008 Jan 15;18(2):762-6.
- Zhang XK, Elbin CS, Turecek F, Scott R, Chuang WL, Keutzer JM, Gelb M. Multiplex lysosomal enzyme activity assay on dried blood spots using tandem mass spectrometry. *Methods Mol Biol*. 2010;603:339-50.
- Zheng X, Zhang L, Wang AP, Araneda RC, Lin Y, Zukin RS, Bennett MV. Mutation of structural determinants lining the N-methyl-D-aspartate receptor channel differentially affects phencyclidine block and spermine potentiation and block. *Neuroscience*. 1999;93(1):125-34.
- Zhu MX, Evans AM, Ma J, Parrington J, Galione A. Two-pore channels for integrative Ca signaling. *Commun Integr Biol*. 2010 Jan;3(1):12-7.
- Zong X, Schieder M, Cuny H, Fenske S, Gruner C, Rötzer K, Griesbeck O, Harz H, Biel M, Wahl-Schott C. The two-pore channel TPCN2 mediates NAADP-dependent Ca²⁺-release from lysosomal stores. *Pflugers Arch*. 2009 Sep;458(5):891-9.
- Zong X, Krause S, Chen CC, Krüger J, Gruner C, Cao-Ehlker X, Fenske S, Wahl-Schott C, Biel M. Regulation of hyperpolarization-activated cyclic nucleotide-gated (HCN) channel activity by cCMP. *J Biol Chem*. 2012 Aug 3;287(32):26506-12.

7. Appendix

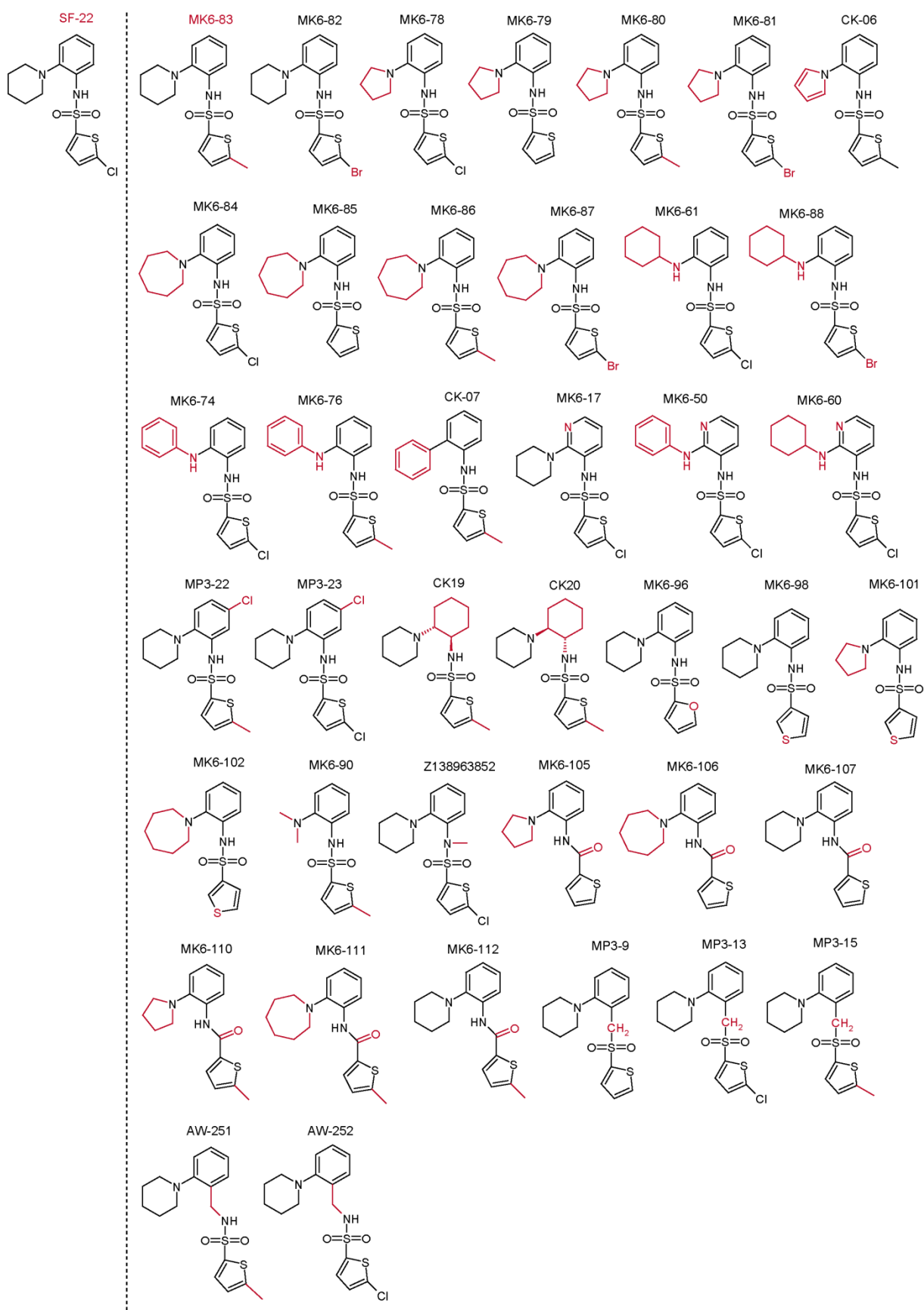
7.1. Abbreviations

μg	microgram
μl	microliter
μm	micromolar
ACS	American Chemical Society
ADP	Adenosine diphosphate
ATP	Adenosine triphosphate
ATPase	adenylpyrophosphatase
Ca^{2+}	calcium
CaCl_2	calcium chloride
cAMP	cyclic adenosine monophosphate
cDNA	Complementary DNA
Cl^-	chloride
CIC	chloride channel
CMV	cytomegalovirus
CO_2	Carbon dioxide
COS7 cells	cells being cv-1 (simian) in origin and carrying the sv40 genetic material
ddH ₂ O	double deionized water
DMEM	dulbecco's modified eagle medium
DMSO	dimethylsulfoxide
DNA	deoxyribonucleic acid
EDTA	ethylenediaminetetraacetic acid
EGTA	ethylene glycol tetraacetic acid
ER	Endoplasmic reticulum
E_{rev}	reversal potential
F	Floride
Fab1	Fatty acid biosynthesis 1
FBS	fetal bovine serum
Fe^{3+}	ferric
G	gram
GFP	green fluorescent protein
H	hour
HCl	hydrochloric acid
HCN channel	hyperpolarization-activated cyclic nucleotide-gated channel
HEK293 cells	human embryonic kidney cells
HEPES	4-(2-hydroxyethyl)piperazine-1-ethanesulfonic acid, n-(2-hydroxyethyl)piperazine- n ¹ -(2-ethanesulfonic acid)
IP3	1,4,5-triphosphate
LSD	lysosomal storage disease
LTS	Lysosomal targeting sequence
K^+	potassium
KO	knockout
MEF	Mouse embryonic fibroblast
MES	2-(N-morpholino)ethanesulfonic acid
mg	milligram
Mg^{2+}	Magnesium
ml	milliliter

MLIV	Mucopolipidosis type IV
mm	millimeter
min	minute
MSA	methanesulfonate
mv	millivoltage
Na ⁺	sodium
NAADP	nicotinic acid adenine dinucleotide phosphate
NaCl	sodium chloride
NaOH	sodium hydroxide
NSF	n-ethylmaleimide-sensitive fusion
Ω	Ohm
pA	picoampere
Pen/strep	penicillin / streptomycin
pH	power of hydrogen
PI(3)P	Phosphatidylinositol 3-phosphate
PI(3,5)P ₂	Phosphatidylinositol 3,5-bisphosphate
PI(4,5)P ₂	phosphatidylinositol 4,5-bisphosphate
PI5-kinase	Phosphoinositide 5-kinase
PIKfyve	FYVE finger-containing phosphoinositide kinase
PIP	phosphoinositide
rpm	rotations per minute
SNARE	soluble NSF attachment protein
TM	Transmembrane domain
TPC	two pore channel
TRP	transient receptor potential channel
TRPML	Transient receptor potential channel mucolipin
Va	Varicella-zoster virus
VGCC	Voltage-gated cation channel
w/o	without
WT	wildtype
YFP	Yellow Fluorescent Protein

6.2 Chemical structures of the lead compound SF-22 and novel SF-22 analogues

The SF-22 analogues were designed and synthesized by Dr. Marco Keller and Dr. Annette Wolfgardt under the supervision of Prof. Dr. Franz Bracher at the Department of Pharmacy, LMU Munich.



7.2. Curriculum vitae

Personal Information

Name: Cheng-Chang Chen
Place of birth: Tainan, Taiwan
Date of birth: 21.02.1983
Adress: Riesstr. 65, 80993 München
Email: cheng-chang.chen@cup.uni-muenchen.de

Educaiton

2010-present PhD at the Department of Pharmacy - Center for Drug Research, Ludwig-Maximilians-Universität München, Germany

2007-2009 Institute of Biophotonics Engineering, National Yang-Ming University, Taiwan
Master's Degree of Science (M.Sc.)

2002-2006 Department of Clinical Laboratory Sciences and Medical Biotechnology,
National Taiwan University, Taiwan
Bachelor Degree of Medical Biotechnology

1998-2001 National Tainan First Senior High School, Taiwan

Publication

C.-C. Chen*, M. Keller*, M. Hess, R. Schiffmann, N. Urban, Michael Schaefer, F. Bracher, M. Biel, C. A. Wahl-Schott, and C. Grimm. A small molecule to restore function of TRPML1 mutant isoforms causing mucopolidosis type IV. *Nature Communication* (2014) 14;5:4681. doi:10.1038/ncomms5681

C. Grimm, **C.-C. Chen***, L. M. Holdt*, S. Hassan*, S. Jörs, H. Cuny, S. Kissing, B. Schröder, E. Butz, B. Northoff, C. Müller, S. Spahn, J. Castonguay, C. A. Lubber, M. Moser, R. Lüllmann-Rauch, C. Fendel, N. Klugbauer, O. Griesbeck, A. Haas, M. Mann, F. Bracher, D. Teupser, P. Saftig, M. Biel, and C. Wahl-Schott. High susceptibility to fatty liver disease in two-pore channel 2 deficient mice. *Nature Communication* (2014) 21;5:4699. doi: 10.1038/ncomms5699

M. P. Cuajungco, L. C. Basilio, T. Hart, **C.-C. Chen**, J. Silva, M. Biel, and C. Grimm; Cellular zinc levels are modulated by trpml1-tmeme163 interactions. *Traffic* (2014) doi: 10.1111/tra.12205

Y. Sakurai, A. A. Kolokoltsov, **C.-C. Chen**, M. W. Tidwell, W. E. Bauta, N. Klugbauer, C. Grimm, C. Wahl-Schott, M. Biel, R. A. Davey. Two pore channels control Ebolavirus entry into host cells and are targets for disease treatment. *Nature* (2014) (submitting)

M. Ruas, L. C. Davis, **C.-C. Chen**, K.-T. Chuang, T. Walseth, C. Grimm, A. J. Morgan, M. Biel, C. Wahl-Schott, J. Parrington, A. Galione. Two-pore channels are essential for NAADP-induced Ca²⁺ signaling. *EMBO* (2014) (submitting)

X. Zong, S. Krause, **C.-C. Chen**, J. Krüger, C. Gruner, X. Cao-Ehlker, S. Fenske, C. Wahl-Schott and M. Biel; Regulation of HCN channel activity by cyclic cytidine 3', 5'-monophosphate (cCMP). *Journal of Biological Chemistry* (2012) 287, 26506–26512

M. Skasko, A. Tokarev, **C.-C. Chen**, W. B. Fischer, S. K. Pillai, J. Guatelli; BST-2 is rapidly down-regulated from the cell surface by the HIV-1 protein Vpu: evidence for a post-ER mechanism of Vpu-action. *Virology* (2011) 411, 65-77

C.-C. Chen, J. Krüger, I. Sramala, H.-J. Hsu, P. Henklein, Y.-M. A. Chen, W. B. Fischer; ORF 8a of SARS-CoV forms an ion channel: experiments and molecular dynamics simulations. *Biochim. Biophys. Acta* (2011) 1808, 572-579

* These authors contributed equally

7.3. Acknowledgements

First and foremost, I want to express my deepest regards and sincere gratitude to my advisors, Prof. Martin Biel and Prof. Christian Wahl-Schott for providing the best opportunity and research environment of studying in LMU Munich. The completion of this PhD work would not have been possible without their priceless guidance and constant encouragement. Prof. Biel showed me how to think like a scientist and gave me so many invaluable chances to prove and improve myself. Prof. Wahl taught me how to solve problems and influenced me with his great research insight. My sincere thanks also go to all the current and past members from their research group. I will never forget their great support. I would like to express my immense gratitude to Dr. Christian Grimm for the excellent collaboration on TPC and TRPML1 projects. His professional support and tutorial enormously helped me throughout my PhD years and thesis. Meeting him in my second PhD year is definitely crucial for my academic performance in these years. Special thanks to Bayerische Forschungsstiftung for the financial support during my first three PhD years. It allowed me to reach my dream over the ocean. I also owe my gratitude to Dr. Xiangang Zong for his tremendous assistance with electrophysiological technique, and many inspiring and helpful discussions. Big thanks to Dr. Michael Schieder for teaching me Nanion Patch in my first PhD year. If I have seen further it is by standing on the shoulder of Michael. I want to thank my great colleagues Sami Hassan, Zhuolu Niu, Dr. Verena Hammelmann, Dr. Stefanie Fenske, Dr. Stylianos Michalakis, Dr. Lior Shaltiel, Dr. Andreas Scharr, Christos Paparizos, Dr. Christian Gruner, Dr. Stefanie Krause, Dr. Elvir Becirovic, Dr. Susanne Koch, Dr. Xiaochun Cao-Ehlker, Dr. Christian Schön, Arshan Perera, Phuong Nguyen, Vanessa Marks, Henrik Hülle, Fred Koch, Elisabeth Butz, Mirja Koch, Verena Schludi, Saskia Spahn and Maria Barthmes. And many thanks to the technicians Katrin Rötzer, Elisabeth Schulze, Berit Noack, Daniela Hölle and the secretary Monika Grethe for their great help. Thanks to the LSM graduate program and LMU staff who helped me a lot. I also want to thank Prof. Dejian Ren and Dr. Chunlei Cang in University of Pennsylvania for generously exhibiting the whole-lysosome patch-clamp approach. Many thanks to all the co-authors of my publications for being such nice collaborators. I am very grateful to the members of my thesis committee, Prof. Franz Bracher, Prof. Stefan Zahler, Prof. Wolfgang Frieß and Dr. Martin Heß for being so helpful. Last but not least, thanks to my family and friends, C.-T. Chen, S.-J. Yang, C.-C. Chen, Y.-H. Tasi, S.-H. Yeh and other friends who supported me during these years. I would like to especially express my deepest gratitude to my lovely partner Bei-Bei Chuang who takes care of me in Germany. I would not have survived in this country without her around me. I feel extremely fortunate to be a PhD student in this Lab and enjoyed the research life in Munich.